

# **Masur-Veech Volumes of the Moduli Space of Quadratic Differentials**

**Quan Nguyen**

A thesis submitted for the degree of  
Master of Science

Supervised by  
**Paul Norbury**

School of Mathematics and Statistics  
University of Melbourne

January 7, 2026

# Abstract

Many dynamical and enumerative problems can be recast in terms of translation surfaces, and studying the associated moduli spaces can reveal fascinating insights into their behaviour. We develop combinatorial tools to compute volumes of these moduli spaces and provide a new extension to recent techniques to evaluate volumes of strata. Kontsevich’s proof of Witten’s conjecture provided a link between intersection theory and counts of ribbon graphs which was later developed to evaluate volumes of principal strata. We discuss this approach and some applications to combinatorial problems of meander counts.

# Acknowledgements

I would like to thank my supervisor, [Name], for his support and guidance throughout this project, and for introducing me to a beautiful area of mathematics. I am also grateful to everyone in G90, as well as my family and friends, for their support throughout my Master's degree.

# Contents

<b>1</b>	<b>Introduction</b>	<b>5</b>
<b>2</b>	<b>Flat surfaces</b>	<b>8</b>
2.1	Three equivalent definitions . . . . .	9
2.2	Moduli space and strata . . . . .	17
2.3	Period and cohomological coordinates . . . . .	21
<b>3</b>	<b>Masur-Veech Volumes</b>	<b>23</b>
3.1	Counting square-tiled surfaces . . . . .	24
3.2	Stable graphs . . . . .	26
3.3	Ribbon graphs . . . . .	29
3.4	The volume formula . . . . .	36
3.5	Computation of volumes . . . . .	43
3.6	Refinement of volume contributions . . . . .	48
<b>4</b>	<b>Principal Strata of Quadratic Differentials</b>	<b>50</b>
4.1	Intersection numbers . . . . .	50
4.2	Kontsevich's Theorem . . . . .	52
4.2.1	Combinatorial moduli space . . . . .	53
4.2.2	Combinatorial classifying space . . . . .	55
4.2.3	Main identity . . . . .	57
4.3	Trivalent ribbon graphs with leaves . . . . .	59
4.4	Examples of volume computations . . . . .	63
<b>5</b>	<b>Application of Volumes</b>	<b>67</b>
5.1	Enumeration of meanders . . . . .	67
5.2	Siegel-Veech constants and Lyapunov exponents . . . . .	70
<b>6</b>	<b>Conclusion</b>	<b>73</b>
<b>A</b>	<b>Riemann surfaces and differentials</b>	<b>74</b>
<b>B</b>	<b>Moduli space examples</b>	<b>76</b>
<b>C</b>	<b>Additional proofs</b>	<b>77</b>

# Chapter 1

## Introduction

Many interesting problems in geometry, dynamical systems, and physics lead to the study of translation surfaces. Roughly speaking, a translation surface is a polygon in the plane with opposite and equal edges identified via translation. Geodesics in a translation surface are straight lines, which upon hitting an edge, continue in the same direction from the opposite identified edge. One of the original motivations for translation surfaces comes from studying billiard trajectories.

Consider a polygonal billiard table with a point moving around at constant speed, representing an idealised billiard ball. When the point hits an edge, it bounces off in such a way that the incidence angle is equal to the reflection angle. When it hits a vertex, it stops moving. The path traced out by the point as it moves is called a billiard trajectory.

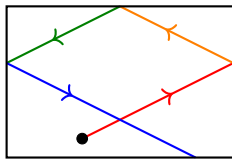
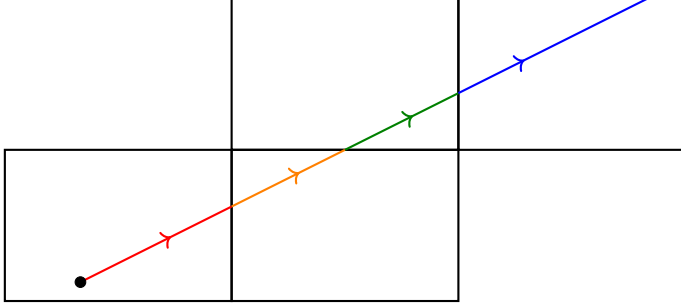


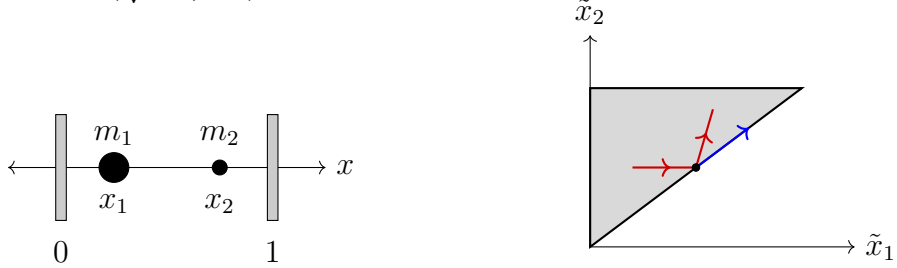
Figure 1.1: A billiard trajectory on a rectangular billiard table.

The study of billiard trajectories have been of interest in mathematics and physics, with still many unsolved open problems. For example, a surprising problem which can be stated in elementary terms is the question on the existence of periodic trajectories on any billiard table. The problem has an affirmative answer in the case of rational billiard tables (where the angles are rational multiples of  $\pi$ ), and remains unsolved in the general case. The rational case was proven by Katok and Zemlyakov in [KaZe] and uses the technique of “unfolding” a billiard table. This reframes billiard trajectories in terms of geodesics on a translation surface. The key idea is instead of reflecting

the billiard trajectory, we reflect the polygon and allow the trajectory to continue in a straight line.



Many physical models can be recast in terms of a billiard trajectory. Consider a simple model of a Boltzmann gas consisting of two particles modelled by point masses  $m_1$  and  $m_2$  confined to the unit interval  $[0, 1]$ . The points are assumed to collide elastically with each other and the walls at the endpoints. Let  $x_1, x_2 \in [0, 1]$  be the coordinates of the points and suppose that  $x_1 \leq x_2$ . Then the configuration space of the system is the right triangle  $0 \leq x_1 \leq x_2 \leq 1$ . Consider rescaling the coordinates by  $\tilde{x}_i = \sqrt{m_i}x_i$  which transforms the configuration space into a right triangle with an acute angle  $\tan^{-1}(\sqrt{m_1/m_2})$ .



Assuming there are no external forces acting on the system, its evolution corresponds to a straight-line path  $\gamma$  in the configuration space of constant velocity. Consider a collision of the two particles, which corresponds to a path reaching the wall  $x_1 = x_2$ . Let  $(u_1, u_2)$  and  $(v_1, v_2)$  be the velocities before and after the collision. By the conservation laws for momentum and energy, we have

$$m_1 u_1 + m_2 u_2 = m_1 v_1 + m_2 v_2 \quad \text{and} \quad \frac{1}{2} m_1 u_1^2 + \frac{1}{2} m_2 u_2^2 = \frac{1}{2} m_1 v_1^2 + \frac{1}{2} m_2 v_2^2.$$

Rewriting in rescaled coordinates, we obtain

$$\sqrt{m_1} \tilde{u}_1 + \sqrt{m_2} \tilde{u}_2 = \sqrt{m_1} \tilde{v}_1 + \sqrt{m_2} \tilde{v}_2 \quad \text{and} \quad \tilde{u}_1^2 + \tilde{u}_2^2 = \tilde{v}_1^2 + \tilde{v}_2^2.$$

The first equation tells us the scalar product of the vector  $(\tilde{u}_1, \tilde{u}_2)$  and  $(\tilde{v}_1, \tilde{v}_2)$  with  $(\sqrt{m_1}, \sqrt{m_2})$  is identical. Since  $(\sqrt{m_1}, \sqrt{m_2})$  is the vector parallel to the wall  $x_1 = x_2$ , the incidence and reflection angle of the path  $\gamma$  off the wall  $x_1 = x_2$  coincide. The second

equation tells us the velocity of  $\gamma$  is preserved before and after the collision. Therefore, the trajectory of the system reflects in the wall  $x_1 = x_2$ . One can also check collisions on the walls  $x_1 = 0$  and  $x_2 = 1$  corresponds to reflections. We conclude that our dynamical system is equivalent to billiards in a right triangle. When  $\tan^{-1}(\sqrt{m_1/m_2})$  is a rational multiple of  $\pi$ , it is equivalent to a geodesic on a translation surface.

### Structure of the thesis

In Chapter 2, we begin by providing three equivalent definitions of a translation surface from geometric and analytic perspectives. We consider families of translation surfaces called *strata*, their moduli spaces, and the Masur-Veech measure defined using local coordinates we construct on the moduli space.

In Chapter 3, we define the Masur-Veech volumes and reduce the computation down to counting lattice points, which involve counting metric ribbon graphs. We provide a new extension of an existing count in Lemma 3.5 to strata of quadratic differentials under certain conditions.

In Chapter 4, we derive an intersection theory approach to computing volumes in the special case of principal strata of quadratic differentials. We follow the work of [DGZZ1] and provide an exposition of Kontsevich’s proof of Witten’s conjecture.

We conclude in Chapter 5 by applying some volume computations to problems involving the enumeration of meanders and discuss some further applications of volumes.

### Notation

A partition is a finite unordered collection of numbers  $\mu = [\mu_1, \dots, \mu_n]$  where  $\mu_i \in S$  for some subset  $S \subseteq \mathbb{Z}$ . We will usually either take  $S = \mathbb{N}_0$  or  $\mathbb{N} \cup \{-1\}$  which is made clear when used. We will also use exponential notation for partitions. For example,  $[1, 1, 2, 2, 2, 4] = [1^2, 2^3, 4]$ . The concatenation of two partitions  $\mu$  and  $\nu$  is denoted  $\mu \cup \nu$ . For example,  $[1, 2] \cup [2, 3] = [1, 2^2, 3]$ . We denote the length of a partition by  $\ell(\mu) = n$  and the sum  $\mu_1 + \dots + \mu_n$  by  $|\mu|$ . We denote  $\lambda_i(\mu)$  as the number of terms in the partition  $\mu$  equal to  $i$ .

A multi-index is a finite ordered collection of numbers or indeterminates  $\mathbf{d} = (d_1, \dots, d_n)$ . We denote the sum  $d_1 + \dots + d_n$  by  $|\mathbf{d}|$  and the product  $d_1! \cdots d_n!$  by  $\mathbf{d}!$ . For another multi-index  $\mathbf{b} = (b_1, \dots, b_n)$ , we denote  $\mathbf{b}^\mathbf{d}$  to be the product  $b_1^{d_1} \cdots b_n^{d_n}$ . For a sequence  $\tau_{d_1}, \dots, \tau_{d_n}$  indexed by a multi-index  $\mathbf{d}$ , we denote the product  $\tau_{d_1} \cdots \tau_{d_n}$  by  $\tau_\mathbf{d}$ .

For a set  $X$  and a finite set  $E$ , we denote by  $X^E$  the set of functions  $E \rightarrow X$ . We interpret this as the set of tuples containing elements in  $X$  indexed by  $E$ .

# Chapter 2

## Flat surfaces

This chapter introduces the necessary background on translation surfaces and their moduli space as needed for our purposes. This area of research is vast, containing many fascinating ideas and results. The interested reader may consult the survey [Zo] or the textbook [AtMa] for introductions into many key topics in the field, with selected topics relating to counting problems, equidistribution, renormalisation, dynamics, and ergodic theory. Although our constructions are primarily formulated to build up to the computation of volumes, Chapter 5 will offer a brief glimpse into adjacent areas in this field where volumes make an appearance.

The Gauss-Bonnet Theorem from geometry provides a bridge between the geometry and topology of a surface. An orientable genus  $g$  surface  $X$  with constant Gaussian curvature  $K$  satisfies  $K \cdot \text{Area}(X) = 2\pi(2 - 2g)$ . Thus, we generally associate a constant positive curvature to a sphere, a constant zero curvature to a torus and a constant negative curvature to a higher genus surface. In fact, any surface regardless of genus can be equipped with a metric of zero curvature, that is, a flat metric. This is provided we allow for singular points where there may be an accumulation of excess or surplus curvature, creating cone points. Consider, for example, the unit sphere which has constant curvature 1, and a total curvature of  $4\pi$ . We can deform the sphere until it is everywhere flat except for eight points where the curvature has accumulated. At each of these points, the cone angle is  $3\pi/2$  so the angle deficit is  $\pi/2$ . Since the surface is now everywhere else flat, the local Gauss-Bonnet Theorem tells us the total curvature is the sum of angle deficits. Therefore, the curvature of the flat sphere is  $8 \cdot \pi/2 = 4\pi$  which matches the smooth case.

Consider parallel transporting a vector around a closed loop. The *holonomy* of a metric can roughly be described by the extent to which the vector has been rotated after traversing the loop. In the case of the flat sphere, we observe that parallel transporting a vector around a cone point with cone angle  $3\pi/2$  induces a rotation by an angle of  $\pi/2$ . Thus, we say the flat metric on the sphere has nontrivial holonomy.

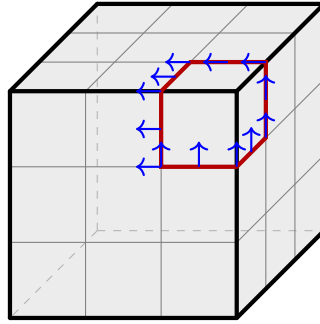


Figure 2.1: Parallel transport of a vector along a loop around a conical singularity induces a rotation by  $\pi/2$ .

We will be considering flat surfaces with trivial or  $\mathbb{Z}/2$ -holonomy, also called *translation surfaces* or *half-translation surfaces* respectively. Some authors also refer to these as *very flat surfaces* however we will use the term flat surface to mean either a translation or half-translation surface. On a translation surface, parallel transporting a vector along any path is equivalent to a translation, while on a half-translation surface, it is equivalent to translation up to a sign. Due to the direction being preserved on a translation surface, the orientation of any geodesic is well defined (and up to sign for a half-translation surface), in particular, geodesics will either close up or never self-intersect. Moreover, cone angles for a translation surface can only be integer multiples of  $2\pi$ , whereas for half-translation surfaces, we allow for integer multiples of  $\pi$ .

## 2.1 Three equivalent definitions

We will now present a formal treatment of translation and half-translation surface. We provide three equivalent definitions of a translation surface; geometric, analytic, and polygonal. The polygonal definition is constructive, and how we will be representing most of the translation surfaces in this thesis. Some of the organisation of results in the following exposition is inspired by [BC; Wr], which are also an excellent starting point for a general audience.

**Definition 2.1** (First definition). A *translation surface* is a connected, compact, orientable (real two-dimensional) surface  $X$  equipped with a special subset of points  $\Sigma = \{p_1, \dots, p_n\}$  called *singularities* satisfying the following:

1. There exists an atlas on the punctured surface  $X \setminus \Sigma$  such that all chart transition maps are translations;
2. At each  $p_i \in \Sigma$ , the cone angle is  $2\pi(k_i + 1)$  for some  $k_i \in \mathbb{Z}^+$ . We refer to  $k_i$  as the *degree* or *order* of the singularity  $p_i$ .

Since all chart transition maps are translations, the atlas naturally induces a flat metric away from any singularities given by the usual Euclidean metric.

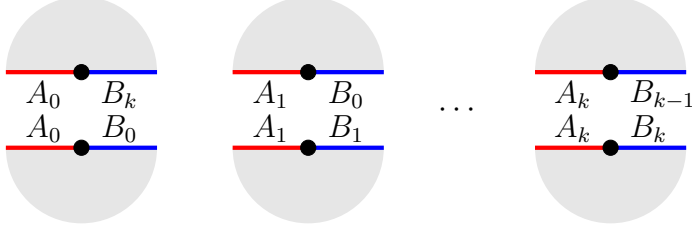


Figure 2.2: A cone angle of  $2\pi(k + 1)$  formed by gluing  $2(k + 1)$  half-planes under the above identifications. A neighbourhood of any order  $k$  singularity is isometric to the neighbourhood constructed above.

**Definition 2.2** (Second definition). An *Abelian differential*  $\omega$  on a Riemann surface  $X$  is a global section of the cotangent bundle of  $X$ . A *translation surface* is a non-zero Abelian differential.

The terms “Abelian differential” and “translation surface” are often used interchangeably. It will always be clear from context when we assume an Abelian differential is non-zero, and is thus a translation surface. We will now prove these two definitions are equivalent. First, we introduce the following results.

**Proposition 2.1.** *Let  $\omega$  be a non-zero Abelian differential on a Riemann surface  $X$  and let  $\Sigma$  be the zeros of  $\omega$ .*

1. *For any point  $p \in X \setminus \Sigma$ , there exist a local coordinate  $z$  around  $p$  such that  $\omega = dz$ .*
2. *For a zero  $p \in \Sigma$  of order  $k$ , there exists a local coordinate  $z$  around  $p$  such that  $\omega = z^k dz$ .*

*Proof.* Let  $p$  be a zero of order  $k$ . Without loss of generality, choose a local coordinate  $w$  such that  $w(p) = 0$ . Then there exists a holomorphic function  $g$  with  $g(0) \neq 0$  such that  $\omega = w^k g(w) dw$ . Define the holomorphic function

$$F(w) = \int_0^w \zeta^k g(\zeta) d\zeta. \quad (2.1)$$

In a neighbourhood of  $w(p)$ ,  $g(w)$  is non-zero so  $F(w)$  has a zero of order  $k + 1$  at  $w(p)$ . Therefore,  $F(w)$  has a  $(k + 1)$ -st root, and we define the local coordinate  $z$  by

$$z^{k+1} = (k + 1)F(w).$$

Taking the derivative of both sides gives us  $z^k dz = F'(w)dw = \omega$ . □

**Proposition 2.2.** *There exists an atlas on  $X \setminus \Sigma$  such that all chart transition maps are translations.*

*Proof.* Define a local coordinate  $(U, z)$  of  $X \setminus \Sigma$  around a point  $p$  by

$$z(x) = \int_{\gamma_{p,x}} \omega$$

where  $\gamma_{p,x}$  is a path from  $p$  to  $x$ . Holomorphicity of  $\omega$  implies well-definition of  $z$ . Now let  $(V, w)$  be another such local coordinate around a point  $q$ . For any  $x \in U \cap V$ , we have

$$z(x) = \int_{\gamma_{p,x}} \omega = \underbrace{\int_{\gamma_{p,q}} \omega}_{C} + \int_{\gamma_{q,x}} \omega = w(x) + C$$

and thus the chart transition maps are translations.  $\square$

**Proposition 2.3.** *The first and second definition of a translation surface are equivalent.*

*Proof.* Let  $X$  be a translation surface with singularities  $\Sigma$  from Definition 2.1. The atlas on  $X \setminus \Sigma$  induces a complex structure since the chart transition maps are translations, which are biholomorphisms. On each chart, the local coordinate  $z$  defines the one-form  $dz$ . Furthermore, the one-forms agree on chart intersections since the transition maps are translations, so extends to a global one-form  $\omega$  on  $X \setminus \Sigma$ .

Consider a chart around a singularity  $p \in \Sigma$  of degree  $k$  with the local coordinate  $w$ . In this chart, we can also write  $\omega = dw$ . Since  $p$  has cone angle  $2\pi(k+1)$  the metric can be realised as the pullback of the flat metric induced by  $dw$  under the map  $w = \phi(z) = z^{k+1}$ . This is a local isometry in a punctured neighbourhood of 0 and  $dw$  pulls back under  $\phi$  to  $(k+1)z^k dz$ .

We show this is compatible with the complex structure on  $X \setminus \Sigma$ . Let  $z$  be a local coordinate at a singularity  $p$  such that  $\omega = (k+1)z^k dz$  and  $w$  a local coordinate in a neighbourhood of  $p$  but not containing  $p$  such that  $\omega = dw$ . On the intersection,  $dw = (k+1)z^k dz$  so the transition map is  $w(z) = z^{k+1} + c$  which is a biholomorphism away from the singularity at  $z = 0$  and thus Definition 2.2 is implied.

Conversely, let  $(X, \omega)$  be a translation surface from Definition 2.2. By Proposition 2.1,  $\omega$  defines a flat metric on  $X \setminus \Sigma$  where  $\Sigma$  are the zeros of  $\omega$ . At a zero, we can write  $\omega = (k+1)z^k dz$ . Following the same argument previously,  $\omega$  is the pullback of a flat metric induced by  $dw$  under  $\phi$  so has cone angle  $2\pi(k+1)$ . Using Proposition 2.2 gives us the first condition of Definition 2.1.  $\square$

**Definition 2.3** (Third definition). A *translation surface* is a finite union of polygons in  $\mathbb{C}$  together with a choice of pairing of edges which are parallel, equal in length, and occur on opposite sides. The last condition is to ensure orientability of the resulting surface after identifying edges. Two such collections of polygons are considered equivalent if there is a series of cut and paste operations transforming one collection into another. Cuts are made along straight lines between the vertices, and gluings respect edge pairings, with the cut piece moved only by translation. Cuts introduce two new edges which form a new edge pair, whereas gluings along two edges removes the pairing.

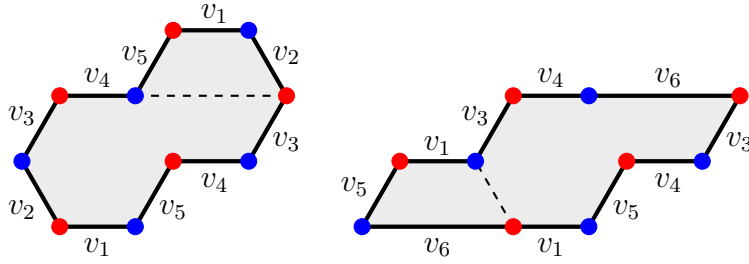


Figure 2.3: Two polygon presentations of a genus  $g$  translation surface with two conical singularities.

We now prove the first and third definitions are equivalent. Some preliminary definitions are required. A *saddle connection* on a translation surface  $X$  is a geodesic, or straight line, joining two singularities without passing any other singularities. A *triangulation* of a translation surface is a collection of non-intersecting saddle connections  $S$  such that every singularity is incident to a saddle connection, and  $X \setminus S$  is a collection of disjoint triangles.

**Proposition 2.4.** *Every translation surface  $X$  from Definition 2.1 can be triangulated.*

*Proof.* Take any set  $S$  of non-intersecting saddle connections on  $X$  such that all finitely many singularities are incident to a saddle connection. Only a finite number of saddle connections are required to add to  $S$  until all components of  $X \setminus S$  are triangles.  $\square$

**Theorem 2.5.** *The first and third definition of a translation surface are equivalent.*

*Proof.* Let  $X$  be a translation surface from Definition 2.1 and let  $S$  be a collection of saddle connections defining a triangulation. Then  $X \setminus S$  can be considered a set of disjoint triangles in  $\mathbb{C}$  with the appropriate edge identifications made by translations. Conversely, given a translation surface from Definition 2.3, the interior of each polygon has a natural coordinate  $z = x + iy$  inducing the flat metric  $|dz|^2$ . On the interior of an edge, the two polygons can be glued together forming a well-defined coordinate. Since gluings are made via translations, the holonomy is trivial. The cone angle at a vertex can be obtained by adding up the angles at all vertices that are identified. It must be an integer multiple of  $2\pi$  otherwise the surface admits non-trivial holonomy.  $\square$

**Remark 2.4.** We will often refer to the polygon construction in Definition 2.3 as a *polygon presentation* of a translation surface. Polygon presentations provide a concrete and visual model for Abelian differentials, which otherwise is an abstract construction. This perspective makes it very accessible to represent an Abelian differential and study its properties. Translation surfaces provide a natural setting to study dynamical problems, and many interesting questions and ideas can arise solely by studying them through this geometric perspective. Often, their study is enriched when viewing them as Abelian differentials, since some of the most deep and profound connections to other areas of mathematics emerge when viewing them through this lens.

A natural extension of Abelian differentials are quadratic differentials, which are locally represented on a Riemann surface  $X$  by  $q = f(z)dz^2$ . Just as with Abelian differentials in Proposition 2.1, we can parameterise our chart so that  $q = dz^2$  away from any singularities and  $q = z^k dz^2$  at an order  $k$  singularity. Since  $dz^2$  is invariant under translations and rotations by  $\pi$ , chart translation maps take the form  $z \mapsto \pm z + c$ , which is analogous to Proposition 2.2. Quadratic differentials also have a polygon presentation which is identical to Definition 2.3, however, we now allow edges to be identified under translation and half-rotations. Thus, we give the name *half-translation surface* to these objects. Similarly to a translation surface, there are three equivalent definitions which we now present.

**Definition 2.5.** A *half-translation surface* is equivalently:

1. A surface with the properties in Definition 2.1, but allowing chart transition maps to be translations composed with a possible rotation by an angle of  $\pi$ , and at a singularity of order  $k$ , the cone angle is  $\pi(k + 2)$ ;
2. A non-zero quadratic differential on a Riemann surface;
3. A collection of polygons with the properties in Definition 2.3, but allowing equal and opposite edges to be identified by translation with a possible rotation by an angle of  $\pi$ .

**Remark 2.6.** It is convenient to write the cone angle of a order  $k$  singularity for an Abelian differential resp. quadratic differential as  $2\pi + 2\pi k$  resp.  $2\pi + \pi k$ . When  $k = 0$ , we locally have a flat metric, so the cone angle is  $2\pi$ . Higher-order zeros correspond an *excess angle* of  $2\pi k$  resp.  $\pi k$ . One could also ask if it makes geometric sense to have singularities of negative order. For an Abelian differential, the geometric perspective suggests that a simple pole would correspond to a cone angle of 0. In fact, the local model looks like an infinite cylinder which has infinite area. Thus, we consider only holomorphic differentials when working with finite translation surfaces. In contrast, a quadratic differential with a simple pole yields a cone angle of  $\pi$  which makes geometric sense, see for instance, Figure 2.4. Thus, it is admissible for us to consider meromorphic quadratic differentials with at most simple poles. When we refer to quadratic differentials in this thesis, we will implicitly assume that is meromorphic with at most simple poles unless otherwise stated.

**Proposition 2.6.** Let  $X$  be a genus  $g$  translation surface resp. half-translation surface with cone angle  $2\pi(k_i + 1)$  resp.  $\pi(k_i + 1)$  with  $k_i \in \mathbb{Z}_0^+$  at each marked point  $p_i$  for  $i = 1, \dots, n$ . Then

$$\sum_{i=1}^n k_i = 2g - 2 \quad \text{resp.} \quad \sum_{i=1}^n k_i = 4g - 4. \quad (2.2)$$

*Proof.* Use Proposition 2.4 to take any triangulation of a polygon presentation. There are  $n$  vertices, and let  $e$  and  $f$  be the number edges and faces of this triangulation respectively. Since each edge borders two triangles, we have  $2e = 3f$ . A simple Euler characteristic computation tells us that  $f = 4g - 4 + 2n$ . Each triangle has an angle sum of  $\pi$  so the total angle sum of all vertices is  $\pi f$ . This must coincide with the sum of cone angles giving us

$$\sum_{i=1}^n 2\pi(k_i + 1) = \pi(4g - 4 + 2n) \quad \text{resp.} \quad \sum_{i=1}^n \pi(k_i + 1) = \pi(4g - 4 + 2n). \quad (2.3)$$

which is equivalent to 2.2.  $\square$

**Remark 2.7.** The analytic version of Proposition 2.6 is the Riemann-Roch Theorem, which states that the sum of multiplicities of zeros of a genus  $g$  Abelian differential resp. quadratic differential is  $2g - 2$  resp.  $4g - 4$ . See for instance, [Fo, Theorem 17.12].

**Example 2.8.** The simplest example of a half-translation surface is the *pillowcase*  $\mathcal{P}$ , constructed from two squares with four cone angles of  $\pi$ . It is also a quotient of the flat torus  $\mathbb{C}/\mathbb{Z}[i]$  by a  $\mathbb{Z}_2$  action, given by the automorphism  $z \mapsto -z$ . From an analytic perspective,  $\mathcal{P}$  can be realised as a quadratic differential on  $\mathbb{C}P^1$  with four simple poles. In fact, the quotient map  $\mathbb{C}/\mathbb{Z}[i] \rightarrow \mathbb{C}P^1$  is given by the Weierstrass  $\wp$ -function, and the quadratic differential  $dz^2$  on  $\mathbb{C}/\mathbb{Z}[i]$  is  $\mathbb{Z}_2$ -invariant so descends to a well-defined quadratic differential  $q$  on  $\mathbb{C}P^1$ .

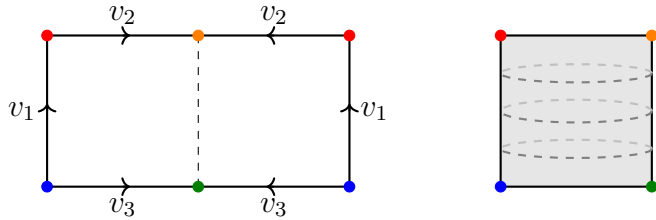


Figure 2.4: Pillowcase

**Definition 2.9.** A *cylinder*  $C$  in a (half-)translation surface  $X$  is an isometric image of  $\{\frac{c}{2\pi}e^{i\theta}, t : \theta \in [0, 2\pi], t \in (0, h)\} \subseteq \mathbb{C} \times \mathbb{R}$  in  $X$  where  $c$  is the *circumference* and  $h$  is the *height*. A *waist curve* of  $C$  is a closed geodesic  $\gamma$  of length  $c$  with respect to the flat metric of  $X$ . The *direction* of a cylinder is the angle  $\phi$  determined by the geodesic  $\gamma$ .

Every cylinder has a unique waist curve considered up to a free homotopy. A cylinder is *maximal* if the both boundaries are unions of saddle connections.

**Definition 2.10.** A *cylinder decomposition* of a translation surface  $X$  in the direction  $\phi$  is the disjoint union

$$X = \text{cyl}_1 \sqcup \cdots \sqcup \text{cyl}_k \sqcup G$$

where  $\text{cyl}_i$  are maximal cylinders in the direction of  $\phi$  and  $G$  is a union of saddle connections in the direction of  $\phi$ .

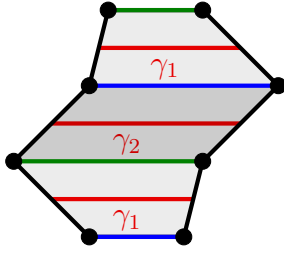


Figure 2.5: A horizontal cylinder decomposition of a genus 2 translation surface into two maximal cylinders and two connected singular layers. Waist curves are shown in red, and singular layers are shown in green and blue

**Definition 2.11.** A *(abelian) square-tiled surface* is a translation surface  $(X, \omega)$  where the complex numbers representing the edges lie in the integer lattice  $\mathbb{Z}[i]$ . Equivalently, it is a cover of the flat torus  $(\mathbb{C}/\mathbb{Z}[i], dz)$  branched over 0. In particular, there is a branched covering map

$$p : X \rightarrow \mathbb{C}/\mathbb{Z}[i]$$

such that  $\omega = p^*dz$ . The ramification points corresponds to the zeros of  $\omega$ , and the degree of the cover corresponds to the number of unit squares from which  $(X, \omega)$  can be tiled. Similarly, a *(quadratic) square-tiled surface* is a half translation surface with edges lying in the integer lattice  $\mathbb{Z}[i]$  and is a branched cover of the pillowcase  $\mathcal{P}$ .

**Remark 2.12.** Using a polygon presentation of a flat surface with edges lying in the integer lattice, one can observe by there are always a series of cut and paste actions such that the surface and be presented as a collection of squares.

**Proposition 2.7.** *Every square-tiled surface admits a cylinder decomposition in the horizontal and vertical direction.*

In fact, square-tiled surface lie in a special class of differentials, called *Jenkins-Strebel* differentials. Roughly speaking, these are differentials where the horizontal foliation consists entirely of closed trajectories away from the singularities.

We conclude this section by analysing the behaviour of the horizontal foliation and the saddle connections of a horizontal cylinder decomposition at a singularity. We only treat the quadratic case, since the Abelian case is included when the singularity orders are even. Locally, a quadratic differential can be represented as the differential of a function, that is,  $q = (df)^2$  for some holomorphic function  $f$ . The horizontal foliation corresponds to level curves where  $\text{Im}(f)$  is constant. Locally, write  $q = z^k dz^2$ . Then  $f$  is given by

$$f(z) = \frac{2}{k+1} z^{(k+2)/2}.$$

In particular, the total angle is  $\pi(k+2)$ . Locally, there are  $k+2$  horizontal trajectories emanating from the singularity, which are called *separatrix rays*. The angle in each chamber is  $\pi$ . Therefore, an order  $k$  singularity of a quadratic differential corresponds to  $k+2$  separatrix rays coming together on the singular layer at an angle of  $\pi$ .

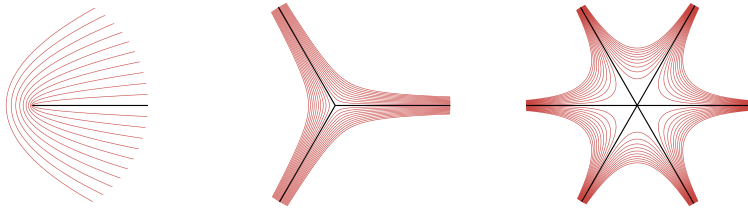


Figure 2.6: A local model of the horizontal foliation around a simple pole (left), a simple zero (middle) and zero of order 4 (right) of a quadratic differential.

**Remark 2.13.** Beyond translation and half-translation surfaces, and equivalently Abelian and quadratic differentials, one can also study  $j$ -differentials  $\xi = f(z)dz^j$  for  $j > 2$ . Geometrically, these correspond to flat surfaces with cone angle  $\frac{2\pi}{j}(k+1)$  at every order  $k$  singularity of  $\xi$ . From the polygon perspective, we allow gluings by angle  $2\pi/j$  and translations. Since the area of the flat surface is finite for positive cone angles, we allow for meromorphic  $j$ -differentials with at most  $j-1$  order poles.

## 2.2 Moduli space and strata

In this section, we define the moduli space of Abelian and quadratic differentials, which is a geometric space parameterising their isomorphism classes. These spaces admit a stratification by the degrees of the singularities of the differential.

**Definition 2.14.** The moduli space  $\mathcal{H}_g$  is the space of genus  $g$  Abelian differentials considered up to isomorphism. Two Abelian differentials  $(X_1, \omega_1)$  and  $(X_2, \omega_2)$  are isomorphic if there exists a biholomorphism  $f : X_1 \rightarrow X_2$  such that  $\omega_1 = f^*\omega_2$ .

**Remark 2.15.** Consider a polygon presentation of an Abelian differential in the plane corresponding to a point in  $\mathcal{H}_g$ . The above definition implies that rotating this polygon generally takes us to a different point in  $\mathcal{H}_g$ . In very symmetrical cases, there may be rotations that fix the point in  $\mathcal{H}_g$ . For example, consider the flat torus  $(\mathbb{C}/\mathbb{Z}[i], dz)$ . A biholomorphism  $f : \mathbb{C}/\mathbb{Z}[i] \rightarrow \mathbb{C}/\mathbb{Z}[i]$  lifts to a biholomorphism  $\tilde{f} : \mathbb{C} \rightarrow \mathbb{C}$  that fixes the lattice  $\mathbb{Z}[i]$ . A rotation by an angle of  $\theta$  corresponds to a map  $\tilde{f}(z) = e^{i\theta}z$  so the only rotations that fix the lattice are integer multiples of  $\frac{\pi}{2}$ , which determine the same point in  $\mathcal{H}_1$ . Every other rotation moves us to a different point in  $\mathcal{H}_1$ .

**Definition 2.16.** The moduli space  $\mathcal{Q}_{g,n}$  is the space of isomorphism classes of pairs  $(X, q)$ . Here,  $X$  is a genus  $g$  Riemann surface with  $n$  distinct labeled marked points and  $q$  is a meromorphic quadratic differential with at most simple poles at the marked points and no other poles. Two quadratic differentials  $(X_1, q_1)$  and  $(X_2, q_2)$  are isomorphic if there exists a biholomorphism  $f : X_1 \rightarrow X_2$  such that  $q_2 = f^*q_1$ . The moduli space of holomorphic quadratic differentials is defined to be  $\mathcal{Q}_g = \mathcal{Q}_{g,0}$ .

In the polygon presentation of an Abelian/quadratic differential, consider the edges as complex numbers. We will see in Section 2.3 that these complex numbers give rise to local coordinates in our moduli space. Perturbing these complex numbers slightly gives us a new differential that is “nearby” to our original point in the moduli space. Using this construction, one can induce a topology on the moduli spaces  $\mathcal{H}_g$  and  $\mathcal{Q}_{g,n}$  which at present we only consider as a set. Observe that by deforming our flat surfaces preserves the degree of the singularities. This leads us to consider special subsets of the moduli space  $\mathcal{H}_g$  and  $\mathcal{Q}_{g,n}$  called *strata*, which are families of differentials sharing the same orders of singularities. These singularity orders are encoded in a partition  $\mu$  which satisfy the statements of Proposition 2.6 and Remark 2.7.

**Definition 2.17.** Let  $\mu$  be a positive partition of  $2g - 2$ , that is,  $\sum_i \mu_i = 2g - 2$  and  $\mu_i \in \mathbb{N}$ . The *Abelian stratum* of type  $\mu$  is the subset

$$\mathcal{H}(\mu) = \{(X, \omega) \in \mathcal{H}_g \mid \text{div}(\omega) = \sum_i \mu_i p_i\}.$$

**Definition 2.18.** Let  $\mu$  be a partition of  $4g - 4$  with  $\mu_i \in \mathbb{N} \cup \{-1\}$ . The *quadratic stratum* of type  $\mu$  is the subset

$$\mathcal{Q}(\mu) = \{(X, q) \in \mathcal{Q}_{g,n} \mid \text{div}(q) = \sum_i \mu_i p_i, \lambda_{-1}(\mu) = n, q \neq \omega^2 \forall \omega \in \mathcal{H}_g\}.$$

**Remark 2.19.** By convention, a quadratic stratum only includes quadratic differentials that do not arise as the square of an Abelian differential. The reasoning is that the square locus can be identified with an Abelian stratum, and the square of an Abelian differential defines the same flat structure as the Abelian differential itself. Some authors, for instance [Go], use the notation  $\tilde{\mathcal{Q}}(\mu)$  to allow for squares of Abelian differentials. Note that a quadratic stratum with at least one odd singularity will not contain any squares of Abelian differentials, since such quadratic differentials necessarily have all even order singularities. Therefore,  $\tilde{\mathcal{Q}}(\mu) = \mathcal{Q}(\mu)$  when there is an odd singularity and  $\tilde{\mathcal{Q}}(\mu) = \mathcal{Q}(\mu) \cup \mathcal{H}(\mu/2)$  otherwise.

**Remark 2.20.** The strata  $\mathcal{H}(\mu)$  and  $\mathcal{Q}(\mu)$  are in general not connected. The classification of connected components of Abelian strata was done by Kontsevich and Zorich in [KoZo]. They showed that all strata are non-empty with at most three connected components. Lanneau in [La] provided the classification for quadratic strata and proved that the strata  $\mathcal{Q}(0)$ ,  $\mathcal{Q}(-1, 1)$ ,  $\mathcal{Q}(1, 3)$  and  $\mathcal{Q}(4)$  are empty. We will not pursue the details of connected components further in this thesis beyond the current section.

**Proposition 2.8** ([KoZo, Proposition 4]). *The closure of any connected component of  $\mathcal{H}(\mu_1, \dots, \mu_m)$  contains a connected component of  $\mathcal{H}(\mu_1 + \mu_2, \mu_3, \dots, \mu_n)$ .*

Strata of differentials are never compact, which is suggested by Proposition 2.8 when there are multiple singularities. Consider a flat surface with at least two singularities and a saddle connection joining any two singularities with order  $\mu_1$  and  $\mu_2$ . By contracting this saddle connection, the two singularities merge to form singularity of order  $\mu_1 + \mu_2$ . That is, we can construct a sequence of differentials that does not converge within the same stratum.

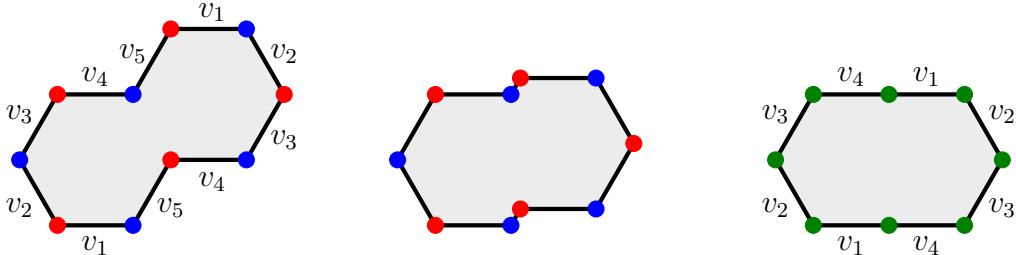


Figure 2.7: A surface in  $\mathcal{H}(1, 1)$  degenerating into a surface in  $\mathcal{H}(2)$  given by contracting the edge  $v_5$ .

**Proposition 2.9.** *The dimension of a stratum  $\mathcal{H}(\mu)$  of genus  $g$  Abelian differentials is given by*

$$\dim_{\mathbb{C}} \mathcal{H}(\mu) = 2g + \ell(\mu) - 1 = |\mu| + \ell(\mu) + 1.$$

*The dimension of a stratum  $\mathcal{Q}(\mu)$  of genus  $g$  quadratic differentials, is given by*

$$\dim_{\mathbb{C}} \mathcal{Q}(\mu) = 2g + \ell(\mu) - 2 = \frac{1}{2}|\mu| + \ell(\mu).$$

All dimension counts in this thesis will be considered over  $\mathbb{C}$  unless otherwise stated. In the dimension count for Abelian strata, observe that the edges defining a translation surface can vary independently. Using the Euler characteristic, the number of edges is  $2g + \ell(\mu) - 1$  which matches the expected dimension. For quadratic strata, first orient all edges in a polygon presentation such that the interior of the polygon is to the left. These define complex numbers  $v_1, \dots, v_k$  such that  $v_1 + \dots + v_k = 0$  and  $v_{\sigma(i)} = \pm v_i$  for some permutation  $\sigma$ . If two edges are glued by translation, then  $v_{\sigma(i)} = -v_i$ . Such edges can vary freely without being constrained by the relation  $v_1 + \dots + v_n = 0$ . Since we work with non-square quadratic differentials, there exist two edges glued by a half-translation. That is  $v_{\sigma(i)} = v_i$  for some  $i$  and so it is determined by all other edges. Indeed,  $v_1 + \dots + \hat{v}_i + \dots + \hat{v}_{\sigma(i)} + \dots + v_n = -2v_i$  so, we lose one complex parameter giving us  $2g + \ell(\mu) - 2$ .

**Definition 2.21.** The *principal stratum* is the unique stratum of largest dimension. In  $\mathcal{H}_g$ , it is given by  $\mathcal{H}(1^{2g-2})$  with dimension  $4g-3$ . In  $\mathcal{Q}_{g,n}$ , it is given by  $\mathcal{Q}(-1^n, 1^{4g-4+n})$  with dimension  $6g-6+2n$ .

Principal strata in fact form dense and open subsets in their respective moduli space of Abelian or quadratic differentials. We have already described openness preceding the definition of strata - small perturbations to the edges of a translation surface preserve the singularity degrees. Density follows from Proposition 2.8 - for any translation surface, we split higher order zeros to simple zeros, giving us a sequence of differentials in the principal strata that converge to the given translation surface. Therefore, the dimension of  $\mathcal{H}_g$  and  $\mathcal{Q}_{g,n}$  coincides with the dimension of their principal strata.

We now introduce a classical object of study in geometry, the moduli space of complex curves. It is closely related to the moduli space  $\mathcal{H}_g$  and  $\mathcal{Q}_{g,n}$  previously defined.

**Definition 2.22.** The moduli space  $\mathcal{M}_{g,n}$  is the space of isomorphism classes of genus  $g$  Riemann surfaces with  $n$  distinct labelled marked points. If there are no markings, we write  $\mathcal{M}_g = \mathcal{M}_{g,0}$ .

**Theorem 2.10.** *The complex dimension of  $\mathcal{M}_{g,n}$  is  $3g-3+n$ .*

Details for the proof can be found in [Jo, Section 4.3] or which proves the result on Teichmuller space, or [Al, Theorem 5.4.14] for an algebraic proof. A rough idea for this dimension found is as follows. First use the fact that any Riemann surface in  $\mathcal{M}_g$  with  $g \geq 2$  can be equipped with a unique hyperbolic metric. Decompose the surface into  $2g-2$  pairs of pants by cutting along  $3g-3$  simple closed geodesics. The hyperbolic metric on a pair of pants is uniquely determined by the length of its boundary components. Gluing the pair of pants together, we have  $3g-3$  choices of length parameters, and an additional  $3g-3$  twist parameters. These  $6g-6$  real parameters are called *Fenchel-Nielsen coordinates* which gives us the  $3g-3$  complex dimensions. Finally, each marked point adds an additional complex dimension.

The moduli space  $\mathcal{H}_g$  is in fact a holomorphic vector bundle of rank  $g$  over  $\mathcal{M}_g$ , also known as the *Hodge bundle*. The bundle projection  $\mathcal{H}_g \rightarrow \mathcal{M}_g$  simply forgets the Abelian differential and remembers only the complex curve. The fibre over a curve  $X \in \mathcal{M}_g$  is the space of holomorphic one-forms on  $X$  given by  $H^0(X, K_X)$ . It is well known that this space is  $g$  dimensional, see [Fo, Remark 17.10]. Thus, we can deduce from Theorem 2.10 that the dimension of  $\mathcal{H}_g$  is  $4g - 3$  which matches the dimension of the principal stratum as expected. Similarly, the moduli space  $\mathcal{Q}_{g,n}$  is a holomorphic vector bundle over  $\mathcal{M}_{g,n}$ . The bundle projection forgetting the quadratic differential and the fibre over a curve  $(X, p_1, \dots, p_n) \in \mathcal{M}_{g,n}$  is the space of meromorphic quadratic differentials with simple poles at  $p_1, \dots, p_n$ . What is interesting in the quadratic case is the following result.

**Theorem 2.11** ([Jo, Corollary 5.4.2]). *There is a natural vector bundle isomorphism  $\mathcal{Q}_{g,n} \cong T^*\mathcal{M}_{g,n}$ . In particular, there is an isomorphism of vector spaces*

$$T_{[(X, p_1, \dots, p_n)]}^*\mathcal{M}_{g,n} \cong H^0(X, K_X^{\otimes 2}(p_1 + \dots + p_n)).$$

Thus, the dimension of  $\mathcal{Q}_{g,n}$  is  $6g - 6 + 2n$  which is twice the dimension of  $\mathcal{M}_{g,n}$ , matching the dimension of the principal stratum. This provides another way to verify the dimension of  $\mathcal{Q}(\mu)$ , since merging two singularities drops the dimension by 1.

We will only consider the moduli spaces  $\mathcal{M}_{g,n}$  satisfying the condition  $2g+n-2 > 0$ , called the *stability condition*. This ensures the curves have finite automorphism group, so the moduli space can be endowed with a complex orbifold structure, see for instance [Mi95, pp. III.3, VII.1] and [Si09, p. III.10]. Moreover, enforcing the stability condition allows us to compactify the moduli space, which are in general non-compact, giving us the space  $\overline{\mathcal{M}}_{g,n}$  called the Deligne-Mumford compactification. This is done by adding in points called *stable curves*, which are curves with nodal singularities corresponding to certain degenerations. This compactification is again a complex orbifold, see [HM98, Chapter 4] and [Zvo, Chapter 1] for detailed constructions. Considering the compactified moduli space is desirable for studying them using geometric tools, such as intersection theory in Chapter 4. Some small examples of  $\mathcal{M}_{g,n}$  and  $\overline{\mathcal{M}}_{g,n}$  are provided in Appendix B.

## 2.3 Period and cohomological coordinates

In this section, we construct local coordinate charts on strata which are used to define a measure. We have loosely described coordinates on strata as the complex numbers defining the edges in a polygon presentation of a flat surface. Recovering these complex numbers is done by integrating the differential over certain homology cycles.

**Construction in Abelian strata:** Fix an Abelian differential  $(X, \omega) \in \mathcal{H}(\mu_1, \dots, \mu_m)$  and let  $\Sigma$  denote the set of zeros of  $\omega$ . Consider the first relative homology group  $H_1(X, \Sigma; \mathbb{Z})$  which fits into the long exact sequence

$$0 \rightarrow H_1(X; \mathbb{Z}) \rightarrow H_1(X, \Sigma; \mathbb{Z}) \rightarrow H_0(\Sigma; \mathbb{Z}) \rightarrow H_0(X; \mathbb{Z}) \rightarrow 0.$$

This reduces to a short exact sequence

$$0 \rightarrow \mathbb{Z}^{2g} \rightarrow H_1(X, \Sigma; \mathbb{Z}) \rightarrow \mathbb{Z}^{m-1} \rightarrow 0$$

giving us  $H_1(X, \Sigma; \mathbb{Z}) \cong \mathbb{Z}^{2g+m-1}$ . Choose a basis  $[\gamma_1], \dots, [\gamma_{2g+m-1}]$  for this relative homology group. The representatives of each class are paths on  $X$  starting and ending at the zeros  $\Sigma$ . In a local coordinate, we have  $\omega = dz$  and integrating against along the paths  $\gamma_i$  recovers the complex numbers joining two vertices in the polygon representation. Note that only under an appropriate basis do these complex numbers represent the edges, and a change of basis corresponds to a series of cut and paste operations on the polygon. We now define a local chart in the stratum around  $(X, \omega)$  by

$$\Phi : U \subseteq \mathcal{H}(\mu) \rightarrow \mathbb{C}^{2g+m-1}, (X', \omega') \mapsto \left( \int_{\gamma_i} \omega' \right)_{i=1}^{2g+m-1}.$$

The complex numbers  $\Phi(X, \omega)$  are called the *period coordinates* of  $(X, \omega)$  and  $\Phi$  is called the *period map*. It is well-known that the period map provides local coordinates in a stratum. The proof is rather technical and the details can be found in [FoMa, Section 2.3]. One can also define a local chart into the first relative cohomology  $H^1(X, \Sigma; \mathbb{C})$  called *cohomological coordinates* by considering the map

$$\Psi : U \subseteq \mathcal{H}(\mu) \rightarrow H^1(X, \Sigma; \mathbb{C}), (X', \omega') \mapsto \left( [\gamma] \mapsto \int_{\gamma} \omega' \right).$$

The cohomological perspective is useful since it is canonical, that is, it does not depend on the choice of a basis of relative cycles.

Using these coordinates, we can define a natural linear measure on the stratum  $\mathcal{H}(\mu)$ , called the *Masur-Veech measure*. Let  $\lambda$  be the standard Lebesgue measure on  $\mathbb{C}^{2g+m-1}$ . Define a measure  $\nu$  on  $\mathcal{H}(\mu)$  by pulling back  $\lambda$  along the period map, that is, for any Borel measurable set  $A \subseteq U$ , we set  $\nu(A) = \lambda(\Phi(A))$ . This measure is well-defined since the change of basis matrix for  $H_1(X, \Sigma; \mathbb{Z})$  is an element in  $GL_{2g+m-1}(\mathbb{Z})$  which has unit determinant.

We can also define the Masur-Veech measure in cohomological coordinates. First note that every finite dimensional vector space admits a linear (translation invariant) measure  $\lambda$  that is unique up to scaling. To fix this scale, we identify an integer lattice  $\Lambda$  in  $H^1(X, \Sigma, \mathbb{C})$  and normalise  $\lambda$  so that the fundamental domain of  $\Lambda$  has unit volume. The lattice  $\Lambda$  corresponds to surfaces with periods lying in  $\mathbb{Z} \oplus i\mathbb{Z}$ , in particular, it is the lattice of square-tiled surfaces. Given more precisely, it is the subset of linear forms in  $H^1(X, \Sigma; \mathbb{C})$  taking values in  $\mathbb{Z} \oplus i\mathbb{Z}$  on  $H_1(X, \Sigma; \mathbb{Z})$ . The measure  $\nu$  on  $\mathcal{H}(\mu)$  is again given by pulling back  $\lambda$ , that is,  $\nu(A) = \lambda(\Psi(A))$ . This is equivalent to the measure defined using period coordinates since the lattice  $\Lambda$  corresponds to differentials  $(X, \omega)$  such that  $\Phi(X, \omega) \in (\mathbb{Z} \oplus i\mathbb{Z})^{2g+m-1}$  which has covolume 1 in  $\mathbb{C}^{2g+m-1}$ .

**Construction in quadratic strata:** Fix a quadratic differential  $(X, q) \in \mathcal{Q}(\mu)$ . To mimic the constructions from Abelian strata, one would like to integrate  $\sqrt{q}$  over a basis of first relative homology, however,  $q$  is not a global square. Geometrically, there exist edges in the flat representation of  $q$  that appear in opposite directions, so we cannot construct a well-defined period map using  $q$ . To resolve this issue, we pass to the canonical double cover  $(\widehat{X}, \widehat{\omega}^2)$  using Proposition A.1 where the induced quadratic differential is a global square, and repeat the construction from the Abelian case. By Proposition A.2, the induced involution  $\tau$  on the double cover acts on the differential  $\widehat{\omega}$  by  $\tau^* \widehat{\omega} = -\widehat{\omega}$ . Therefore, the differentials in  $H^1(\widehat{X}, \widehat{\Sigma}; \mathbb{C})$  that come from a quadratic differential downstairs lie in the  $(-1)$ -eigenspace of  $\tau^*$ , which we denote by  $H_-^1(\widehat{X}, \widehat{\Sigma}; \mathbb{C})$  where  $\widehat{\Sigma}$  are the zeros of the induced differential  $\widehat{\omega}$ . Thus, the local cohomological coordinates of  $\mathcal{Q}(\mu)$  around  $(X, q)$  is given by

$$\Psi : U \subseteq \mathcal{Q}(\mu) \rightarrow H_-^1(\widehat{X}, \widehat{\Sigma}; \mathbb{C}), (X', q') \mapsto \left( [\gamma] \mapsto \int_{\gamma} \widehat{\omega}' \right).$$

Dually, by considering the  $(-1)$ -eigenspace  $H_1^-(\widehat{X}, \widehat{\Sigma}; \mathbb{C})$  of  $\tau_*$ , it is also possible to define period coordinates in the quadratic setting using the map

$$\Phi : U \subseteq \mathcal{Q}(\mu) \rightarrow \mathbb{C}^{2g+m-2}, (X', q') \mapsto \left( \int_{\gamma_i} \widehat{\omega} \right)_{i=1}^{2g+m-2}$$

where  $[\gamma_1], \dots, [\gamma_{2g+m-2}]$  is a basis of  $H_1^-(\widehat{X}, \widehat{\Sigma}; \mathbb{C})$ . Under an appropriate basis, the complex numbers  $\Phi(X, q)$  correspond to the complex numbers defining the edges in a polygon presentation of the double cover that come from the edges of  $(X, q)$ .

The Masur-Veech measure on  $\mathcal{Q}(\mu)$  is defined identically to the Abelian case on the double cover. That is, we choose the lattice  $\Lambda$  of forms in  $H_-^1(\widehat{X}, \widehat{\Sigma}; \mathbb{C})$  that take values in  $\mathbb{Z} \oplus i\mathbb{Z}$  on  $H_1^-(\widehat{X}, \widehat{\Sigma}; \mathbb{Z})$  and normalise the linear measure in  $H_-^1(\widehat{X}, \widehat{\Sigma}; \mathbb{C})$  such that the fundamental domain of  $\Lambda$  has unit volume. The lattice  $\Lambda$  contains Abelian square-tiled surfaces that are double covers of a quadratic differential. Since the double cover doubles the length of periods in certain directions, the corresponding quadratic differentials are square-tiled surfaces tiled from squares of size  $(1/2 \times 1/2)$ .

# Chapter 3

## Masur-Veech Volumes

We now turn to the main topic of this thesis: the computation of volumes of the moduli space  $\mathcal{Q}_{g,n}$  and its strata. Several approaches by different authors have been developed to compute these volumes over the past three decades. Zorich in [Zo] first obtained explicit values in low dimension strata by directly counting square-tiled surfaces. Eskin and Okounkov in [EO] counted square-tiled surfaces by enumerating branched covers of the torus, which can be encoded using permutations in  $S_n$ . Using the representation theory of  $S_n$ , they collected these counts into a generating function

$$\sum_{N=1}^{\infty} q^N \sum_{\substack{X \in \mathcal{H}(\mu) \\ \text{square-tiled} \\ \text{with } N \text{ squares}}} \frac{1}{|\text{Aut}(X)|}$$

and proved it was a quasi-modular form, expressible as a polynomial in the Eisenstein series  $G_2(q)$ ,  $G_4(q)$  and  $G_6(q)$ . This provided an efficient algorithm to compute volumes. These techniques were later extended to quadratic strata in [EO2] and implemented up to strata of dimension 12 in [Go], although the algorithm is computationally inefficient. The Eskin and Okounkov method provides us with the following result.

**Theorem 3.1.** *The Masur-Veech volume of a stratum  $\mathcal{H}(\mu)$  resp.  $\mathcal{Q}(\mu)$  is a rational multiple of  $\pi^{2g}$  resp.  $\pi^{2(\hat{g}-g)}$ . Here,  $\hat{g}$  is the genus of the double cover, see Remark A.6.*

An open problem is to find formulas for volumes of any stratum. Kontsevich conjectured a formula in genus 0 quadratic strata which was proven in [AEZ2] by expressing volumes in terms of Siegel-Veech constants, which are known in genus 0. Volumes of special series of strata and their connected components were found in [Go]. There have been a number of other methods, for example, using linear Hodge integrals in [CMS2]. We will use a geometric approach, following the ideas from [AEZ2], [Go], [DGZZ1] and work with quadratic strata. In high-dimensional strata, this method becomes very inefficient for computations, although provides insights into the volume contributions of certain types of flat surfaces.

### 3.1 Counting square-tiled surfaces

In this section, we define the Masur-Veech volume and reduce the computation to a counting problem. Each stratum contains a lattice of square-tiled surfaces, and counting these lattice points under a finer mesh will recover the volume in the limit. This mimics the Riemann sum construction. The total measure of any Abelian or quadratic stratum is infinite, since a differential can be rescaled arbitrarily. However, the Masur-Veech measure induces a finite measure on the level hypersurface of differentials of fixed finite area, which is a result proved independently by Masur [Ma] and Veech [Ve]. We will define the Masur-Veech volume of a stratum to be the corresponding induced volume on the level hypersurface of differentials with area 1 for the Abelian case, and area  $1/2$  for the quadratic case. Recall that quadratic strata are modelled on a double cover, so the convention to use the area  $1/2$  hypersurface is so the double cover has area 1. For an Abelian and quadratic differential  $(X, \omega)$  and  $(X, q)$ , the area is given by

$$\text{Area}(X, \omega) = \frac{i}{2} \int_X \omega \wedge \bar{\omega} \quad \text{and} \quad \text{Area}(X, q) = \int_X |q|.$$

Given a stratum  $\mathcal{H}(\mu)$  or  $\mathcal{Q}(\mu)$  and  $a > 0$ , define the following level hypersurfaces:

$$\begin{aligned} \mathcal{H}_a(\mu) &= \{(X, \omega) \in \mathcal{H}(\mu) : \text{Area}(X, \omega) = a\} \\ \mathcal{Q}_a(\mu) &= \{(X, q) \in \mathcal{Q}(\mu) : \text{Area}(X, q) = a/2\}. \end{aligned}$$

We also have a natural scaling action on  $\mathcal{H}(\mu)$  and  $\mathcal{Q}(\mu)$  given respectively by  $r \cdot (X, \omega) = (X, r\omega)$  and  $r \cdot (X, q) = (X, r^2q)$ . For what follows, we present the formulation of Masur-Veech volumes for Abelian strata. The construction is identical for quadratic strata by making the obvious replacements. Every  $(X, \omega) \in \mathcal{H}(\mu)$  can be represented as  $r \cdot (X_1, \omega_1)$  for some  $(X_1, \omega_1) \in \mathcal{H}_1(\mu)$  and  $r \in \mathbb{R}^+$ . This action also rescales the area by a squared factor, that is,

$$r \cdot \mathcal{H}_a(\mu) = \mathcal{H}_{r^2a}(\mu).$$

Let  $d\nu$  denote the volume element induced by the Masur-Veech measure. The volume element  $d\nu_1$  on the level hypersurface  $\mathcal{H}_1(\mu)$  is then defined by

$$d\nu = r^{2d-1} dr d\nu_1$$

where  $2d = \dim_{\mathbb{C}} \mathcal{H}(\mu) = 2 \dim_{\mathbb{R}} \mathcal{H}(\mu)$ . The total volume of  $\mathcal{H}(\mu)$  is then given by

$$\text{Vol } \mathcal{H}(\mu) = \int_{\mathcal{H}_1(\mu)} d\nu_1.$$

We aim to compute volumes using a lattice point counts so it is useful to rewrite the induced volume of the hypersurface in terms of a volume in the original stratum. Define the cone of a subset  $E \subseteq \mathcal{H}(\mu)$  to be

$$C(E) = \{r \cdot (X, \omega) \mid r \in (0, 1], (X, \omega) \in E\}.$$

The volume of the cone of the hypersurface can be expressed as

$$\nu(C(\mathcal{H}_1(\mu))) = \int_{C(\mathcal{H}_1(\mu))} d\nu = \int_0^1 r^{2d-1} dr \int_{\mathcal{H}_1(\mu)} d\nu_1 = \frac{1}{2d} \cdot \text{Vol } \mathcal{H}(\mu). \quad (3.1)$$

The volume can also be computed by considering the limit of Riemann sums under an appropriate normalisation. Denote the union of all differentials in  $\mathcal{H}(\mu)$  corresponding to a lattice point of  $\Lambda$  in local cohomological coordinates by  $\mathcal{L}$ . In particular,  $\mathcal{L}$  consists of all square-tiled surfaces in the stratum. Define the set of square-tiled surfaces in  $\mathcal{H}(\mu)$  constructed from at most  $N$  unit squares by  $\mathcal{ST}(\mathcal{H}(\mu), N)$ .

Consider scaling down the lattice  $\mathcal{L}$  to obtain a finer lattice  $\varepsilon\mathcal{L}$  where  $0 < \varepsilon \leq 1$  and  $\varepsilon^{-1} \in \mathbb{N}$  so that  $\mathcal{L}$  is an  $\varepsilon^{-2d}$ -index sublattice of  $\varepsilon\mathcal{L}$ . Recall from Section 2.3 that the measure  $\nu$  is defined such that in a local neighbourhood of a point  $(X, \omega) \in \mathcal{H}(\mu)$ , the fundamental domain of the lattice  $\Lambda$  has volume 1. We observe that  $(X, \omega)$  is a point in the  $\varepsilon\mathcal{L}$  lattice if and only if  $\varepsilon^{-1} \cdot (X, \omega)$  is a point in the  $\mathcal{L}$  lattice. To compute the volume of the cone  $C(\mathcal{H}_1(\mu))$ , we take the Riemann integral of the characteristic function over this subset. Rewriting in terms of Riemann sums, we count the number of points in the cone that lie in  $\varepsilon\mathcal{L}$  and multiply by the covolume of this lattice. Therefore, the volume of the cone can be expressed as

$$\begin{aligned} \nu(C(\mathcal{H}_1(\mu))) &= \int_{\mathcal{H}(\mu)} \chi_{C(\mathcal{H}_1(\mu))} d\nu \\ &= \lim_{\varepsilon \rightarrow 0} \sum_{(X, \omega) \in \varepsilon\mathcal{L}} \chi_{C(\mathcal{H}_1(\mu))}((X, \omega)) \varepsilon^{2d} \\ &= \lim_{\varepsilon \rightarrow 0} \varepsilon^{2d} \cdot \#(\varepsilon\mathcal{L} \cap C(\mathcal{H}_1(\mu))) \\ &= \lim_{\varepsilon \rightarrow 0} \varepsilon^{2d} \cdot \#(\mathcal{L} \cap C(\mathcal{H}_{\varepsilon^{-2}}(\mu))) \\ &= \lim_{N \rightarrow \infty} \frac{1}{N^d} \cdot \#\mathcal{ST}(\mathcal{H}(\mu), N). \end{aligned} \quad (3.2)$$

Combining the above results, the Masur-Veech volume of a stratum  $\mathcal{H}(\mu)$  can be expressed in terms of the asymptotics of counts of squared tiled surface as

$$\text{Vol } \mathcal{H}(\mu) = 2d \lim_{N \rightarrow \infty} \frac{1}{N^d} \cdot \#\mathcal{ST}(\mathcal{H}(\mu), N). \quad (3.3)$$

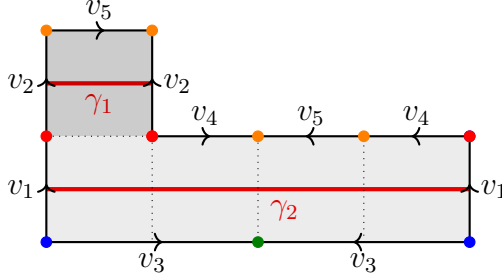
For quadratic strata, the integer lattice chosen in cohomological coordinates corresponds to square-tiled surfaces constructed from squares of size  $(1/2 \times 1/2)$ . Therefore, such a surface in  $\mathcal{Q}_N(\mu)$  of area  $N/2$  is built from  $2N$  squares, giving us the expression

$$\text{Vol } \mathcal{Q}(\mu) = 2d \lim_{N \rightarrow \infty} \frac{1}{N^d} \cdot \#\mathcal{ST}(\mathcal{Q}(\mu), 2N). \quad (3.4)$$

The remainder of this chapter develops the techniques to evaluate  $\#\mathcal{ST}(\mathcal{Q}(\mu), 2N)$  allowing us to compute volumes of quadratic strata. We will not pursue the computation of Abelian strata. We refer the interested reader to [Zo2] where direct counts of square-tiled surfaces are computed for low dimensional Abelian strata.

## 3.2 Stable graphs

Computing the count  $\#\mathcal{ST}(\mathcal{Q}(\mu), 2N)$  directly is difficult. The problem becomes much more tractable by considering square-tiled surfaces of a fixed type, given by a *stable graph*  $\Gamma$ . We will denote this subset of square-tiled surfaces by  $\mathcal{ST}_\Gamma(\mathcal{Q}(\mu), 2N)$ . Consider the following square-tiled surface in the principal stratum  $\mathcal{Q}(-1^2, 1^2)$ .



The horizontal cylinder decomposition consists of two cylinders glued onto two singular layers. We will see in Section 3.3 that these singular layers correspond to ribbon graphs. We wish to encode the decomposition into cylinders and the attachments onto each singular layer. This data can be encapsulated by a stable graph, for which we now provide a formal construction.

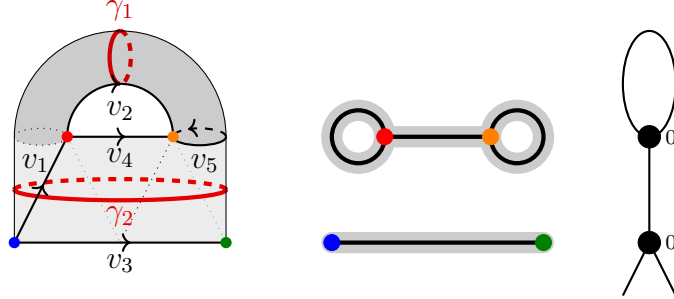


Figure 3.1: The horizontal cylinder decomposition after folding up a square-tiled surface, its singular layers, and associated stable graph.

Let  $S$  be the underlying topological surface of a square-tiled surface  $(X, q)$  and let  $S = \bigsqcup_{j=1}^M \text{cyl}_j \sqcup G$  be its cylinder decomposition. Associate to each cylinder  $\text{cyl}_j$  a waist curve  $\gamma_j$  and let  $\gamma = \bigsqcup_{j=1}^M \gamma_j$ . Consider the decomposition  $S \setminus \gamma = \bigsqcup_{i=1}^N S_i$  into connected components where each  $S_i$  is disjoint. We observe that every singular layer corresponds to a deformation retract of a connected component  $S_i$ . Moreover, a boundary of a cylinder in the cylinder decomposition glues to a singular layer if and only if the corresponding waist curve of the cylinder shares a boundary with the connected component that deformation retracts onto the singular layer. The stable graph  $\Gamma$  of  $S$  is the decorated dual graph associated to the decomposition  $S \setminus \gamma$  constructed as follows:

1. Assign a vertex  $v_i$  to each connected component  $S_i$  and decorate by the genus  $g_{v_i} = g(S_i)$  of the component  $S_i$ .
2. Assign an edge  $b_j$  to each component  $\gamma_j$  of  $\gamma$ . If  $\gamma$  is the boundary of a component of  $S_i$ , then  $b_j$  is adjacent to  $v_i$ . If  $\gamma_j$  shares the same component of  $S_i$  on each side, then  $b_j$  is a loop at  $v_i$ .
3. Assign a leg  $b_p$  adjacent to  $b_i$  to each marked point  $p \in S_i$ .

This is equivalent to assigning to each singular layer a vertex and each cylinder an edge. The incidence relations between edges and vertices encode which boundaries of each cylinder glue onto the singular layers. The genus decoration of a vertex corresponds to the genus of the singular layer, which we will make precise in Section 3.3. We will now provide a formal definition of a stable graph, its isomorphisms, and set of isomorphism classes.

**Definition 3.1.** A *stable graph* is the data  $\Gamma = (V, H, \iota, \alpha, \mathbf{g}, L)$  where

- $V$  is a finite set of *vertices*. We may also denote this set by  $V(\Gamma)$ ;
- $H$  is a finite set of *half-edges*;
- $\iota : H \rightarrow H$  is an involution. The 2-cycles are called the *edges* and the fixed points are called *legs*. Denote the set of edges by  $E(\Gamma)$  and the set of legs by  $l(\Gamma)$ ;
- $\alpha : H \rightarrow V$  is the attaching map. Denote the number of full-edges incident to  $v$  by  $n_v$  and the number of legs incident to  $v$  by  $p_v$ . The *valence* of a vertex  $v$  is the number of half-edges incident to  $v$  given by  $\#\alpha^{-1}(v) = n_v + p_v$ ;
- $\mathbf{g} = \{g_v\}_{v \in V(\Gamma)}$  is a set of nonnegative numbers. We call  $g_v$  the *genus decoration* at the vertex  $v$ . Moreover, it satisfies the stability condition  $2g_v - 2 + n_v > 0$ .
- $L : l(\Gamma) \rightarrow \{1, \dots, n\}$  is a bijection labelling the legs.

**Remark 3.2.** Stable graphs also encode boundary classes in the Deligne-Mumford compactification  $\overline{\mathcal{M}}_{g,n}$ . Pinching the underlying surface along the waist curves produces a stable curve. The vertices correspond to irreducible components labelled by the genus and the edges correspond to nodes connecting the components. The legs correspond to marked points. Each irreducible component is stable, suggesting the stability condition at each vertex in the stable graph. Additionally, there is a stratification of the Deligne-Mumford compactification  $\overline{\mathcal{M}}_{g,n}$  by stable graphs given by  $\overline{\mathcal{M}}_{g,n} = \bigsqcup_{\Gamma \in \mathcal{G}_{g,n}} \mathcal{M}_\Gamma$  where  $\mathcal{M}_\Gamma = \prod_{v \in V(\Gamma)} \mathcal{M}_{g_v, n_v}$ .

**Definition 3.3.** The *genus* of a stable graph is the number  $g(\Gamma) = h_1(\Gamma) + \sum_{v \in V} g_v$  where  $h_1(\Gamma)$  denotes the first Betti number of  $\Gamma$ . In particular,  $h_1$  is the number of edges that form a loop at a vertex and is given by  $h_1(\Gamma) = \#E(\Gamma) - \#V(\Gamma) + 1$ .

Note that the genus of  $\Gamma$  coincides with the genus of the underlying surface.

**Definition 3.4.** Two stable graphs  $\Gamma = (V, H, \iota, \alpha, \mathbf{g}, L)$  and  $\Gamma' = (V', H', \iota', \alpha', \mathbf{g}', L')$  are *isomorphic* if there is a pair of bijections  $\phi : V \rightarrow V'$  and  $\psi : H \rightarrow H'$  such that

- half-edge pairings are preserved:  $\iota' \circ \psi = \psi \circ \iota$ ;
- genus decorations are preserved:  $g'_{\phi(v)} = g_v$ ;
- leg labelings are preserved:  $L' \circ \psi = L$ .

Each vertex in a stable graph represents a singular layer of the cylinder decomposition of a square-tiled surface which contains the zeros and poles of the differential. The zeros and poles induce fixed valences on the vertices of the singular layer which we will record in a partition  $\kappa$ . The partition  $\kappa$  associated to a stratum  $\mathcal{Q}(\mu)$  is given by  $\kappa_i = \mu_i$  by the discussion above Section 2.1. The partition  $\kappa$  must also be compatible with the genus decoration and valences of the corresponding vertex in the stable graph, which will be explained in Remark 3.17. This motivates the following definition.

**Definition 3.5.** A *decorated stable graph* is a pair  $(\Gamma, \kappa)$  where

- $\Gamma$  is a stable graph;
- $\kappa = \{\kappa_{(v)}\}_{v \in V(\Gamma)}$  is a set of partitions indexed over vertices of  $\Gamma$ ;
- $\kappa_{(v)}$  satisfies  $|\kappa_{(v)}| - 2\ell(\kappa_{(v)}) = 4g_v - 4 + 2n_v$  and  $\lambda_1(\kappa_{(v)}) = p_v$  at each vertex  $v$ .

The concatenation  $\kappa = \cup_{v \in V(\Gamma)} \kappa_{(v)}$  of partitions is called the *total decoration* of  $(\Gamma, \kappa)$ . An *isomorphism* of decorated stable graphs  $(\Gamma, \kappa)$  and  $(\Gamma', \kappa')$  is an isomorphism of stable graphs  $(\phi, \psi) : \Gamma \rightarrow \Gamma'$  such that  $\kappa'_{(\phi(v))} = \kappa_{(v)}$ .

**Definition 3.6.** The set of isomorphism classes of stable graphs is denoted by  $\mathcal{G}_{g,n}$ . The set of isomorphism classes of *unlabelled* stable graphs is given by  $\mathcal{G}_{g,n}/S_n$  where  $S_n$  acts by permuting the legs. We denote the size of the orbit of this action by  $n_\Gamma$ . We also define the subsets  $\mathcal{G}_{g,n}(k)$  consisting of stable graphs with  $k$  edges. For decorated stable graphs with total decoration  $\kappa$ , similar definitions follow for  $\mathcal{G}_{g,n}^\kappa$ .

We also denote the automorphism group of a stable graph  $\Gamma$  by  $\text{Aut}(\Gamma)$ . We will be interested in knowing the number  $|\text{Aut}(\Gamma)|$  in volume computations. Once we are able to compute the counts  $\#\mathcal{ST}_\Gamma(\mathcal{Q}(\mu), 2N)$  for all appropriate stable graphs, we can add the contributions to recover the count  $\#\mathcal{ST}(\mathcal{Q}(\mu), 2N)$ . In particular, we can define

$$\text{Vol}(\Gamma) = 2d \lim_{N \rightarrow \infty} \frac{1}{N^d} \cdot \#\mathcal{ST}_\Gamma(\mathcal{Q}(\mu), 2N) \quad (3.5)$$

to be the volume contribution from square-tiled surfaces of type  $\Gamma$ , and the original volume is recovered by

$$\text{Vol } \mathcal{Q}(\mu) = \sum_{\Gamma \in \mathcal{G}_{g,n}^\kappa} \text{Vol}(\Gamma). \quad (3.6)$$

### 3.3 Ribbon graphs

For a square tiled surface with associated stable graph  $\Gamma$ , a vertex  $v \in V(\Gamma)$  represents a singular layer and the valence  $n_v$  is the number of cylinder boundaries glued to the singular layer. A cylinder may have both boundaries attached to the same singular layer, in which case, the corresponding edge in  $\Gamma$  forms a loop at a vertex as in Figure 3.2. In this section, we count the number of ways to attach cylinders of fixed circumferences onto a singular layer. This corresponds to fixing the boundary lengths of a singular layer, and counting the number of positive integer metrics. The idea of a singular layer is made precise using ribbon graphs, which are graphs endowed with the extra structure of a cyclic ordering at the vertices.

**Definition 3.7.** A *ribbon graph* is the data  $G = (X, \tau_0, \tau_1)$  where

- $X$  is a finite set of *half-edges*;
- $\tau_0 : X \rightarrow X$  is a permutation. This defines the set of vertices  $V(G) = X/\langle \tau_0 \rangle$ . The *valence* of a vertex is the length of the corresponding cycle.
- $\tau_1 : X \rightarrow X$  is an involution with no fixed points. This pairs half-edges into edges and defines the set of edges  $E(G) = X/\langle \tau_1 \rangle$ .

Moreover,  $\tau_2 := \tau_0\tau_1$  defines a “walk” along the edges respecting the cyclic ordering at vertices. The boundary set is given by  $F(G) = X/\langle \tau_2 \rangle$ . For a half-edge  $x \in X$ , we also denote by  $[x]_i$  for  $i = 0, 1, 2$  the image of  $x$  under the projection  $X \rightarrow X/\langle \tau_i \rangle$ .



Figure 3.2: The “theta” and “twisted theta” graphs are isomorphic as graphs but non-isomorphic as ribbon graphs. The cyclic ordering of half-edges at each vertex is given by the projection onto the plane.

**Remark 3.8.** We can endow a ribbon graph with an orientation by defining the cyclic ordering at each vertex to be anticlockwise in the planar projection. Thus, a ribbon graph defines an embedding of a graph onto an orientable surface. The genus of the ribbon graph coincides with the minimal genus surface for which the graph can be embedded. Explicitly, it is the integer  $g$  such that  $2k - 2g = \#V(G) - \#E(G) + \#F(G)$  where  $k$  is the number of connected components. A genus 0 ribbon graph can be embedded in a sphere, so after removing a point, we have an embedding into space homeomorphic to  $\mathbb{R}^2$ . Therefore, genus 0 ribbon graphs are equivalent to planar graphs.

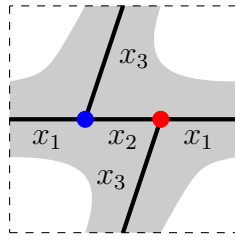


Figure 3.3: An embedding of  $G_{\tilde{\Theta}}$  into genus 1 surface with one boundary component.

**Definition 3.9.** A *labelled ribbon graph* is a pair  $(G, L)$  where  $G$  is a ribbon graph and  $L$  is a bijection  $L : F(G) \rightarrow \{1, \dots, n\}$  labelling the boundary components.

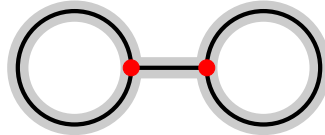
From now on, we will only consider labelled ribbon graphs. We will refer to them simply as ribbon graphs.

**Definition 3.10.** Two ribbon graphs  $G = (X, \tau_0, \tau_1, L)$  and  $G' = (X', \tau'_0, \tau'_1, L')$  are *isomorphic* if there is a bijection  $\phi : X \rightarrow X'$  such that:

- half-edge cycles are preserved:  $\tau'_0 \circ \phi = \phi \circ \tau_0$ ;
- half-edge pairings are preserved:  $\tau'_1 \circ \phi = \phi \circ \tau_1$ ;
- boundary labellings are preserved:  $L' \circ \phi_2 = L$  where  $\phi_2$  is the induced map under the quotient  $X \rightarrow X/\langle \tau_2 \rangle$ .

In Figure 3.3, there is only one possible labelling on  $G_{\tilde{\Theta}}$ . In fact,  $G_{\Theta}$  also admits one unique labelling, since all labellings are isomorphic. This can be seen by embedding  $G_{\Theta}$  onto the sphere.

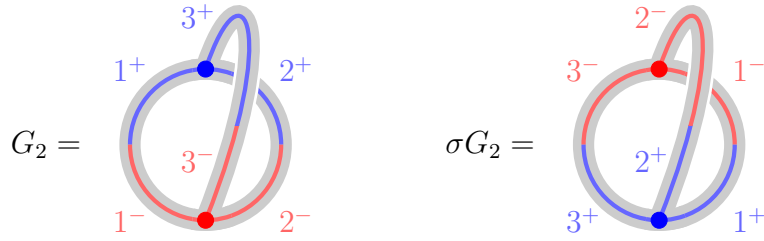
**Example 3.11.** Consider the following unlabelled genus 0 “dumbbell” ribbon graph. There are three possible labellings up to isomorphism. For use in Example 3.22, we will refer to these ribbon graphs by  $G_i$  for  $i = 1, 2, 3$  where  $G_i$  is the ribbon graph with the outer boundary labelled by  $i$ .



**Remark 3.12.** Given a ribbon graph  $G$ , we will be interested in computing the order of the automorphism group  $\text{Aut}(G)$ . Here we will provide a rough bound. An automorphism  $g \in \text{Aut}(G)$  is a permutation of half-edges such that  $g$  commutes with  $\tau_0$  and  $\tau_1$  so  $\text{Aut}(G)$  is a subgroup of the centralisers of  $\tau_0$  and  $\tau_1$ . If a permutation  $\sigma$  has  $m_i$  cycles of length  $i$ , the order of the centraliser  $C_{S_n}(\sigma)$  is  $\prod_i m_i! i^{m_i}$ . Thus, we can deduce that  $|\text{Aut}(G)|$  divides the number

$$\gcd \left( |C_{S_{|X|}}(\tau_0)|, \#E(G)! \cdot 2^{\#E(G)} \right).$$

**Example 3.13.** We show that  $\text{Aut}(G_{\tilde{\Theta}}) \cong \mathbb{Z}_6$  for the twisted theta graph. First, label the six half-edges by  $i^+, i^-$  for  $i = 1, 2, 3$  where  $i^+$  is the half-edge incident to the blue vertex and  $i^-$  is the half-edge incident to the red vertex. Consider the automorphism  $\sigma = (1^+ 3^- 2^+ 1^- 3^+ 2^-)$  which corresponds to a half-rotation. By Remark 3.12,  $|\text{Aut}(G_{\tilde{\Theta}})| \leq \gcd(3^2 2!, 2^3 3!) = 6$  and since  $\sigma$  has order 6 the bound is attained.



**Definition 3.14.** Let  $G$  be a ribbon graph. Enumerate the edges and boundary components by  $E(G) = \{e_1, \dots, e_m\}$  and  $F(G) = \{f_1, \dots, f_n\}$ . For each edge  $e_i$ , let  $x_i \in X$  be a half-edge representative. The *incidence matrix* of  $G$  is an  $m \times n$  matrix  $A_G$  defined by

$$(A_G)_{ij} = \mathbb{1}([x_i]_2 = f_j) + \mathbb{1}([\tau_1 x_i]_2 = f_j)$$

We observe that the sum of every column in an incidence matrix is 2 since

$$((1, \dots, 1) A_G)_i = \sum_{j=1}^n (A_G)_{ij} = \sum_{j=1}^n \mathbb{1}([x_i]_2 = f_j) + \sum_{j=1}^n \mathbb{1}([\tau_1 x_i]_2 = f_j) = 2.$$

**Definition 3.15.** A *metric* on a ribbon graph  $G$  is a length function  $\ell : E(G) \rightarrow \mathbb{R}^+$ . The length function is then defined on boundary components by

$$\ell : F(G) = X/\langle \tau_2 \rangle \rightarrow \mathbb{R}^+, [x]_2 \mapsto \sum_{i=1}^{\# [x]_2} \ell([\tau_2^i x]_1).$$

The matrix  $A_G$  determines a linear map  $\mathbb{R}E(G) \rightarrow \mathbb{R}F(G)$  mapping an edge to the sum of its two incident boundary components. Given a vector  $\mathbf{x} = (x_1, \dots, x_m)^\top \in \mathbb{R}_+^m$  where  $x_i = \ell(e_i)$  is the edge length, the vector  $\mathbf{b} = A_G \mathbf{x} \in \mathbb{R}_+^n$  gives us the resulting lengths  $b_i = \ell(f_i)$  of boundary components. We will be interested in the possible edge length assignments given a fixed boundary length. Thus, for a fixed  $\mathbf{b} \in \mathbb{R}_+^n$ , define the subset

$$P_G(\mathbf{b}) = \{\mathbf{x} \in \mathbb{R}_+^m : A_G \mathbf{x} = \mathbf{b}\}.$$

This set is a convex polytope and describing all metrics on  $G$  with boundary lengths  $\mathbf{b}$ . We wish to count the lattice points in  $P_G(\mathbf{b})$  corresponding to positive integer metrics on  $G$ . Define the number

$$\mathcal{N}_G(\mathbf{b}) = \# P_G(\mathbf{b}) \cap \mathbb{Z}_+^m.$$

It is a piecewise polynomial in the variable  $\mathbf{b}$  and may be 0 on certain subsets. Observe that for  $\mathbf{x} \in \mathbb{Z}_+^m$ , we have

$$\sum_{i=1}^m b_i = (1, \dots, 1)\mathbf{b} = (1, \dots, 1)A_G\mathbf{x} = (2, \dots, 2)\mathbf{x} \in 2\mathbb{Z},$$

in particular,  $\mathcal{N}_G(\mathbf{b})$  is zero whenever  $\sum_{i=1}^m b_i$  is odd. The following elementary result from combinatorics is useful for computing the counts  $\mathcal{N}_G(\mathbf{b})$ .

**Lemma 3.2** (Stars and Bars). *For positive integers  $n$  and  $k$ , the number of tuples  $(x_1, \dots, x_k) \in \mathbb{Z}_+^k$  such that  $x_1 + \dots + x_k = n$  is equal to  $\binom{n-1}{k-1}$ .*

*Proof.* Given  $n$  stars, there are  $n - 1$  possible placements of  $k - 1$  bars to group the stars into  $k$  groups.  $\square$

**Example 3.16.** The incidence matrices from Figure 3.3 are

$$A_{G_1} = \begin{pmatrix} 1 & 1 & 0 \\ 1 & 0 & 1 \\ 0 & 1 & 1 \end{pmatrix}, \quad A_{G_2} = \begin{pmatrix} 2 & 2 & 2 \end{pmatrix}.$$

The matrix  $A_{G_1}$  is full rank hence has a unique solution. A positive solution exists on the cone

$$C_0 = \{(b_1, b_2, b_3) \in \mathbb{R}_+^3 : b_1 + b_2 > b_3, b_1 + b_3 > b_2, b_2 + b_3 > b_1\}.$$

An integer solution exists on the lattice  $\mathbb{L}$  defined by  $b_1 + b_2 + b_3 \in 2\mathbb{Z}$ . Therefore,

$$\mathcal{N}_{G_1}(\mathbf{b}) = \mathbb{1}_{C \cap \mathbb{L}}(\mathbf{b}).$$

Since the lattice condition is always implied for an integer solution, we may omit this detail when writing down the lattice count functions, so  $\mathcal{N}_{G_1}(\mathbf{b}) = 1$  on  $C$ . For  $A_{G_2}$ , points in  $P_{G_2}(b_1)$  satisfy  $x_1 + x_2 + x_3 = b_1/2$ . By the Stars and Bars Theorem, we obtain

$$\mathcal{N}_{G_2}(\mathbf{b}) = \binom{\frac{b_1}{2} - 1}{2} = \frac{(b_1 - 4)(b_1 - 2)}{8}.$$

**Remark 3.17.** The *valence profile* of a ribbon graph  $G$  is a positive partition  $\kappa$  encoding the vertex valences. Observing that  $\ell(\kappa) = \#V(G)$  and  $|\kappa| = 2 \cdot \#E(G)$ , the Euler characteristic gives us  $|\kappa| - 2\ell(\kappa) = 4g - 4 + 2n$  when  $G$  is connected. This condition is sufficient to check that  $\kappa, g, n$  are compatible hand computations

**Definition 3.18.** Denote by  $\mathcal{R}_{g,n}$  the set of isomorphism classes of connected genus  $g$  ribbon graphs with  $n$  boundary components where all vertices have valence at least 3. The subset containing only trivalent ribbon graphs is denoted by  $\mathcal{R}_{g,n}^{\text{tri}}$ . Denote by  $\mathcal{R}_{g,n}^\kappa$  the set of isomorphism classes of connected genus  $g$  ribbon graphs with  $n$  boundary components with valence profile specified by  $\kappa$ . Note that  $\mathcal{R}_{g,n}^\kappa$  is a subset of  $\mathcal{R}_{g,n}$  only when there are no univalent vertices. The valence condition on  $\mathcal{R}_{g,n}$  is to ensure the number of edges is bounded.

**Remark 3.19.** The number  $\mathcal{N}_G(\mathbf{b})$  does not count the number of unique integral metrics on  $G$ , in fact, it overcounts. If there are nontrivial automorphisms of a ribbon graph, two tuples  $\mathbf{x}_1, \mathbf{x}_2 \in \mathbb{R}_+^m$  that are equal up to permutation of their entries may determine the same underlying metric ribbon graph. If we wish to count unique metrics, we will divide the total count  $\mathcal{N}_G(\mathbf{b})$  by  $|\text{Aut}(G)|$ . This will not recover the exact count, for example, if all edges are assigned the same length, we will obtain a fractional count for that metric. However, for the purposes of volume computation, we will be interested in this quantity for large  $\mathbf{b}$  and the set of automorphism-invariant metrics in  $\mathcal{N}_G(\mathbf{b})$  will become negligible. This motivates the following definition.

**Definition 3.20.** The *lattice count function* of genus  $g$  with  $n$  boundary components is the weighted sum

$$\mathcal{N}_{g,n}(\mathbf{b}) = \sum_{G \in \mathcal{R}_{g,n}} \frac{1}{|\text{Aut}(G)|} \mathcal{N}_G(\mathbf{b}).$$

We have an analogous definition for ribbon graphs with valence profile specified by  $\kappa$ .

$$\mathcal{N}_{g,n}^\kappa(\mathbf{b}) = \sum_{G \in \mathcal{R}_{g,n}^\kappa} \frac{1}{|\text{Aut}(G)|} \mathcal{N}_G(\mathbf{b}).$$

The lattice count functions were defined by Norbury in [Nor] to count the number of lattice points in a combinatorial moduli space introduced by Kontsevich in [K92]. We will encounter these objects again in Chapter 4. One would expect these functions to be piecewise polynomials given the nature of the contributions. Remarkably, summing the weighted contributions produces a polynomial function.

**Theorem 3.3** ([Nor, Theorem 1]). *The function  $\mathcal{N}_{g,n}(b_1, \dots, b_n)$  is a degree  $3g - 3 + n$  polynomial in the variables  $b_1^2, \dots, b_n^2$  depending on the parity of  $b_i$ .*

Hence, we will refer to  $\mathcal{N}_{g,n}(\mathbf{b})$  as the *lattice count polynomial*. As remarked in Example 3.16, the polynomial is only defined on the lattice  $b_1 + \dots + b_n = 0$  and is 0 otherwise. We will again omit these details when writing down lattice count functions. The lattice count function given with valence profile  $\kappa$  in general does not exhibit polynomial behaviour and is at best a piecewise polynomial.

**Remark 3.21.** The lattice count function can be interpreted as the number of unique integer metrics that can be assigned to any genus  $g$  ribbon graph with valence profile  $\kappa$  and  $n$  boundary components of fixed lengths  $\mathbf{b}$ . These count functions will appear in our proof for the formula to count the number  $\#\mathcal{ST}_\Gamma(\mathcal{Q}(\mu), 2N)$  in Lemma 3.5. There, we will glue  $n$  cylinders of circumferences given by  $\mathbf{b}$  together onto a genus  $g$  ribbon graph with valence profile  $\kappa$ . The number of ways to do so corresponds to the number of unique integer metrics that can be assigned to such a ribbon graph, that is, the lattice count function  $\mathcal{N}_{g,n}^\kappa(\mathbf{b})$ .

**Example 3.22.** Let us compute the polynomial  $\mathcal{N}_{0,3}(b_1, b_2, b_3)$ . For a ribbon graph in this set, a simple Euler characteristic computation tells us that  $E = V + 1$ . The sum of vertex valences is  $2E = 2V + 2$ . Since we only consider at least trivalent vertices, we have a bound  $2V + 2 \geq 3V$  so  $V \leq 2$ . Therefore, the only possible valence profiles are  $[3, 3]$  and  $[4]$ . There are four possible ribbon graphs in  $\mathcal{R}_{0,3}^{[3,3]}$  given by the twisted theta graph  $G_{\tilde{\Theta}}$  and the three dumbbell graphs  $G_i$ . All graphs have trivial automorphism group. It is easily checked that the incidence matrices  $A_{G_i}$  are full rank so  $\mathcal{N}_{G_i}(\mathbf{b}) = \mathbb{1}_{C_i}$  where  $C_i = \{(b_1, b_2, b_3) \in \mathbb{R}_+^3 : b_i > \sum_{j \neq i} b_j\}$ . Observe that  $C = \bigsqcup_{i=0}^3 C_i$  where  $C_0$  is given in Example 3.16 fill up the space  $\mathbb{R}_+^3$  except for three codimension 1 walls on the boundaries where  $b_i = \sum_{j \neq i} b_j$ . So far, we have the piecewise polynomial

$$\mathcal{N}_{0,3}^{[3,3]}(\mathbf{b}) = \mathbb{1}_C(\mathbf{b}).$$

In  $\mathcal{R}_{0,3}^{[4]}$ , there are three 4-valent ribbon graphs given by contracting the middle edge in the graphs  $G_i$ . The incidence matrix is again full rank so on the codimension 1 walls we have

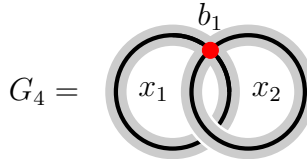
$$\mathcal{N}_{0,3}^{[4]}(\mathbf{b}) = \mathbb{1}_{\mathbb{R}_+^3 \setminus C}(\mathbf{b})$$

Combining both contributions, we obtain the polynomial  $\mathcal{N}_{0,3}(\mathbf{b}) = 1$ . The degree is as expected by Theorem 3.3 for  $g = 0$  and  $n = 3$ .

**Example 3.23.** We now compute  $\mathcal{N}_{1,1}(b_1)$ . Following an identical argument to Example 3.22, the possible valence profiles are  $[3, 3]$  and  $[4]$ . Using Example 3.13, we have

$$\mathcal{N}_{1,1}^{[3,3]}(b_1) = \frac{1}{|\text{Aut}(G_{\tilde{\Theta}})|} \mathcal{N}_{\tilde{\Theta}}(b_1) = \frac{(b_1 - 4)(b_1 - 2)}{48}.$$

Observe that this is not yet a polynomial in even powers of  $b_1$ . In  $\mathcal{R}_{1,1}^{[4]}$ , there is only one ribbon graph  $G_4$  given below, which can be produced by “sliding” the vertices of the twisted theta graph  $G_{\tilde{\Theta}}$  together. Its incidence matrix  $A_{G_4} = (2 \ 2)$ .



Points in  $P_{G_4}(b_1)$  satisfy  $x_1 + x_2 = b_1/2$ . Using Lemma 3.2 and a similar argument to Example 3.13, obtain an automorphism group of  $\mathbb{Z}_4$ . Therefore,

$$\mathcal{N}_{1,1}^{[4]}(b_1) = \frac{1}{4} \begin{pmatrix} \frac{b_1}{2} - 1 \\ 1 \end{pmatrix} = \frac{b_1 - 2}{8}$$

and the overall lattice count polynomial is

$$\mathcal{N}_{1,1}(b_1) = \mathcal{N}_{1,1}^{[4]}(b_1) + \mathcal{N}_{1,1}^{[3,3]}(b_1) = \frac{1}{48}(b_1^2 - 4).$$

This is a polynomial in  $b_1^2$  with degree matching the statement of Theorem 3.3.

**Remark 3.24.** The cardinality of the set  $\mathcal{R}_{g,n}$  grows rapidly for larger  $g$  and  $n$ . There exists a recursion for the polynomials  $\mathcal{N}_{g,n}$  constructed in [Nor], which determines every such polynomial from  $\mathcal{N}_{0,3}$  and  $\mathcal{N}_{1,1}$ . For the special case of trivalent ribbon graphs, we will see in Chapter 4 that the top degree terms of  $\mathcal{N}_{g,n}$  coincide with the Kontsevich volume polynomials  $N_{g,n}$  which are defined using well-known intersection numbers.

Connected ribbon graphs represent a connected component of a singular layer in the cylinder decomposition of a quadratic square-tiled surface. We will investigate the Abelian case which is more restrictive and requires extra structure. Firstly, the vertex valences of an Abelian singular layer are always even. Moreover, there is a global oriented horizontal flow that must be respected by the ribbon graph. This can be done by endowing the half-edges with an orientation. Therefore, all singular layers must be taken into account at once, so our ribbon graphs are not necessarily connected.

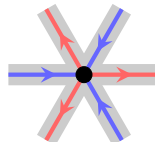
**Definition 3.25.** A *separatrix diagram* is the data  $S = (G, s, P)$  where

- $G$  is a (possibly disconnected) ribbon graph;
- $s : X \rightarrow \{-1, 1\}$  assigns a sign such that  $s \circ \tau_i = -s$  for  $i = 1, 2$ ;
- $P : F(G) \rightarrow F(G)$  is fixed-point free bijection such that  $s_2 \circ P = -s_2$  where  $s_2$  is the induced map of  $s$  under the quotient  $X \rightarrow X/\langle \tau_2 \rangle$ .

In particular, the assignment of signs to half-edges determines an orientation on each boundary component, and  $P$  determines a pairing of boundary components with opposite orientation. We say a ribbon graph  $G$  admits a *separatrix structure* if there exists data  $s, P$  such that  $(G, s, P)$  is a separatrix diagram.

**Definition 3.26.** A separatrix diagram is called *realisable* if there exists a metric  $\ell$  on the underlying ribbon graph such that  $\ell \circ P = \ell$ , that is, paired boundaries share the same length.

**Example 3.27.** Let us find all separatrix diagrams with valence profile  $\kappa = [6]$  which corresponds to the stratum  $\mathcal{H}(2)$ . Note that there are necessarily 6 half-edges. We first endow each half-edge with a sign  $s$ . We represent a positive sign by an outgoing arrow, and a negative sign by an ingoing arrow.



The half-edge pairing  $\tau_1$  must pair opposite signs. Up to isomorphism, there are 3 possible pairings of white two yield valid separatrix diagrams.

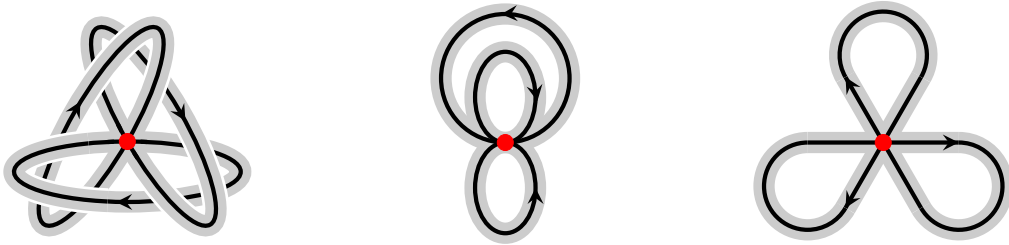


Figure 3.4: The first two diagrams are realisable separatrix diagrams. The final diagram is not realisable - there are three boundary components with the same orientation.

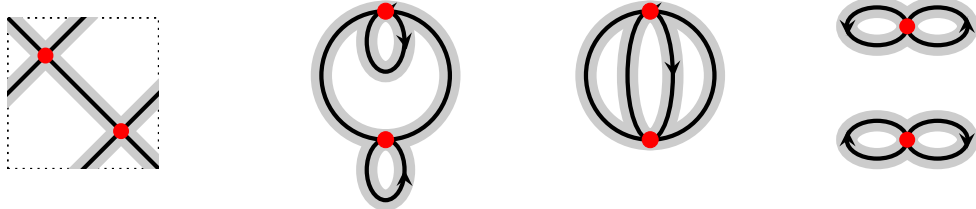


Figure 3.5: Realisable separatrix diagrams in the stratum  $\mathcal{H}(1, 1)$ .

### 3.4 The volume formula

We are now ready to assemble all the objects previously established to prove a formula for the Masur-Veech volumes of quadratic strata. The volume computations of some small Abelian strata for the interested reader can be found in [Zo2]. The Abelian case is rather restrictive, and only allows for feasible hand computations using the geometric method in very low dimensional strata. The ideas and constructions in this section mostly follow [DGZZ1] where a formula for volumes of principal quadratic strata was provided using intersection theory. We will postpone the intersection theory discussion until Chapter 4 and mostly work with direct hand computations using some of the examples provided in Section 3.3.

The geometric approach we will follow has been known since [AEZ2] where volumes of principal strata were computed in genus 0 principal strata, and extended in [DGZZ1] to all principal strata. In [Go], examples of volumes computations in low dimensional quadratic strata were provided by directly counting configurations of diagrams, similar to the computations done in [Zo2] for Abelian strata. We will recast some of these computations in [Go] in terms of the framework provided in [DGZZ1], providing a more systematic approach to evaluating volumes. In particular, Lemma 3.5 proves that the method from [DGZZ1] extends to quadratic strata. There are some pitfalls which we discuss, however, it is valid in sufficiently nice cases.

In [AEZ1] and [DGZZ1], a formal operator  $\mathcal{Z}$  was defined on polynomials to give us numbers related to certain volume contributions. The authors in these papers worked in principal strata, where they only encountered polynomials. When working with

non-principal strata, we may come across certain piecewise polynomials, so applying the operator  $\mathcal{Z}$  is no longer valid. We will also discuss in this section some possible extensions of this operator to piecewise polynomials in such a way that it mimics the behaviour of the operator  $\mathcal{Z}$ . This is done in Lemma 3.11.

We first provide a brief overview of the road ahead to compute volumes of strata. Recall from Section 3.1 that our goal is to compute the count  $\#\mathcal{ST}_\Gamma(\mathcal{Q}(\mu), 2N)$ , and using Equations. (3.5) and (3.6) we recover the volume  $\text{Vol } \mathcal{Q}(\mu)$ . We first consider all possible dimensions of cylinders in the cylinder decomposition of a square-tiled surface of type  $\Gamma$ . The dimensions are encoded in vectors  $\mathbf{w}$  and  $\mathbf{h}$  representing the circumference and heights of the cylinders. The number of ways to glue these cylinders together is given in terms of a product of lattice count functions  $\mathcal{N}_{g,n}^\kappa(\mathbf{b})$ , along with appropriate twist parameters. After including necessary prefactors, taking the limit recovers the volume. We can repackage this computation nicely by interpreting this limit as a certain operator  $\mathcal{Z}$  on polynomials, which we also extend to some piecewise polynomials.

This first Lemma describes the admissible dimensions of cylinders in the cylinder decomposition. In particular, we only have constraints on the circumference parameter  $\mathbf{w}$  which determine the boundary faces of ribbon graphs. The height parameters are free to vary.

**Lemma 3.4** ([DGZZ1, Corollary 2.2]). *Let  $X$  be a square-tiled surface of type  $\Gamma \in \mathcal{G}_{g,n}$  tiled by squares of size  $(1/2 \times 1/2)$ . Denote the circumference of the cylinder associated to an edge  $e \in E(\Gamma)$  by the positive half-integer  $w_e \in \frac{1}{2}\mathbb{N}$ . Collect these numbers into a tuple  $\mathbf{w} = (w_e)_{e \in E(\Gamma)}$ . Transforming into integer parameters,  $\mathbf{b} = 2\mathbf{w}$  lies in a lattice  $\mathbb{L}_\Gamma \subseteq \mathbb{Z}^{E(\Gamma)}$  of index  $2^{\#V(\Gamma)-1}$ . Conversely, every such collection  $\mathbf{b} \in \mathbb{L}_\Gamma \cap \mathbb{Z}_+^{E(\Gamma)}$  is realised by a square-tiled surface of type  $\Gamma$  with cylinder circumference given by  $b_i/2$ .*

*Proof.* At a vertex  $v \in V(\Gamma)$ , define  $E_v(\Gamma)$  to be the set of edges in  $E(\Gamma)$  incident to  $v$ , with loops appearing twice. Define the linear forms

$$\ell_v : \mathbb{Z}^{E(\Gamma)} \rightarrow \mathbb{Z}/2\mathbb{Z}, \mathbf{b} \mapsto \sum_{e \in E_v(\Gamma)} b_e \pmod{2}$$

in the module  $\text{Hom}(\mathbb{Z}^{E(\Gamma)}, \mathbb{Z}/2\mathbb{Z}) \cong (\mathbb{Z}/2\mathbb{Z})^{E(\Gamma)}$ . Considering a vertex  $v$  as a singular layer in the cylinder decomposition,  $\ell_v(\mathbf{b})$  gives us the parity of the boundary length of the underlying ribbon graphs. For integral metric ribbon graphs, a metric is only realised on a ribbon graph when we have even parity. Adding all linear forms  $\ell_v$  double counts the edge parameters, so

$$\left( \sum_{v \in V(\Gamma)} \ell_v \right) (\mathbf{b}) = \sum_{v \in V(\Gamma)} \sum_{e \in E_v(\Gamma)} b_e \pmod{2} = 2 \sum_{e \in E(\Gamma)} b_e \pmod{2} = 0.$$

Therefore, the submodule  $\langle \ell_v \rangle_{v \in V(\Gamma)}$  has rank  $\#V(\Gamma) - 1$ . The sublattice  $\mathbb{L}_\Gamma \subseteq \mathbb{Z}^k$  is defined by

$$\mathbb{L}_\Gamma = \{\mathbf{b} \in \mathbb{Z}^k : l_v(\mathbf{b}) = 0 \text{ for all } v \in V(\Gamma)\}$$

and thus has index  $2^{\#V(\Gamma)-1}$ .  $\square$

We are now ready to state the main Lemma which gives the count  $\#\mathcal{ST}(\mathcal{Q}(\mu), 2N)$ . The special case for principal quadratic strata was proven as part of [DGZZ1, Theorem 1.5]. We extend the proof to all quadratic strata with the condition that there is at least one odd singularity. The reasoning for this is explained at the end of the proof.

**Lemma 3.5.** *If  $\kappa$  has at least one odd component, the total number of square-tiled surfaces of type  $\Gamma \in \mathcal{G}_{g,n}^\kappa$  constructed from at most  $2N$  squares of size  $(1/2 \times 1/2)$  is*

$$\#\mathcal{ST}_\Gamma(\mathcal{Q}(\mu), 2N) = \frac{2^d \cdot c_\kappa}{|\text{Aut}(\Gamma)|} \sum_{\substack{\mathbf{b}, \mathbf{H} \in \mathbb{N}^{E(\Gamma)} \\ \mathbf{b} \cdot \mathbf{H} \leq N \\ \mathbf{b} \in \mathbb{L}_\Gamma}} \prod_{e \in E(\Gamma)} b_e \cdot \prod_{v \in V(\Gamma)} \mathcal{N}_v(\mathbf{b}) \quad (3.7)$$

where  $c_\kappa = \prod_{i \geq 3} \lambda_i(\kappa)!$  and  $\mathcal{N}_v$  is the function counting the number of ways the cylinders of width  $b_i$  can be glued at vertex  $v$ . In particular, it is given by

$$\mathcal{N}_v(\mathbf{b}) = \mathcal{N}_{g_v, n_v}^{\kappa_v}((b_e)_{e \in E_v(\Gamma)}) \quad (3.8)$$

where  $E_v(\Gamma)$  is defined in the proof of Lemma 3.4.

*Proof.* Associate to each cylinder  $\text{cyl}_i$  represented by an edge  $e_i \in E(\Gamma)$  the width and height dimensions  $w_i$  and  $h_i$ . Since each cylinder is constructed from squares of size  $(1/2 \times 1/2)$ , the parameters  $w_i$  and  $h_i$  are half-integer. Let  $\mathbf{w}, \mathbf{h}$  be half-integer  $\#E(\Gamma)$ -dimensional vectors collecting all values  $w_i$  and  $h_i$ . The area of the square-tiled surface constructed from the cylinders  $\text{cyl}_i$  is given by the dot product  $\mathbf{w} \cdot \mathbf{h}$ .

The first step to compute the count  $\#\mathcal{ST}_\Gamma(\mathcal{Q}(\mu), 2N)$  is to sum over all pairs  $(\mathbf{w}, \mathbf{h})$  where  $\mathbf{w} \cdot \mathbf{h} \leq N/2$  (a square-tiled surface built from at most  $2N$  squares has area at most  $N/2$ ). By Lemma 3.4, a square-tiled surface is only realised when  $2\mathbf{w} \in \mathbb{L}_\Gamma$ . Given an admissible pair  $(\mathbf{w}, \mathbf{h})$ , we count the number of ways to attach the corresponding cylinders onto the singular layers represented by the vertices  $V(\Gamma)$ .

Given the boundary lengths  $\mathbf{w}$ , we first observe that counting half-integer metrics on a ribbon-graph is equivalent to counting integer metrics given boundary lengths  $2\mathbf{w}$ . Consider now a vertex  $v \in V(\Gamma)$  representing a singular layer with valence profile  $\kappa_v$  of genus  $g_v$  with  $n_v$  boundary components. The number of ways to attach  $n_v$  cylinders to any singular layer of this type is given by the lattice count function  $\mathcal{N}_{g_v, n_v}^{\kappa_v}(2\mathbf{w}_v)$  by Remark 3.21 where  $\mathbf{w}_v$  is a vector of boundary lengths corresponding to the vertex  $v$  depending on the attachment of cylinders.

If an edge  $e \in E(\Gamma)$  is incident to the vertex  $v$  and it not a loop, then the corresponding length variable  $w_e$  only appears once in the vector  $\mathbf{w}_v$  since only a single

side of the cylinder is glued onto a boundary component. If the edge  $e$  forms a loop at  $v$ , then both ends of the cylinder attach onto a boundary component, so appears twice in  $\mathbf{w}_v$ . Therefore, the lattice count function at  $v$  is precisely  $\mathcal{N}_v(2\mathbf{w}_v)$  as given in Equation (3.8).

After attaching one end of a cylinder onto a singular layer, there is freedom to twist the cylinder before attaching the other end. Since full Dehn twists produce isomorphic surfaces, we can assume that the twist parameter  $\phi_e$  measured in arc length lies in the range  $0 \leq \phi_e < w_e$ . We allow half-integer twists, so there are  $2w_e$  possible twists. Therefore, given an admissible pair  $(\mathbf{w}, \mathbf{h})$ , the number of square-tiled surfaces is the product of all  $\mathcal{N}_v(2\mathbf{w})$  for each vertex  $v \in V(\Gamma)$ , together with the product of all  $2w_e$  for each edge  $e \in E(\Gamma)$ . Summing over the constraints  $\mathbf{w} \cdot \mathbf{h} \geq N/2$  gives us

$$\sum_{\substack{\mathbf{w}, \mathbf{h} \in (\frac{1}{2}\mathbb{N})^{E(\Gamma)} \\ \mathbf{w} \cdot \mathbf{h} \leq N/2 \\ 2\mathbf{w} \in \mathbb{L}_\Gamma}} \prod_{e \in E(\Gamma)} (2w_e) \cdot \prod_{v \in V(\Gamma)} \mathcal{N}_v(2\mathbf{w}).$$

We now make the change of variables  $\mathbf{b} = 2\mathbf{w}$  and  $\mathbf{H} = 2\mathbf{h}$  so that  $b_i, H_i \in \mathbb{N}$ . This transforms the second restriction in the sum to  $\mathbf{b} \cdot \mathbf{H} \leq 2N$ . Using instead the restriction  $\mathbf{b} \cdot \mathbf{H} \leq N$  introduces a factor of  $2^d$ . We also divide by the number of automorphisms of  $\Gamma$  to count unique square-tiled surfaces. The constant  $c_\kappa$  takes into account the number of ways the zeros of the same multiplicity can be rearranged. Combining these transformations and constants gives us the expression in Equation (3.7).

Finally, we comment on the condition for there to be at least one odd singularity. If all singularities are even, this method does not rule out the possibility that the resulting square-tiled surfaces come from the associated Abelian strata. In computations, one would have to filter out all configuration of ribbon graph diagrams that give rise to a separatrix structure.  $\square$

**Proposition 3.6.** *Given a stable graph  $\Gamma$ , if  $\mathcal{N}_v(\mathbf{b})$  is a polynomial on  $\mathbb{L}_\Gamma$  for all  $v \in V(\Gamma)$ , then*

$$\prod_{e \in E(\Gamma)} b_e \cdot \prod_{v \in V(\Gamma)} \mathcal{N}_v(\mathbf{b}) \tag{3.9}$$

*is also a polynomial on  $\mathbb{L}_\Gamma$  with degree equal to  $d - \#E(\Gamma)$  where  $d = \dim \mathcal{Q}(\mu)$ .*

*Proof.* This fact will be made clear in Lemma 3.7. In light of Equation (3.7), Equation (3.13) produces asymptotics of order  $|\mathbf{m}| + k$  where  $|\mathbf{m}|$  is the sum of all powers in the top multinomial of Equation (3.9) and  $k$  is the number of variables, which is exactly  $\#E(\Gamma)$ . The order of the asymptotics must correspond to the dimension of the stratum, as seen by Equation (3.4).  $\square$

In some special cases, Equation (3.9) is a polynomial. This is always the case in the principal strata by Theorem 3.3 and also later by Theorem 4.9. The following Lemma

is useful for computing limits of the form given in Lemma 3.8. It was proven in [AEZ2, Theorem 3.7], however we provide a complete proof for a more general form which is also used in [DGZZ1]. Define the operator  $\mathcal{Z}$  on monomials by

$$\mathcal{Z} \left( \prod_{i=1}^k b_i^{m_i} \right) = \prod_{i=1}^k m_i! \cdot \zeta(m_i + 1).$$

**Lemma 3.7.** *Let  $\mathbb{L} \subseteq \mathbb{Z}^k$  be a sub-lattice with finite index  $|\mathbb{Z}^k : \mathbb{L}| < \infty$ . Let  $m_1, \dots, m_k \in \mathbb{N}$  be positive integers. The following limit holds.*

$$\lim_{N \rightarrow \infty} \frac{1}{N^{|\mathbf{m}|+k}} \sum_{\substack{\mathbf{b}, \mathbf{H} \in \mathbb{N}^k \\ \mathbf{b} \cdot \mathbf{H} \leq N \\ \mathbf{b} \in \mathbb{L}}} \prod_{i=1}^k b_i^{m_i} = \frac{1}{|\mathbb{Z}^k : \mathbb{L}|} \frac{1}{(|\mathbf{m}| + k)!} \mathcal{Z} \left( \prod_{i=1}^k b_i^{m_i} \right) \quad (3.10)$$

*Proof.* Since  $\mathbb{L} \subseteq \mathbb{Z}^k$  is a sub-lattice, there is a full-rank integer matrix  $A : \mathbb{Z}^k \rightarrow \mathbb{Z}^k$  with image  $\mathbb{L}$  and  $|\det A| = |\mathbb{Z}^k : \mathbb{L}|$ . We first re-index the sum using  $\mathbf{b} = A\mathbf{y}$  for  $\mathbf{y} \in \mathbb{Z}^k$  and perform an integral approximation, giving us

$$\sum_{\substack{\mathbf{b}, \mathbf{H} \in \mathbb{N}^k \\ \mathbf{b} \cdot \mathbf{H} \leq N \\ \mathbf{b} \in \mathbb{L}}} \prod_{i=1}^k b_i^{m_i} = \sum_{\mathbf{H} \in \mathbb{N}^k} \sum_{\substack{\mathbf{y} \in \mathbb{Z}^k \\ A\mathbf{y} \in \mathbb{N}^k \\ (A\mathbf{y}) \cdot \mathbf{H} \leq N}} \prod_{i=1}^k (A\mathbf{y})_i^{m_i} \sim \sum_{\mathbf{H} \in \mathbb{N}^k} \int_E \prod_{i=1}^k (A\mathbf{y})_i^{m_i} d\mathbf{y}$$

where  $E$  is the set  $\{\mathbf{y} \in \mathbb{R}^k : A\mathbf{y} \in \mathbb{R}_+^k, (A\mathbf{y}) \cdot \mathbf{H} \leq N\}$ . Next, we perform the substitution  $\mathbf{x} = A\mathbf{y}$  so  $d\mathbf{x} = |\det A|d\mathbf{y} = |\mathbb{Z}^k : \mathbb{L}|d\mathbf{y}$  which gives us a new domain of integration  $E' = \{\mathbf{x} \in \mathbb{R}_+^k : \mathbf{x} \cdot \mathbf{H} \leq N\}$ . We follow this by performing a rescaling  $x_i \mapsto Nx_i/H_i$  which transforms  $E'$  into the simplex  $\Delta = \{\mathbf{x} \in \mathbb{R}_+^k : x_1 + \dots + x_k \leq 1\}$ . Thus we obtain the following simplification where the desired limit directly follows:

$$\begin{aligned} &= \frac{1}{|\mathbb{Z}^k : \mathbb{L}|} \sum_{\mathbf{H} \in \mathbb{N}^k} \int_{E'} \prod_{i=1}^k x_i^{m_i} dx_i = \frac{1}{|\mathbb{Z}^k : \mathbb{L}|} \sum_{\mathbf{H} \in \mathbb{N}^k} \int_{\Delta} \prod_{i=1}^k \left( \frac{Nx_i}{H_i} \right)^{m_i} d\left( \frac{Nx_i}{H_i} \right) \\ &= \frac{1}{|\mathbb{Z}^k : \mathbb{L}|} N^{|\mathbf{m}|+k} \left( \int_{\Delta} \prod_{i=1}^k x_i^{m_i} dx_i \right) \left( \sum_{\mathbf{H} \in \mathbb{N}^k} \prod_{i=1}^k \frac{1}{H_i^{m_i+1}} \right) \\ &= \frac{1}{|\mathbb{Z}^k : \mathbb{L}|} N^{|\mathbf{m}|+k} \frac{\prod_{i=1}^k m_i!}{\left( \sum_{i=1}^k (m_i + 1) \right)!} \prod_{i=1}^k \zeta(m_i + 1) \\ &= \frac{1}{|\mathbb{Z}^k : \mathbb{L}|} \frac{N^{|\mathbf{m}|+k}}{(|\mathbf{m}| + k)!} \prod_{i=1}^k m_i! \cdot \zeta(m_i + 1). \end{aligned}$$

Note that the second last equality follows from the integral representation of the multinomial beta function.  $\square$

**Lemma 3.8.** Suppose the top degree of the summand in Equation (3.7) is a polynomial. Define

$$P_\Gamma = \frac{1}{2^{\#V(\Gamma)-1}} \cdot \frac{1}{|\text{Aut}(\Gamma)|} \cdot \prod_{e \in E(\Gamma)} b_e \cdot \prod_{v \in V(\Gamma)} \mathcal{N}_v(\mathbf{b})$$

The volume contribution of type  $\Gamma$  is given by

$$\text{Vol}(\Gamma) = C_\kappa \cdot n_\Gamma \cdot \mathcal{Z}(P_\Gamma) \quad (3.11)$$

where

$$C_\kappa = \frac{2^{d+1} c_\kappa}{(d-1)!}, \quad \text{and} \quad C_\kappa = C_{g,n} = \frac{2^{6g-5+2n} \cdot (4g-4+n)!}{(6g-7+2n)!}.$$

where the latter constant is in the case of the principal stratum.

*Proof.* Recall from Equation (3.5) that

$$\text{Vol}(\Gamma) = 2d \lim_{N \rightarrow \infty} \frac{1}{N^d} \cdot \#\mathcal{ST}_\Gamma(\mathcal{Q}(\mu), 2N).$$

After rewriting

$$\prod_{e \in E(\Gamma)} b_e \cdot \prod_{v \in V(\Gamma)} \mathcal{N}_v(\mathbf{b}) = b_1^{m_1} \cdots b_k^{m_k} =: \tilde{P}_\Gamma,$$

the limit of their sum (with the appropriate summation domain from Lemma 3.5) evaluates to  $\mathcal{Z}(\tilde{P}_\Gamma)$  by Lemma 3.7 with additional factors  $1/2^{\#V(\Gamma)-1}$  and  $1/(|\mathbf{m}|+k)!$ . The first factor is dependent on  $\Gamma$  so appears in  $P_\Gamma$ . By Proposition 3.6,  $|\mathbf{m}| = d - k$  so the second factor is  $1/d!$ . Combining the factors not involving  $\Gamma$  gives us

$$2d \cdot \frac{2^d c_\kappa}{d!} = \frac{2^{d+1} c_\kappa}{(d-1)!}$$

which is the prefactor in (3.11). In the principal stratum, the dimension is  $d = 6g-6+2n$  and the number of simple zeros is  $4g-4+n$ , so  $c_\kappa = (4g-4+n)!$ . We obtain  $C_{g,n}$  after substituting these constants into  $C_\kappa$ . We observe that  $P_\Gamma$  is invariant under permutation of legs labellings, so it suffices to compute the volume contribution for an unlabelled stable graph, then multiply by the number of legs labellings  $n_\Gamma$ .  $\square$

**Corollary 3.9.** The volume of the principal stratum  $\mathcal{Q}(-1^n, 1^{4g-4+n})$  is given by

$$\text{Vol } \mathcal{Q}(-1^n, 1^{4g-4+n}) = C_{g,n} \sum_{\Gamma \in \mathcal{G}_{g,n}^\kappa / S_n} n_\Gamma \cdot \mathcal{Z}(P_\Gamma).$$

Only for some stable graphs of sufficiently nice strata do we obtain a polynomial after multiplying the lattice count functions. We describe one such case below.

**Proposition 3.10.** *Let  $\Gamma \in \mathcal{G}_{g,n}^\kappa(1)$  be a stable graph with one edge. The following function is a polynomial.*

$$\prod_{v \in V(\Gamma)} \mathcal{N}_v(b) \quad (3.12)$$

*Proof.* If  $\Gamma$  has two vertices, the lattice count function  $\mathcal{N}_v(b)$  has only boundary component. For any ribbon graph  $G$  contributing to this count, the count function  $\mathcal{N}_G(b)$  is polynomial since it is given by Stars and Bars Lemma 3.2. If  $\Gamma$  has one vertex, contributions to the lattice count function are of the form  $\mathcal{N}_G(b, b)$  where  $G$  has two boundary components of the same length. An edge in  $G$  is either bordered by both components, or one of the two. Using this observation, split the edge lengths into three groups  $\{x_i\}_i$ ,  $\{y_j\}_j$  and  $\{z_k\}_k$  respectively. Then we obtain the equations

$$b = \sum_i x_i + 2 \sum_j y_j = \sum_i x_i + 2 \sum_k z_k.$$

The count of integer metrics can be expressed as sums and products of binomial coefficients which can be expressed as a polynomial again using Stars and Bars Lemma 3.2.  $\square$

It is common in non-principal strata for Equation (3.9) to be piecewise polynomial on the lattice  $\mathbb{L}_\Gamma$ , for instance,  $b_1^{m_1} \cdots b_k^{m_k} \mathbf{1}_{\{b_1=2b_2\}}$  for  $i \neq j$ . In such cases, one would resort to a direct computation of Lemma 3.8. These computations are often tedious, involving a change of variables and integral approximations, following the idea in the proof of Lemma 3.7. One would hope to be able to extend the operator  $\mathcal{Z}$  to easily take asymptotics of piecewise polynomials that are common in this context. We present a possible extension below for the aforementioned piecewise polynomial. First, define the extension of the operator  $\mathcal{Z}$  by

$$\mathcal{Z} \left( \prod_{i=1}^k b_i^{m_i} \mathbf{1}_{\{b_1=2b_2\}} \right) = (m_1 + m_2)! \cdot \xi(m_1, m_2) \prod_{i \geq 3} m_i! \cdot \zeta(m_i + 1)$$

where

$$\xi(m_1, m_2) := 2^{m_1} \zeta(m_1 + m_2) - (2^{m_1} + 2^{-m_2-1}) \zeta(m_1 + m_2 + 1).$$

**Lemma 3.11.** *Let  $\Gamma$  be a stable graph. Suppose there is a vertex  $v$  with a loop represented by the variable  $b_1$ , and the only other incident edge is represented by a variable  $b_2$ . Let  $m_1, \dots, m_k \in \mathbb{N}$  be positive integers. The following limit holds.*

$$\lim_{N \rightarrow \infty} \frac{1}{N^{|\mathbf{m}|+k-1}} \sum_{\substack{\mathbf{b}, \mathbf{H} \in \mathbb{N}^k \\ \mathbf{b} \cdot \mathbf{H} \leq N \\ \mathbf{b} \in \mathbb{L}}} \prod_{i=1}^k b_i^{m_i} \mathbf{1}_{\{b_1=2b_2\}} = \frac{1}{2^{\#V(\Gamma)-2}} \frac{1}{(|\mathbf{m}| + k - 1)!} \mathcal{Z} \left( \prod_{i=1}^k b_i^{m_i} \mathbf{1}_{\{b_1=2b_2\}} \right) \quad (3.13)$$

*Proof.* This follows an identical approach to Lemma 3.7 and is proven in [Go, Lemma 5] when  $k = 2$ . Adding additional variables does not affect the interaction between  $b_1$  and  $b_2$  so contributes zeta values as usual from Lemma 3.7.  $\square$

## 3.5 Computation of volumes

It remains unknown, and considered unlikely, that a closed formula in terms of elementary functions exists for the volume of any stratum of quadratic differentials. In genus 0, however, such a formula exists and was a conjecture by Kontsevich, proven by Athreya, Eskin, and Zorich in [AEZ1] using Siegel-Veech constants which are known in genus 0.

**Theorem 3.12** ([AEZ1, Theorem 1.1]). *The volume of any stratum  $\mathcal{Q}(\mu)$  of genus 0 meromorphic differentials is equal to*

$$\text{Vol } \mathcal{Q}(\mu) = 2\pi^2 \cdot \prod_{i=1}^k v(d_i)$$

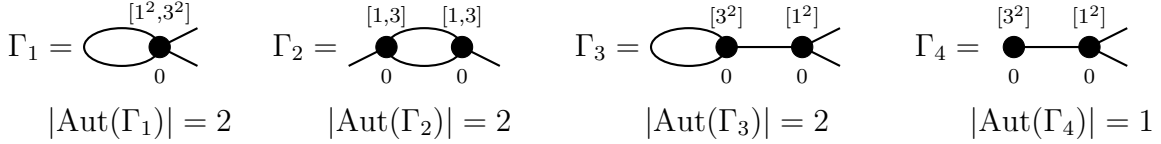
where the function  $v$  is defined on  $\mathbb{Z}_{\geq -1}$  by

$$v(n) := \frac{n!!}{(n+1)!!} \cdot \pi^n \cdot \begin{cases} \pi, & n \text{ odd} \\ 2, & n \text{ even} \end{cases}$$

and the double factorial is given by  $n!! = n \cdot (n-2) \cdots$ . By convention, we define  $(-1)!! = 0!! = 1$ , in particular,  $v(-1) = 1$  and  $v(0) = 2$ .

**Example 3.28.**  $\mathcal{Q}(-1^2, 1^2)$ .

The associated total decoration is  $\kappa = [1^2, 3^2]$ . There are four decorated stable graphs in  $\mathcal{G}_{1,2}^{[1^2, 3^2]}$  given below. Each has a unique leg labelling up to isomorphism.



We now provide the relevant lattice count functions  $\mathcal{N}_{g_v, n_v}^{\kappa_v}$  at each vertex up to lower order terms. Recall that  $g_v$  and  $\kappa_v$  are the genus and partition decorations of  $v$ , and  $n_v$  is the number of full edges incident to  $v$  with loops counted twice.

$$\mathcal{N}_{0,1}^{[1^2]}(b_1) = 1 \quad \mathcal{N}_{0,2}^{[1,3]}(b_1, b_2) = 1 \quad \mathcal{N}_{0,3}^{[3^2]}(b_1, b_2, b_3) = 1$$

$$\mathcal{N}_{1,1}^{[3^2]}(b_1) = \frac{1}{48} \cdot b_1^2 \quad \mathcal{N}_{0,2}^{[1^2, 3^2]}(b_1, b_2) = \frac{1}{4}(b_1^2 + b_2^2)$$

The computations of the first two polynomials is straightforward. The third and fourth polynomials are computed in Examples 3.22 and 3.23. The computation of the fifth polynomial can be found in [AEZ2, Section 3.3]. The polynomials  $P_{\Gamma_i}$  and their evaluation under the operator  $\mathcal{Z}$  are given below.

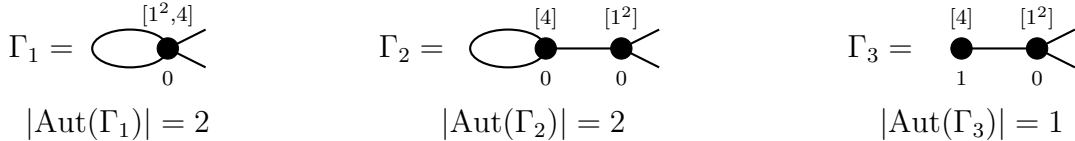
$$\begin{aligned} P_{\Gamma_1} &= \frac{1}{2^0} \cdot \frac{1}{2} \cdot b_1 \cdot \mathcal{N}_{0,2}^{[1^2,3^2]}(b_1, b_1) = \frac{1}{4} b_1^3 & \xrightarrow{\mathcal{Z}} \frac{1}{4} \cdot 3! \cdot \zeta(4) &= \frac{\pi^4}{60} \\ P_{\Gamma_2} &= \frac{1}{2^1} \cdot \frac{1}{2} \cdot b_1 b_2 \cdot \mathcal{N}_{0,2}^{[1,3]}(b_1, b_2)^2 = \frac{1}{4} \cdot b_1 b_2 & \xrightarrow{\mathcal{Z}} \frac{1}{4} \cdot \zeta(2)^2 &= \frac{\pi^4}{144} \\ P_{\Gamma_3} &= \frac{1}{2^1} \cdot \frac{1}{2} \cdot b_1 b_2 \cdot \mathcal{N}_{0,3}^{[3^2]}(b_1, b_1, b_2) \cdot \mathcal{N}_{0,1}^{[1^2]}(b_1) = \frac{1}{4} \cdot b_1 b_2 & \xrightarrow{\mathcal{Z}} \frac{1}{4} \cdot \zeta(2)^2 &= \frac{\pi^4}{144} \\ P_{\Gamma_4} &= \frac{1}{2^1} \cdot \frac{1}{1} \cdot b_1 \cdot \mathcal{N}_{1,1}^{[3^2]}(b_1) \cdot \mathcal{N}_{0,1}^{[1^2]}(b_1) = \frac{1}{96} \cdot b_1^3 & \xrightarrow{\mathcal{Z}} \frac{1}{96} \cdot 3! \cdot \zeta(4) &= \frac{\pi^4}{1440} \end{aligned}$$

This strata is principal so the prefactor  $C_{1,2}$  is  $\frac{32}{3}$  giving us the total volume

$$\text{Vol } \mathcal{Q}(-1^2, 1^2) = \frac{32}{3} \sum_{i=1}^4 \mathcal{Z}(P_{\Gamma_i}) = \frac{\pi^4}{3}.$$

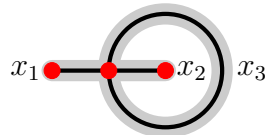
**Example 3.29.**  $\mathcal{Q}(-1^2, 2)$ .

The associated total decoration is  $\kappa = [1^2, 4]$ . There are three unique labelled decorated stable graphs in  $\mathcal{G}_{1,2}^{[1^2,4]}$  given below.



The functions and  $\mathcal{N}_{0,3}^{[4]}$  and  $\mathcal{N}_{1,1}^{[4]}$  are computed in Examples 3.22 and 3.23. It remains to compute  $\mathcal{N}_{0,2}^{[4]}(b_1, b_1)$ . Note that we impose the same boundary length on both components since there is a loop at the vertex in  $\Gamma_1$ . This simplifies the computation to involve only one ribbon graph.

$\mathcal{N}_{0,2}^{[1^2,4]}(b_1, b_1)$ : At a valence 4 vertex, two edges attach to univalent vertices, and the remaining two are joined to create a loop. Having identical boundary lengths implies the univalent vertices appear on opposite sides.



Although both boundaries share the same length, they are still labelled distinctly. There are 2 ways to label the univalent vertices. Observe that swapping the boundary labels

produces the same ribbon graph. Solving  $2x_1 + x_3 = 2x_2 + x_3 = b_1$ , we obtain  $x_1 = x_2$  which are determined by  $x_3$  and  $b_1$ . The parity of  $x_3$  and  $b_1$  must coincide to admit a solution which gives us

$$\mathcal{N}_{0,2}^{[1^2,4]}(b_1, b_1) \sim 2 \cdot \frac{b_1}{2} = b_1.$$

The (piecewise) polynomials and their evaluation under  $\mathcal{Z}$  are given below.

$$\begin{aligned} P_{\Gamma_1} &= \frac{1}{2^0} \cdot \frac{1}{2} \cdot b_1 \cdot \mathcal{N}_{0,2}^{[1^2,4]}(b_1, b_1) = \frac{b_1^2}{2} & \xrightarrow{\mathcal{Z}} \zeta(3) \\ P_{\Gamma_2} &= \frac{1}{2^1} \cdot \frac{1}{2} \cdot b_1 b_2 \cdot \mathcal{N}_{0,3}^{[4]}(b_1, b_1, b_2) \cdot \mathcal{N}_{0,1}^{[1^2]}(b_2) = \frac{b_1 b_2}{4} \cdot \mathbf{1}_{\{b_2=2b_1\}} & \xrightarrow{\mathcal{Z}} \frac{1}{2} \cdot \xi(1, 1) \\ P_{\Gamma_3} &= \frac{1}{2^1} \cdot 1 \cdot b_1 \cdot \mathcal{N}_{1,1}^{[4]}(b_1) \cdot \mathcal{N}_{0,1}^{[1^2]}(b_1) = \frac{b_1^2}{16} & \xrightarrow{\mathcal{Z}} \frac{1}{8} \cdot \zeta(3) \end{aligned}$$

The dimension of this stratum is 3 so  $C_\kappa = 8$ , given us the total volume

$$\text{Vol } \mathcal{Q}(-1^2, 2) = 8 \sum_{i=1}^3 \mathcal{Z}(P_{\Gamma_i}) = 8 \left( \frac{9}{8} \cdot \zeta(3) + \zeta(2) - \frac{9}{8} \cdot \zeta(3) \right) = \frac{4\pi^2}{3}.$$

It is not obvious that the contributions with an odd zeta value would cancel, however, this is guaranteed by Theorem 3.1.

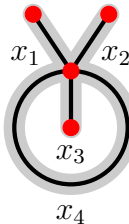
**Example 3.30.**  $\mathcal{Q}(-1^3, 3)$ .

The associated partition is  $\kappa = [1^3, 5]$ . There are three unique decorated stable graphs in  $\mathcal{G}_{1,3}^{[1^3,5]}/S_3$  given below.

$$\begin{array}{ccc} \Gamma_1 = \begin{array}{c} [1^3, 5] \\ \text{---} \\ \text{---} \end{array} & \Gamma_2 = \begin{array}{c} [1, 5] \quad [1^2] \\ \text{---} \quad \text{---} \\ 0 \quad 0 \end{array} & \Gamma_3 = \begin{array}{c} [1, 5] \quad [1^2] \\ \text{---} \quad \text{---} \\ 1 \quad 0 \end{array} \\ |\text{Aut}(\Gamma_1)| = 2 & |\text{Aut}(\Gamma_2)| = 2 & |\text{Aut}(\Gamma_3)| = 1 \end{array}$$

The count of distinct leg labellings are  $n_{\Gamma_1} = 1$  and  $n_{\Gamma_2} = n_{\Gamma_3} = 3$ . We now compute the relevant lattice count functions.

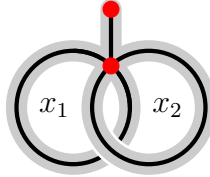
$\mathcal{N}_{0,2}^{[1^3,5]}(b_1, b_1)$ : At a valence 5 vertex, three edges must be attached to the univalent vertices which leaves us with two half-edges to form a loop. Since we enforce identical boundary components, the two edges cannot be cyclically consecutive, otherwise one boundary component is strictly larger than the other. Thus, up to relabelling of the univalent vertices, the only admissible ribbon graph is given below.



There are 6 ways to label the univalent vertices. Again, the two boundaries have distinct labellings, and swapping the labellings produces a non-isomorphic ribbon graph. This gives us an additional factor of 2. The incidence matrix gives us the equations  $2x_1 + 2x_2 + x_4 = 2x_3 + x_4 = b_1$ . Letting  $y = x_1 + x_2$ , the parameters  $x_3$  and  $x_4$  are completely determined by  $b_1$  and  $y$ . The parameter  $y$  can vary between 0 and  $b_1/2$ , and for each  $y$ , there are on the order of  $y$  solutions for the pair  $(x_1, x_2)$ . Thus we obtain the asymptotic

$$\mathcal{N}_{0,2}^{[1^3,5]}(b_1, b_1) = 12 \sum_{y=1}^{b_1/2} y \sim 12 \cdot \frac{(b_1/2)^2}{2} = \frac{3b_1^2}{2}.$$

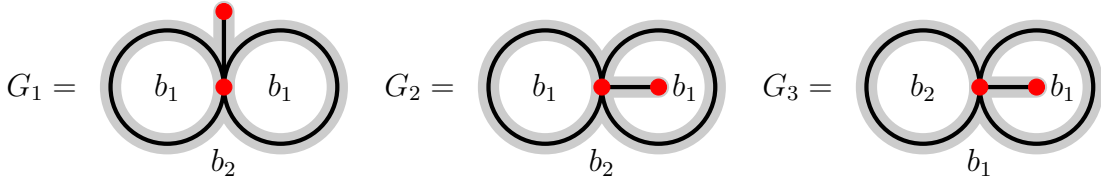
$\mathcal{N}_{1,1}^{[1,5]}(b_1)$ : At a valence 5 vertex, one edge must be attached to the univalent vertex. A genus 1 ribbon graph cannot be produced if two cyclically consecutive half-edges are attached. The only admissible ribbon graph is given below.



In fact, the other choices of half-edge pairings give us the two unlabelled ribbon graphs in  $\mathcal{N}_{0,3}^{[1,5]}$  in the subsequent computation. The incidence matrix gives us the equation  $2x_1 + 2x_2 + 2x_3 = b_1$ . Using Stars and Bars Lemma 3.2, we obtain

$$\mathcal{N}_{1,1}^{[1,5]}(b_1) = \binom{\frac{b_1}{2} - 1}{2} \sim \frac{b_1^2}{8}.$$

$\mathcal{N}_{0,3}^{[1,5]}(b_1, b_1, b_2)$ : There are three labelled ribbon graphs.



Clearly, each has a unique solution when  $\mathbf{b}$  is in an appropriate domain. In particular, we have

$$\mathcal{N}_{G_1}(b_1, b_1, b_2) = \mathbb{1}_{\{b_2 > 2b_1\}} \quad \mathcal{N}_{G_2}(b_1, b_1, b_2) = \mathbb{1}_{\{b_1 < b_2 < 2b_1\}} \quad \mathcal{N}_{G_3}(b_1, b_1, b_2) = \mathbb{1}_{\{b_1 < b_2\}}$$

giving us  $\mathcal{N}_{0,3}^{[1,5]}(b_1, b_1, b_2) = 1$ . Note that this is only true on  $\mathbb{R}_+^2$  away from the two codimension 1 walls  $b_1 = b_2$  and  $2b_1 = b_2$  however this defect has negligible effects on our asymptotics.

The polynomials for  $P_{\Gamma_i}$  and their evaluation under the operator  $\mathcal{Z}$  are given below.

$$\begin{aligned} P_{\Gamma_1} &= \frac{1}{2^0} \cdot \frac{1}{2} \cdot b_1 \cdot \mathcal{N}_{0,2}^{[1^3,5]}(b_1, b_1) = \frac{3b_1^3}{4} & \xrightarrow{\mathcal{Z}} \frac{3}{16} \cdot 3! \cdot \zeta(4) &= \frac{\pi^4}{20} \\ P_{\Gamma_2} &= \frac{1}{2^1} \cdot \frac{1}{2} \cdot b_1 b_2 \cdot \mathcal{N}_{0,3}^{[1,5]}(b_1, b_1, b_2) \cdot \mathcal{N}_{0,1}^{[1^2]}(b_1) = \frac{b_1 b_2}{2} & \xrightarrow{\mathcal{Z}} \frac{1}{2} \cdot \zeta(2)^2 &= \frac{\pi^4}{72} \\ P_{\Gamma_3} &= \frac{1}{2^1} \cdot 1 \cdot b_1 \cdot \mathcal{N}_{1,1}^{[1,5]}(b_1) \cdot \mathcal{N}_{0,1}^{[1^2]}(b_1) = \frac{b_1^3}{16} & \xrightarrow{\mathcal{Z}} \frac{1}{16} \cdot 3! \cdot \zeta(4) &= \frac{\pi^4}{240} \end{aligned}$$

We also take into account the number of leg labellings  $n_{\Gamma_i}$  when adding the contributions. The dimension of this stratum is 4 so the prefactor  $C_\kappa$  is  $\frac{16}{3}$ . The total volume is then

$$\text{Vol } \mathcal{Q}(-1^3, 3) = \frac{16}{3} \left( \mathcal{Z}(P_{\Gamma_1}) + 3\mathcal{Z}(P_{\Gamma_2}) + 3\mathcal{Z}(P_{\Gamma_3}) \right) = \frac{5\pi^4}{9}.$$

### 3.6 Refinement of volume contributions

Recall that edges in a stable graph represent cylinders in the cylinder decomposition of a square-tiled surface. In the formulas presented so far, the height of the cylinders is arbitrary which is accounted for in Lemmas 3.5 and 3.7 giving us values of the zeta function. In many contexts, one may be interested in the volume contributions  $\text{Vol}(\Gamma, \mathbf{H})$  of a stable graph with fixed cylinder heights encoded by a vector  $\mathbf{H} \in \mathbb{N}^{E(\Gamma)}$ . We will see a demonstration of these contributions in Chapter 4.

Let  $\mathcal{ST}_{\Gamma, \mathbf{H}}(\mathcal{Q}(\mu), 2N)$  be the set of square-tiled surfaces in  $\mathcal{Q}(\mu)$  of type  $\Gamma$  with cylinder heights  $\mathbf{H}$ . Then

$$\text{Vol}(\Gamma, \mathbf{H}) = 2d \lim_{N \rightarrow \infty} \frac{1}{N^d} \cdot \#\mathcal{ST}_{\Gamma, \mathbf{H}}(\mathcal{Q}(\mu), 2N)$$

Using an identical proof to Lemma 3.5 adapted so we have a fixed  $\mathbf{H}$ , we obtain

$$\#\mathcal{ST}_{\Gamma, \mathbf{H}}(\mathcal{Q}(\mu), 2N) = \frac{2^d \cdot c_\kappa}{|\text{Aut}(\Gamma)|} \sum_{\substack{\mathbf{b}, \mathbf{H} \in \mathbb{N}^{E(\Gamma)} \\ \mathbf{b} \cdot \mathbf{H} \leq N \\ \mathbf{b} \in \mathbb{L}_\Gamma}} \prod_{e \in E(\Gamma)} b_e \cdot \prod_{v \in V(\Gamma)} \mathcal{N}_v(\mathbf{b}) \quad (3.14)$$

For  $\mathbf{H} \in \mathbb{N}^k$ , define the operator  $\mathcal{Y}_{\mathbf{H}}$  by

$$\mathcal{Y}_{\mathbf{H}} : \prod_{i=1}^k b_i^{m_i} \mapsto \prod_{i=1}^k \frac{m_i!}{H_i^{m_i+1}}.$$

This operator is analogous to the operator  $\mathcal{Z}$  in the setting where  $\mathbf{H}$  is fixed. Adapting Lemma 3.7 in this context gives us

$$\lim_{N \rightarrow \infty} \frac{1}{N^{|\mathbf{m}|+k}} \sum_{\substack{\mathbf{b} \in \mathbb{N}^k \\ \mathbf{b} \cdot \mathbf{H} \leq N \\ \mathbf{b} \in \mathbb{L}}} \prod_{i=1}^k b_i^{m_i} = \frac{1}{|\mathbb{Z}^k : \mathbb{L}|} \cdot \frac{1}{(|\mathbf{m}| + k)!} \cdot \mathcal{Y}_{\mathbf{H}} \left( \prod_{i=1}^k b_i^{m_i} \right). \quad (3.15)$$

The proof again follows the same argument. When the right-hand side of Equation (3.14) is a polynomial in  $\mathbf{b}$ , we have the following adaptation of Lemma 3.7.

**Lemma 3.13.** *The volume contribution of type  $\Gamma$  with cylinder heights  $\mathbf{H} \in \mathbb{N}^{E(\Gamma)}$  is given by*

$$\text{Vol}(\Gamma, \mathbf{H}) = C_\kappa \cdot n_\Gamma \cdot \mathcal{Y}_{\mathbf{H}}(P_\Gamma). \quad (3.16)$$

where  $C_\kappa$  and  $P_\Gamma$  are the same constant and polynomial as given in the statement of Lemma 3.8.

**Remark 3.31.** Note that the operators  $\mathcal{Z}$  and  $\mathcal{Y}_{\mathbf{H}}$  are related by

$$\mathcal{Z} \left( \prod_{i=1}^k b_i^{m_i} \right) = \sum_{\mathbf{H} \in \mathbb{N}^k} \mathcal{Y}_{\mathbf{H}} \left( \prod_{i=1}^k b_i^{m_i} \right)$$

and by considering all possible cylinder heights  $\mathbf{H}$ , we obtain the relation

$$\text{Vol}(\Gamma) = \sum_{\mathbf{H} \in \mathbb{N}^{E(\Gamma)}} \text{Vol}(\Gamma, \mathbf{H}).$$

**Example 3.32.** Consider square-tiled surfaces having a single horizontal cylinder, that is, its associated stable graphs has one edge. Also consider the special case where this horizontal cylinder is constructed from a single band of squares. We will denote their volume contributions by

$$c_1(\mathcal{Q}(\mu)) = \sum_{\Gamma \in \mathcal{G}_{g,n}(1)} \text{Vol}(\Gamma) \quad \text{and} \quad \text{cyl}_1(\mathcal{Q}(\mu)) = \sum_{\Gamma \in \mathcal{G}_{g,n}^\kappa(1)} \text{Vol}(\Gamma, (1))$$

respectively. At the unique vertex  $v \in V(\Gamma)$ , the function  $\mathcal{N}_v(b)$  is a polynomial by Proposition 3.10 and using Proposition 3.6, we can write  $P_\Gamma = \alpha \cdot b^{d-1}$  where  $d = \dim_{\mathbb{C}} \mathcal{Q}(\mu)$  and  $\alpha \in \mathbb{Q}^+$  is a constant. By Lemmas 3.8 and 3.13,

$$\text{Vol}(\Gamma, (1)) = C_\kappa \cdot n_\Gamma \cdot \alpha \cdot (d-1)! \quad \text{and} \quad \text{Vol}(\Gamma) = C_\kappa \cdot n_\Gamma \cdot \alpha \cdot (d-1)! \zeta(d).$$

This gives us  $\text{Vol}(\Gamma) = \zeta(d) \cdot \text{Vol}(\Gamma, (1))$  and summing over all single edge stable graphs we obtain

$$c_1(\mathcal{Q}(\mu)) = \zeta(d) \cdot \text{cyl}_1(\mathcal{Q}(\mu)).$$

# Chapter 4

## Principal Strata of Quadratic Differentials

### 4.1 Intersection numbers

One can study the geometry of a space by computing their topological invariants, for instance the cohomology ring. Of much interest on the moduli space  $\overline{\mathcal{M}}_{g,n}$  are certain characteristic classes that live in  $H^*(\overline{\mathcal{M}}_{g,n})$ . Many of these classes arise from taking Chern classes of certain vector bundles, for instance:

**Definition 4.1.** The *tautological bundles*  $\mathcal{L}_1, \dots, \mathcal{L}_n$  over  $\overline{\mathcal{M}}_{g,n}$  are line bundles where the fibre at each point  $[(X, p_1, \dots, p_n)]$  is the cotangent space  $T_{p_i}^* X$  at the point  $p_i$ . The  $\psi$ -classes  $\psi_1, \dots, \psi_n$  are the first Chern class of the tautological bundles, that is,

$$\psi_i = c_1(\mathcal{L}_i) \in H^2(\overline{\mathcal{M}}_{g,n}; \mathbb{Q}).$$

**Remark 4.2.** The definition of the tautological bundles we present is informal. A rigorous construction involves pulling back the relative dualising sheaf over sections of the universal curve. See for instance [MPS].

**Definition 4.3.** Let  $\mathbf{d} = (d_1, \dots, d_n)$  be a partition of  $3g - 3 + n$ . The *correlator* or *intersection number* is given by

$$\langle \tau_{d_1} \cdots \tau_{d_n} \rangle = \langle \tau_{d_1} \cdots \tau_{d_n} \rangle_{g,n} = \int_{\overline{\mathcal{M}}_{g,n}} \psi_1^{d_1} \cdots \psi_n^{d_n}.$$

**Remark 4.4.** We adopt Witten's notation where the indices of  $\tau$  do not specify the marked points, since the intersection number is symmetric with respect to permutations of the  $\psi$ -classes. We may also add a subscript for  $g, n$  to emphasise the genus and number of marked points, however this is already specified by the partition  $\mathbf{d}$ . By convention, we also define the correlator to be 0 if any of the indices  $d_i$  are negative.

**Example 4.5.** The correlator  $\langle \tau_0^3 \rangle = \langle \tau_0 \tau_0 \tau_0 \rangle$  corresponds to the moduli space  $\overline{\mathcal{M}}_{0,3}$  which is a point, so

$$\langle \tau_0^3 \rangle = \int_{\overline{\mathcal{M}}_{0,3}} \psi_1^0 \psi_2^0 \psi_3^0 = 1.$$

On  $\overline{\mathcal{M}}_{1,1}$ , Witten proves in [W91] that

$$\langle \tau_1 \rangle = \int_{\overline{\mathcal{M}}_{1,1}} \psi_1 = \frac{1}{24}.$$

In fact, all values for correlators can be deduced from these first two using the following.

**Theorem 4.1** ([Zvo, Proposition 4.1]). *The correlator satisfies the following recursive relations:*

1. *String equation* [W91, Equation (2.41)]:

$$\langle \tau_0 \tau_{d_1} \cdots \tau_{d_n} \rangle_{g,n+1} = \sum_{i=1}^n \langle \tau_{d_1} \cdots \tau_{d_{i-1}} \cdots \tau_{d_n} \rangle_{g,n}$$

2. *Dilaton equation* [W91, Equation (2.45)]:

$$\langle \tau_1 \tau_{d_1} \cdots \tau_{d_n} \rangle_{g,n+1} = (2g - 2 + n) \langle \tau_{d_1} \cdots \tau_{d_n} \rangle_{g,n}$$

3. *Virasoro constraints:* See [Zvo, Theorem 4.5].

**Proposition 4.2.** *In genus 0, the correlators are given by*

$$\langle \tau_{d_1} \cdots \tau_{d_n} \rangle = \frac{(n-3)!}{d_1! \cdots d_n!}.$$

*Proof.* The base case for  $n = 3$  and  $d_i = 0$  is satisfied by Example 4.5. Suppose the equation holds for a correlator with  $n$  factors. Then for a correlator with  $n+1$  factors carrying indices  $d_0, \dots, d_n$ , there must be a zero index, say  $d_0$ . Also, the sum  $d_1 + \cdots + d_n$  is  $(n+1) - 3$ . Applying the string equation gives us

$$\langle \tau_{d_0} \cdots \tau_{d_n} \rangle = \sum_{i=1}^n \langle \tau_{d_1} \cdots \tau_{d_{i-1}} \cdots \tau_{d_n} \rangle = \sum_{i=1}^n \frac{(n-3)!}{d_1! \cdots (d_i-1)! \cdots d_n!}$$

and some further simplifications completes the induction:

$$= \frac{(n-3)! \sum_{i=1}^n d_i}{d_1! \cdots d_n!} = \frac{((n+1)-3)!}{d_0! d_1! \cdots d_n!}. \quad \square$$

## 4.2 Kontsevich's Theorem

While studying models of two-dimensional quantum gravity, Witten in [W91, Section 2a] proposed a surprising connection between intersection theory and integrable hierarchies from mathematical physics. He conjectured that a certain generating function involving intersection numbers satisfies a partial differential equation. Equivalently, it can be restated in terms of Virasoro operators which satisfy the commutation relations of the Virasoro Lie algebra. In fact, these give rise to all the recursive relations from Theorem 4.1.

The year after Witten's conjecture was stated, Kontsevich provided a proof in [K92], now known as Kontsevich's theorem, as part of his doctoral thesis. He uses a cell decomposition of the moduli space  $\mathcal{M}_{g,n} \times \mathbb{R}_+^n$  indexed by ribbon graphs, and makes a remarkable connection between intersection numbers and the counts of metric ribbon graphs. This is stated as the “*Main Identity*” from which he proves Witten's conjecture using matrix models and Feynman diagrams.

In this section, we provide a brief exposition of the proof for the Main Identity. The original paper contains missing details and is rather terse. Many authors have since provided complete or alternative proofs of Kontsevich's theorem; see, for instance, [Zvo2; Mirz; Do]. Later, Norbury in [Nor] studied the count of lattice points in certain polytopes considered in Kontsevich's proof and related the count of integer metrics of ribbon graphs to intersection numbers which we use.

**Theorem 4.3** (Main Identity).

$$\sum_{\substack{\mathbf{d} \in \mathbb{N}_0^n \\ |\mathbf{d}|=3g-3+n}} \langle \tau_{d_1} \cdots \tau_{d_n} \rangle \prod_{i=1}^n \frac{(2d_i)!}{\lambda_i^{2d_i+1}} = \sum_{G \in \mathcal{R}_{g,n}^{\text{tri}}} \frac{2^{5g-5+2n}}{|\text{Aut}(G)|} \prod_{e \in E(G)} \frac{1}{\tilde{\lambda}(e)}$$

**Definition 4.6.** Let  $g$  and  $n$  be positive integers such that  $2g+n > 2$ . The *Kontsevich volume polynomials* are defined by

$$N_{g,n}(b_1, \dots, b_n) = \sum_{\substack{\mathbf{d} \in \mathbb{N}_0^n \\ |\mathbf{d}|=3g-3+n}} \frac{\langle \tau_{d_1} \cdots \tau_{d_n} \rangle}{2^{5g-6+2n} \mathbf{d}!} \mathbf{b}^{2\mathbf{d}}.$$

**Theorem 4.4.** Let  $b_1, \dots, b_n$  be positive integers such that  $\sum_{i=1}^n b_i$  is even. The weighted count of genus  $g$  trivalent integral metric ribbon graphs with  $n$  labelled boundary components of length  $b_1, \dots, b_n$  is equal to the polynomial  $N_{g,n}(b_1, \dots, b_n)$  up to lower-order terms, that is,

$$\mathcal{N}_{g,n}(b_1, \dots, b_n) = \sum_{G \in \mathcal{R}_{g,n}^{\text{tri}}} \frac{1}{|\text{Aut}(G)|} \mathcal{N}_G(b_1, \dots, b_n) = N_{g,n}(b_1, \dots, b_n) + l.o.t.$$

### 4.2.1 Combinatorial moduli space

For a ribbon graph  $G \in \mathcal{R}_{g,n}^\kappa$ , recall from Section 3.3 that we define the space of metrics on  $G$  with fixed boundary lengths  $\mathbf{b} \in \mathbb{R}_+^n$  by

$$P_G(\mathbf{b}) = \{\mathbf{x} \in \mathbb{R}_+^{E(G)} : A_G \mathbf{x} = \mathbf{b}\}.$$

Let  $P_G$  be the space of all metrics on  $G$ . This space is identically  $\mathbb{R}_+^{E(G)}$  since there are no restrictions on the assignment of positive lengths to each edge. Using an Euler characteristic argument, we have

$$\#E(G) = 6g - 6 + 3n - \sum_{i=1}^{\#V(G)} (\kappa_i - 3),$$

in particular, the dimension of the cell  $P_G$  is maximised when all vertices are trivalent. There is a natural action of  $\text{Aut}(G)$  on each cell  $P_G$  given as follows. Any automorphism of  $G$  induces a permutation on its edges, hence acts on  $P_G$  by permuting the corresponding components in  $\mathbf{x} \in P_G$ . Thus, the space of unique metrics on  $G$  is the quotient  $P_G / \text{Aut}(G)$ . This follows from observations made in Remark 3.19.

**Definition 4.7.** The *combinatorial moduli space* of genus  $g$  and  $n$  marked points is the cell complex

$$\mathcal{M}_{g,n}^{\text{comb}} = \coprod_{G \in \mathcal{R}_{g,n}} P_G / \text{Aut}(G)$$

which parameterises isomorphism classes of genus  $g$  metric ribbon graphs with  $n$  labeled boundary components. The topology is given as follows. We take the usual Euclidean topology in each cell. In a cell  $P_G$ , we identify the limit of a metric  $(\ell(e_i))_i$  as  $\ell(e_i) \rightarrow 0$  with the metric in the cell  $P_{G'}$  where  $G'$  is the ribbon graph with the edge  $e_i$  (that is not a loop) in  $G$  contracted. Consider the projection map

$$\pi : \mathcal{M}_{g,n}^{\text{comb}} \rightarrow \mathbb{R}_+^n, G \mapsto (\ell(f))_{f \in F(G)}$$

which returns the lengths of boundary components. For a fixed  $\mathbf{b} \in \mathbb{R}_+^n$ , we define

$$\mathcal{M}_{g,n}^{\text{comb}}(\mathbf{b}) = \pi^{-1}(\mathbf{b}) = \coprod_{G \in \mathcal{R}_{g,n}} P_G(\mathbf{b}) / \text{Aut}(G). \quad (4.1)$$

The spaces  $P_G(\mathbf{b})$  are convex polytopes in  $\mathbb{R}_+^{E(G)}$  and thus carry a natural Euclidean volume, which we denote by  $V_G(\mathbf{b})$ . We then define the Euclidean volume of  $\mathcal{M}_{g,n}^{\text{comb}}(\mathbf{b})$  to be

$$V_{g,n}^E(\mathbf{b}) = \sum_{G \in \mathcal{G}_{g,n}} \frac{1}{|\text{Aut}(G)|} V_G(\mathbf{b}). \quad (4.2)$$

We will be interested in the computation of the volumes  $V_{g,n}^E(\mathbf{b})$  which are related to the lattice point counts  $\mathcal{N}_{g,n}(\mathbf{b})$  from Definition 3.20. In practice, it is difficult

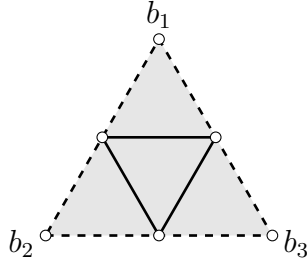
to execute these computations. We will follow Kontsevich's approach to define the symplectic volume  $V_{g,n}^S(\mathbf{b})$  of  $\mathcal{M}_{g,n}^{\text{comb}}(\mathbf{b})$  which can be expressed in terms of intersection numbers on  $\overline{\mathcal{M}}_{g,n}$ . Remarkably, the ratio of volumes  $V_{g,n}^S(\mathbf{b})/V_{g,n}^E(\mathbf{b})$  is a constant, so the lattice point counts  $\mathcal{N}_{g,n}(\mathbf{b})$  can be determined by intersection numbers which are well understood and computable.

**Theorem 4.5.** *The combinatorial moduli space  $\mathcal{M}_{g,n}^{\text{comb}}$  is a connected differentiable orbifold of real dimension  $6g - 6 + 3n$ .*

*Proof.* This is proved in Chapter 3 of [MuPe]. □

There is a natural  $\mathbb{R}_+$ -action on each cell  $P_G$  given by scaling all edge lengths by a constant factor. Thus, one can consider the space  $\Delta_G$  of *unital metrics* on  $G$ , the metrics where the sum of boundary lengths is one. The *rational cell* of  $G$  is the quotient space  $\Delta_G / \text{Aut}(G)$ .

**Example 4.8** ([KaZu]). A model for the space  $\mathcal{M}_{0,3}^{\text{comb}}$ . Using the same names for ribbon graphs from Section 3.3 to identify the cells, we have the following. The central 2-cell corresponds to the theta graph  $G_\Theta$ . The remaining three 2-cells corresponds to the trivalent double loop graphs  $G_i$ , each with a unique labelling of the three boundary components, where  $G_i$  is adjacent to the axis  $b_i$ . The 1-cells are degenerations corresponding to the 4-valent double loop graphs.



**Theorem 4.6.** *There are homeomorphisms*

$$\Psi : \mathcal{M}_{g,n} \times \mathbb{R}_+^n \rightarrow \mathcal{M}_{g,n}^{\text{comb}} \quad \text{and} \quad \Psi_b : \mathcal{M}_{g,n} \rightarrow \mathcal{M}_{g,n}^{\text{comb}}(\mathbf{b}).$$

This is a well-known result due to Harer, Mumford, Thurston [Ha], Penner [Pe], Bowditch and Epstein [BoEp]. Roughly speaking, the boundaries of a ribbon graph correspond to half-infinite cylinders on a Riemann surface, which are determined by a Jenkins-Strebel differential with double poles at  $n$  marked points. Such a differential is uniquely determined by specifying residue of the differential at these points, which take positive real values. Thus, assigning a positive real number at each of the  $n$  marked points on a Riemann surface uniquely determines a Jenkins-Strebel differential and hence a ribbon graph structure.

### 4.2.2 Combinatorial classifying space

**Definition 4.9.** For  $N \in \mathbb{N}$ , define  $BU(1)_{\leq N}^{\text{comb}}$  to be the set of equivalence classes of sequences  $(\ell_1, \dots, \ell_m) \in \mathbb{R}_+^m$  for  $1 \leq m \leq N$  which carries the induced Euclidean topology. The equivalence relation is given by cyclic permutations of the sequence. The *classifying space of combinatorial  $U(1)$ -bundles* is the direct limit

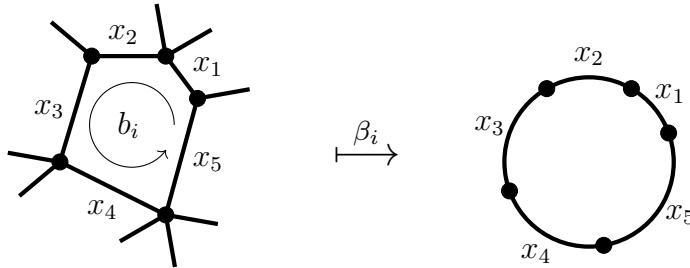
$$BU(1)^{\text{comb}} = \varinjlim BU(1)_{\leq N}^{\text{comb}}.$$

**Remark 4.10.** The classifying space  $BG$  of a group  $G$  is a quotient of a weakly contractible space  $EG$  by a proper free  $G$ -action. In particular,  $EG \rightarrow BG$  is a principal  $G$ -bundle. The isomorphism classes of principal  $G$ -bundles over a space  $X$  is in one-to-one correspondence with homotopy classes of maps  $X \rightarrow BG$ .

We can realise  $BU(1)^{\text{comb}}$  as the moduli space of metric ribbon graphs homeomorphic to  $S^1$ . Since each boundary of every metric ribbon graph is a polygon, there are maps

$$\beta_i : \mathcal{M}_{g,n}^{\text{comb}} \rightarrow BU(1)^{\text{comb}}, G \mapsto \left[ (\ell([\tau_2^k x_i]))_{k=1}^{\# [x_i]_2} \right]$$

where  $x_i$  is a representative for the  $i$ -th boundary component. This map returns the sequence of edge lengths of the  $i$ -th boundary, and is well-defined since we are considering sequences up to cyclic permutations.



Let  $\overline{\mathcal{M}}_{g,n}^{\text{comb}} = \overline{\mathcal{M}}_{g,n} \times \mathbb{R}_+^n$ . A rigorous construction of this space can be found in [Ch].

**Lemma 4.7** ([K92, Appendix B]). *A continuous extension  $\overline{\beta}_i : \overline{\mathcal{M}}_{g,n}^{\text{comb}} \rightarrow BU(1)^{\text{comb}}$  of  $\beta_i$  can be constructed.*

We now construct the  $U(1)$ -bundle  $EU(1)^{\text{comb}}$  over  $BU(1)^{\text{comb}}$ . For each point in the base space represented by a sequence  $(\ell_1, \dots, \ell_m)$ , let  $p = \ell_1 + \dots + \ell_m$  be the perimeter and let  $\phi_{i+1} = \phi_i + \ell_i$  where  $\phi_1 = 0$ . Under the identification  $S^1 = \mathbb{R}/p\mathbb{Z}$ , the points  $[\phi_i] \in S^1$  correspond to the vertices of the polygon and the differences  $\phi_i - \phi_{i-1}$  are the edges of lengths  $\ell_i$  for  $i > 1$  and  $\phi_1 - \phi_m + p$  is the edge length  $\ell_m$ .

There is a natural  $U(1)$  action on the points  $[\phi_i]$  given by  $e^{i\theta} \cdot [\phi_i] = [\phi_i + \theta]$ . Therefore, a point in  $EU(1)^{\text{comb}}$  can be represented by a pair  $(p, S)$  where  $p > 0$  is the perimeter of the underlying polygon and  $S \subseteq \mathbb{R}/p\mathbb{Z}$  is a nonempty finite subset. The representatives  $\phi_i$  of points in  $S$  are chosen such that  $0 \leq \phi_1 < \dots < \phi_m < p$ .

We will now compute the first Chern class of  $EU(1)^{\text{comb}}$ . Define the 1-form

$$\alpha = \sum_{i=1}^m \frac{\ell_i}{p} d\left(\frac{\phi_i}{p}\right)$$

Using the relation  $\phi_{i+1} = \phi_i + \ell_i$ , we can write  $\phi_i = \phi_m - \sum_{j=i}^{m-1} \ell_j$  for  $i \leq m-1$ . This gives us

$$\begin{aligned} \alpha &= \sum_{i=1}^m \frac{\ell_i}{p} d\left(\frac{\phi_i}{p}\right) = \frac{\ell_m}{p} d\left(\frac{\phi_m}{p}\right) + \sum_{i=1}^{m-1} \frac{\ell_i}{p} d\left(\frac{\phi_m}{p} - \sum_{j=i}^{m-1} \frac{\ell_j}{p}\right) \\ &= \underbrace{\sum_{i=1}^m \frac{\ell_i}{p} d\left(\frac{\phi_m}{p}\right)}_{=1} - \sum_{i=1}^{m-1} \sum_{j=i}^{m-1} \frac{\ell_i}{p} d\left(\frac{\ell_j}{p}\right) \\ &= d\left(\frac{\phi_m}{p}\right) - \sum_{1 \leq i \leq j \leq m-1} \frac{\ell_i}{p} d\left(\frac{\ell_j}{p}\right). \end{aligned}$$

The curvature 2-form associated to  $\alpha$  is  $d\alpha + [\alpha \wedge \alpha]$ . Since  $U(1)$  is abelian, the commutator vanishes and we get

$$\omega := d\alpha = - \sum_{1 \leq i < j \leq m-1} d\left(\frac{\ell_i}{p}\right) \wedge d\left(\frac{\ell_j}{p}\right).$$

Since  $\omega$  is free of  $\phi_i$ , it descends to a well-defined 2-form on the base  $BU(1)^{\text{comb}}$ . Therefore, the first Chern class of  $EU(1)^{\text{comb}}$  is

$$[\omega] \in H^2(BU(1)^{\text{comb}}; \mathbb{Q}).$$

Next, we observe that there is an isomorphism

$$\iota^* : H^2(\overline{\mathcal{M}}_{g,n}^{\text{comb}}; \mathbb{Q}) \rightarrow H^2(\overline{\mathcal{M}}_{g,n}; \mathbb{Q})$$

where  $\iota$  is the inclusion of  $\overline{\mathcal{M}}_{g,n}$  given above Lemma 4.7. Let  $\omega_i$  be the pullback of  $\omega$  under the map  $\bar{\beta}_i$ , in particular,  $\omega_i$  is a class on  $\overline{\mathcal{M}}_{g,n}^{\text{comb}}$ . One can show that the image of  $\omega_i$  under  $\iota^*$  represents the first Chern class of the  $i$ -th tautological line bundle  $\mathcal{L}_i$ , in other words,  $\psi_i = (\bar{\beta}_i \circ \iota)^*(\omega)$ . This is done in [Zvo2, Section 5]. The intersection numbers can also be computed from the classes  $\omega_i$  by

$$\langle \tau_{d_1} \cdots \tau_{d_n} \rangle = \int_{\overline{\mathcal{M}}_{g,n}} \psi^d = \int_{\overline{\mathcal{M}}_{g,n}} \omega^d.$$

Define  $\Omega(\mathbf{b}) = \sum_{i=1}^n b_i^2 \omega_i$  which gives rise to a symplectic volume form on the fibre  $\mathcal{M}_{g,n}^{\text{comb}}(\mathbf{b})$ . This can be integrated to obtain the symplectic volume as follows.

$$V_{g,n}^S(\mathbf{b}) = \int_{\overline{\mathcal{M}}_{g,n}(\mathbf{b})} \exp(\Omega(\mathbf{b})) = \int_{\overline{\mathcal{M}}_{g,n}(\mathbf{b})} \frac{\Omega(\mathbf{b})^{3g-3+n}}{(3g-3+n)!}. \quad (4.3)$$

### 4.2.3 Main identity

**Lemma 4.8.** Consider the standard  $n$ -form  $db_1 \wedge \cdots \wedge db_n$  defined on  $\mathbb{R}_+^n$  and the  $(6g - 6 + 2n)$ -form  $\exp(\Omega(\mathbf{b}))$  defined on  $\mathcal{M}_{g,n}^{\text{comb}}(\mathbf{b})$ . Their wedge product defines a top-form in  $\mathcal{M}_{g,n}^{\text{comb}} \cong \mathcal{M}_{g,n}^{\text{comb}}(\mathbf{b}) \times \mathbb{R}_+^n$ . In a cell  $P_G$  of  $\mathcal{M}_{g,n}^{\text{comb}}$ , local coordinates are given by  $(\ell(e))_{e \in E(G)}$ . The corresponding top-form satisfies the following on all cells:

$$\bigwedge_{i=1}^n db_i \wedge \exp(\Omega(\mathbf{b})) = 2^{5g-5+2n} \bigwedge_{e \in E(G)} d\ell(e).$$

*Proof.* This is proved in [K92, Appendix C] using homological algebra. A proof using topological recursion can be found in [CMS].  $\square$

For a ribbon graph  $G \in \mathcal{R}_{g,n}$ , let  $\lambda_i$  be a variable associated with the  $i$ -th labelled boundary component  $f_i \in F(G)$  considered as a function  $\lambda_i = \lambda(f_i)$ . Define the function  $\tilde{\lambda}$  on edges  $e \in E(G)$  by  $\tilde{\lambda}(e) = \lambda([x]_2) + \lambda([\tau_1 x]_2)$ , where  $x$  is a representative of  $e$ . In particular,  $\tilde{\lambda}$  associates an edge with the sum of variables associated with the two incident boundary components. Observe that

$$\sum_{i=1}^n b_i \lambda_i = \sum_{f \in F(G)} \ell(f) \lambda(f) = \sum_{e \in E(G)} \ell(e) \tilde{\lambda}(e) \quad (4.4)$$

where  $b_i$  denotes the length of the  $i$ -th boundary. We provide a derivation using half-edge representative from Definition 3.7 in Lemma C.1.

*Proof of the Main Identity (Theorem 4.3).* Using the multinomial theorem, we rewrite

$$\Omega(\mathbf{b})^{3g-3+n} = \left( \sum_{i=1}^n b_i^2 \omega_i \right)^{3g-3+n} = \sum_{\substack{\mathbf{d} \in \mathbb{N}_0^n \\ |\mathbf{d}|=3g-3+n}} \frac{(3g-3+n)!}{d_1! \cdots d_n!} \prod_{i=1}^n b_i^{2d_i} \omega_i^{d_i}$$

The symplectic fibre volume can then be expressed as

$$V_{g,n}^S(\mathbf{b}) = \sum_{\substack{\mathbf{d} \in \mathbb{N}_0^n \\ |\mathbf{d}|=3g-3+n}} \frac{\mathbf{b}^{2\mathbf{d}}}{\mathbf{d}!} \int_{\overline{\mathcal{M}}_{g,n}^{\text{comb}}(\mathbf{b})} \omega^{\mathbf{d}} = \sum_{\substack{\mathbf{d} \in \mathbb{N}_0^n \\ |\mathbf{d}|=3g-3+n}} \frac{\langle \tau_{\mathbf{d}} \rangle}{\mathbf{d}!} \mathbf{b}^{2\mathbf{d}}. \quad (4.5)$$

We now consider two computations of the Laplace transform of the symplectic fibre volume

$$\widehat{V}_{g,n}^S(\boldsymbol{\lambda}) = \int_{\mathbb{R}_+^n} V_{g,n}^S(\mathbf{b}) \exp(-\boldsymbol{\lambda} \cdot \mathbf{b}) d\mathbf{b}. \quad (4.6)$$

A direct computation by substituting Equation (4.5) into Equation (4.6) gives us

$$\widehat{V}_{g,n}^S(\boldsymbol{\lambda}) = \sum_{\substack{\mathbf{d} \in \mathbb{N}_0^n \\ |\mathbf{d}|=3g-3+n}} \frac{\langle \tau_{\mathbf{d}} \rangle}{\mathbf{d}!} \int_{\mathbb{R}_+^n} \mathbf{b}^{2\mathbf{d}} \exp(-\boldsymbol{\lambda} \cdot \mathbf{b}) d\mathbf{b} = \sum_{\substack{\mathbf{d} \in \mathbb{N}_0^n \\ |\mathbf{d}|=3g-3+n}} \frac{\langle \tau_{\mathbf{d}} \rangle}{\mathbf{d}!} \prod_{i=1}^n \frac{(2d_i)!}{\lambda_i^{2d_i+1}}.$$

Alternatively, substituting Equation (4.3) into Equation (4.6), we obtain

$$\widehat{V}_{g,n}^S(\boldsymbol{\lambda}) = \int_{\mathbb{R}_+^n} \int_{\mathcal{M}_{g,n}^{\text{comb}}(\mathbf{b})} \exp(-\boldsymbol{\lambda} \cdot \mathbf{b}) \frac{\Omega(\mathbf{b})^d}{d!} d\mathbf{b} = \int_{\mathcal{M}_{g,n}^{\text{comb}}} \exp(-\boldsymbol{\lambda} \cdot \mathbf{b}) \frac{\Omega(\mathbf{b})^d}{d!} d\mathbf{b}. \quad (4.7)$$

We then invoke Equation (4.4), Lemma 4.8, and Definition 4.7 and simplify as follows

$$\begin{aligned} &= \sum_{G \in \mathcal{R}_{g,n}^{\text{tri}}} \frac{2^{5g-5+2n}}{|\text{Aut}(G)|} \int_{P_G} \exp\left(-\sum_{i=1}^n \ell(e)\tilde{\lambda}(e)\right) \prod_{e \in E(G)} d\ell(e) \\ &= \sum_{G \in \mathcal{R}_{g,n}^{\text{tri}}} \frac{2^{5g-5+2n}}{|\text{Aut}(G)|} \prod_{e \in E(G)} \int_0^\infty \exp(-\ell(e)\tilde{\lambda}(e)) d\ell(e) \\ &= \sum_{G \in \mathcal{R}_{g,n}^{\text{tri}}} \frac{2^{5g-5+2n}}{|\text{Aut}(G)|} \prod_{e \in E(G)} \frac{1}{\tilde{\lambda}(e)} \end{aligned} \quad (4.8)$$

Note that we only sum over  $\mathcal{R}_{g,n}^{\text{tri}}$  since higher valence ribbon graphs correspond to lower-dimensional cells.  $\square$

*Proof of Theorem 4.4.* We first compute the Laplace transform of the Euclidean fibre volume using Equation (4.1) and Equation (4.2):

$$\widehat{V}_{g,n}^E(\boldsymbol{\lambda}) = \int_{\mathbb{R}_+^n} V_{g,n}^E(\mathbf{b}) e^{-\boldsymbol{\lambda} \cdot \mathbf{b}} d\mathbf{b} = \sum_{G \in \mathcal{R}_{g,n}^{\text{tri}}} \frac{1}{|\text{Aut}(G)|} \int_{\mathbb{R}_+^n} \int_{P_G(\mathbf{b})} e^{-\boldsymbol{\lambda} \cdot \mathbf{b}} \prod_{e \in E(G)} d\ell(e).$$

Integrating instead over the whole polytope  $P_G$  and using Equation (4.4), we can rewrite as

$$= \sum_{G \in \mathcal{R}_{g,n}^{\text{tri}}} \frac{1}{|\text{Aut}(G)|} \int_{P_G} \exp\left(-\sum_{i=1}^n \ell(e)\tilde{\lambda}(e)\right) \prod_{e \in E(G)} d\ell(e).$$

Performing the integral over edge-length coordinates, we have

$$= \sum_{G \in \mathcal{R}_{g,n}^{\text{tri}}} \frac{1}{|\text{Aut}(G)|} \prod_{e \in E(G)} \int_0^\infty \exp(-\ell(e)\tilde{\lambda}(e)) d\ell(e) = \sum_{G \in \mathcal{R}_{g,n}^{\text{tri}}} \frac{1}{|\text{Aut}(G)|} \prod_{e \in E(G)} \frac{1}{\tilde{\lambda}(e)}.$$

Comparing to the expression for the Laplace transform of  $V_{g,n}^S(\mathbf{b})$  in Equation (4.8), we obtain  $2^{5g-5+2n}\widehat{V}_{g,n}^E(\boldsymbol{\lambda}) = \widehat{V}_{g,n}^S(\boldsymbol{\lambda})$ . Inverting the Laplace transform and using Equation (4.5) gives us

$$V_{g,n}^E(\mathbf{b}) = \sum_{\substack{\mathbf{d} \in \mathbb{N}_0^n \\ |\mathbf{d}|=3g-3+n}} \frac{\langle \tau_{d_1} \cdots \tau_{d_n} \rangle}{2^{5g-5+2n} \mathbf{d}!} \mathbf{b}^{2\mathbf{d}}.$$

Since we are working on the index 2 lattice defined by  $b_1 + \cdots + b_n \equiv 0 \pmod{2}$ , we normalise the measure so that the covolume of the lattice is one. Thus, the top degree of  $V_{g,n}^E(\mathbf{b})$  coincides with twice the lattice count polynomial  $N_{g,n}(\mathbf{b})$  proving the Theorem.  $\square$

### 4.3 Trivalent ribbon graphs with leaves

Let  $\mathcal{R}_{g,n,p}^{\text{tri}}$  denote the set of isomorphism classes of genus  $g$  trivalent ribbon graphs with  $n$  labelled boundary components and  $p$  univalent vertices (leaves). In this section, we prove the following extension of Kontsevich's theorem following [DGZZ1]. The authors left out some details of proofs, which we aim to fill in.

**Theorem 4.9** ([DGZZ1, Proposition 2.4]). *Let  $b_1, \dots, b_n$  be positive integers such that  $\sum_{i=1}^n b_i$  is even. The weighted count of genus  $g$  trivalent integral metric ribbon graphs with  $n$  labelled boundary components of length  $b_1, \dots, b_n$  and  $p$  univalent vertices is equal, up to lower order terms, the polynomial*

$$\mathcal{N}_{g,n,p}(b_1, \dots, b_n) = \sum_{G \in \mathcal{R}_{g,n,p}^{\text{tri}}} \frac{1}{|\text{Aut}(G)|} \mathcal{N}_G(b_1, \dots, b_n) = N_{g,n+p}(b_1, \dots, b_n, \underbrace{0, \dots, 0}_p) + l.o.t$$

This theorem is proved via induction on the number of leaves  $p$ . We require two lemmas to carry out this induction. Define the operators  $\mathcal{D}_k$  on monomials by

$$\mathcal{D}_k \left( \prod_{i=1}^n b_i^{m_i} \right) = \frac{b_k^2}{m_k + 2} \prod_{i=1}^n b_i^{m_i}$$

and extend linearly to all polynomials. Then define the operator  $\mathcal{D} = \sum_{k=1}^n \mathcal{D}_k$ . The following extends [AEZ2, Lemma 3.5] which gives the proof for genus 0. We see that this result extends to any genus.

**Lemma 4.10.** *Suppose that the top degree term of the function  $\mathcal{N}_{g,n,p}$  is a homogeneous polynomial  $\mathcal{N}_{g,n,p}^{\text{top}}$ . Then the top degree term of the function  $\mathcal{N}_{g,n,p+1}$  is also a homogeneous polynomial  $\mathcal{N}_{g,n,p+1}^{\text{top}}$  and satisfies the relation*

$$\mathcal{N}_{g,n,p+1}^{\text{top}} = \frac{1}{2} \mathcal{D}(\mathcal{N}_{g,n,p}^{\text{top}}).$$

*Proof.* We will prove the result for the Laplace transform of the polynomials. We observe that

$$\mathcal{L}(\mathcal{D}_k(b_k^{m_k})) = \mathcal{L}\left(\frac{b_k^{m_k+2}}{m_k + 2}\right) = \frac{(m_k + 1)!}{\lambda_k^{m_k+3}} = -\frac{1}{\lambda_k} \frac{\partial}{\partial \lambda_k} \frac{m_k!}{\lambda_k^{m_k+1}} = -\frac{1}{\lambda_k} \frac{\partial}{\partial \lambda_k} \mathcal{L}(b_k^{m_k})$$

so the Laplace transform of the operator  $\mathcal{D}_k$  corresponds to  $\mathcal{L}(\mathcal{D}_k) = -\frac{1}{\lambda_k} \frac{\partial}{\partial \lambda_k}$ . Fix a ribbon graph  $G \in \mathcal{R}_{g,n,p}^{\text{tri}}$  and let  $\rho_{ij}(G)$  be the number of edges of  $G$  incident to boundaries  $i$  and  $j$ . Define the Laplace transform of  $\mathcal{N}_G$  to be

$$\widehat{\mathcal{N}}_G = \prod_{i \leq j} \left( \frac{1}{\lambda_i + \lambda_j} \right)^{\rho_{ij}(G)}.$$

so that the weighted sum over all graphs coincides with Theorem 4.3. Applying the operator  $\mathcal{L}(\mathcal{D}_k)$  gives us

$$\begin{aligned}\mathcal{L}(\mathcal{D}_k)\widehat{\mathcal{N}}_G &= -\frac{1}{\lambda_k}\widehat{\mathcal{N}}_G \frac{\partial}{\partial \lambda_k} \log \widehat{\mathcal{N}}_G \\ &= \frac{1}{\lambda_k}\widehat{\mathcal{N}}_G \sum_{i \leq j} \rho_{ij}(G) \frac{\delta_{ik} + \delta_{jk}}{\lambda_i + \lambda_j} \\ &= \frac{1}{\lambda_k}\widehat{\mathcal{N}}_G \cdot \left( \frac{\rho_{kk}(G)}{\lambda_k} + \sum_{m \neq k} \frac{\rho_{mk}(G)}{\lambda_m + \lambda_k} \right).\end{aligned}$$

We now introduce a new edge and attach one end onto an existing edge away from any vertices. The resulting graph has an additional trivalent vertex and univalent vertex, with the genus and number of boundary components preserved. Suppose the new edge is attached onto an existing edge incident to boundaries  $m$  and  $k$  in such a way that the new edge is only incident to boundary  $k$ . Denote this new graph by  $G_{m,k}$ . There is now one additional edge incident to boundaries  $m$  and  $k$  and one new edge incident to only boundary  $k$ , so the Laplace transform of  $\mathcal{N}_{G_{m,k}}$  becomes

$$\widehat{\mathcal{N}}_{G_{m,k}} = \frac{1}{2\lambda_k} \frac{1}{\lambda_m + \lambda_k} \widehat{\mathcal{N}}_G.$$

We now sum over all possible attachments of an edge onto boundary  $k$ . If the new edge is attached onto an edge only incident to boundary  $k$ , then there are two sides to which the edge can be attached. Let  $\mathcal{N}_G^{(k)}$  be the count of metrics on  $G$  with a univalent vertex added on boundary  $k$ . Then

$$\mathcal{N}_G^{(k)} = 2\rho_{kk}(G) \frac{1}{\lambda_k^2} \widehat{\mathcal{N}}_G + \sum_{m \neq k} \rho_{mk}(G) \widehat{\mathcal{N}}_{G_{m,k}} = \frac{1}{2} \mathcal{L}(\mathcal{D}_k) \widehat{\mathcal{N}}_G.$$

Summing over all  $k$ , we obtain

$$\widehat{\mathcal{N}}_G^+ = \frac{1}{2} \mathcal{L}(\mathcal{D}) \widehat{\mathcal{N}}_G$$

where  $\widehat{\mathcal{N}}_G^+$  is the sum of all Laplace transforms after adding a univalent edge to  $G$ . We note that adding a univalent vertex preserves the automorphism group of the original graph, and the resulting graph can only be obtained by adding a univalent vertex to a unique graph. Therefore,

$$\widehat{\mathcal{N}}_{g,n,p+1} = \frac{1}{2} \mathcal{L}(\mathcal{D}) \widehat{\mathcal{N}}_{g,n,p}$$

and inverting the Laplace transform gives us the statement of the Lemma.  $\square$

**Lemma 4.11.** *The polynomials  $N_{g,n}$  satisfy the relations*

$$N_{g,n+p+1}(b_1, \dots, b_n, \underbrace{0, \dots, 0}_{p+1}) = \frac{1}{2} \mathcal{D}(N_{g,n+p}(b_1, \dots, b_n, \underbrace{0, \dots, 0}_p)).$$

*Proof.* We expand both side in terms of correlators and note that the sum vanishes if the indices of  $\mathbf{d}$  corresponding to slots with 0 are nonzero.

$$\begin{aligned} N_{g,n+p+1}(b_1, \dots, b_n, \underbrace{0, \dots, 0}_{p+1}) &= \sum_{\substack{\mathbf{d} \in \mathbb{N}_0^{n+p+1} \\ |\mathbf{d}|=3g-3+n+p+1}} \frac{\langle \tau_{d_1} \cdots \tau_{d_{n+p+1}} \rangle}{2^{5g-6+2(n+p+1)} \mathbf{d}!} \prod_{i=1}^n b_i^{2d_i} \prod_{j=1}^{p+1} 0^{2d_{n+j}} \\ &= \sum_{\substack{\mathbf{d} \in \mathbb{N}_0^n \\ |\mathbf{d}|=3g-3+n+p+1}} \frac{\langle \tau_{d_1} \cdots \tau_{d_n} \tau_0^{p+1} \rangle}{2^{5g-6+2(n+p+1)} \mathbf{d}!} \prod_{i=1}^n b_i^{2d_i} \end{aligned}$$

For the right hand side, we invoke the string equation to obtain a matching expression.

$$\begin{aligned} &\frac{1}{2} \mathcal{D}(N_{g,n+p}(b_1, \dots, b_n, \underbrace{0, \dots, 0}_p)) \\ &= \frac{1}{2} \mathcal{D} \left( \sum_{\substack{\mathbf{d} \in \mathbb{N}_0^{n+p} \\ |\mathbf{d}|=3g-3+n+p}} \frac{\langle \tau_{d_1} \cdots \tau_{d_{n+p}} \rangle}{2^{5g-6+2(n+p)} \mathbf{d}!} b_1^{2d_1} \cdots b_n^{2d_n} 0^{2d_{n+1}} \cdots 0^{2d_{n+p}} \right) \\ &= \frac{1}{2} \mathcal{D} \left( \sum_{\substack{\mathbf{d} \in \mathbb{N}_0^n \\ |\mathbf{d}|=3g-3+n+p}} \frac{\langle \tau_{d_1} \cdots \tau_{d_n} \tau_0^p \rangle}{2^{5g-6+2(n+p)} \mathbf{d}!} b_1^{2d_1} \cdots b_n^{2d_n} \right) \\ &= \frac{1}{2} \sum_{\substack{\mathbf{d} \in \mathbb{N}_0^n \\ |\mathbf{d}|=3g-3+n+p}} \sum_{j=1}^n \frac{\langle \tau_{d_1} \cdots \tau_{d_n} \tau_0^p \rangle}{2^{5g-6+2(n+p)} \mathbf{d}!} b_1^{2d_1} \cdots b_{j-1}^{2d_{j-1}} \frac{b_j^{2(d_j+1)}}{2(d_j+1)} b_{j+1}^{2d_{j+1}} \cdots b_n^{2d_n} \\ &= \sum_{\substack{\mathbf{d} \in \mathbb{N}_0^n \\ |\mathbf{d}|=3g-3+n+p}} \sum_{j=1}^n \frac{\langle \tau_{d_1} \cdots \tau_{d_{j-1}} \tau_{(d_j+1)-1} \tau_{d_{j+1}} \cdots \tau_{d_n} \tau_0^p \rangle}{2^{5g-6+2(n+p+1)} d_1! \cdots d_{j-1}! (d_j+1)! d_{j+1}! \cdots d_n!} \\ &\quad b_1^{2d_1} \cdots b_{j-1}^{2d_{j-1}} b_j^{2(d_j+1)} b_{j+1}^{2d_{j+1}} \cdots b_n^{2d_n} \\ &= \sum_{\substack{\mathbf{d} \in \mathbb{N}_0^n \\ |\mathbf{d}|=3g-3+n+p+1}} \sum_{j=1}^n \frac{\langle \tau_{d_1} \cdots \tau_{d_{j-1}} \tau_{d_j-1} \tau_{d_{j+1}} \cdots \tau_{d_n} \tau_0^p \rangle}{2^{5g-6+2(n+p+1)} \mathbf{d}!} b_1^{2d_1} \cdots b_n^{2d_n} \\ &= \sum_{\substack{\mathbf{d} \in \mathbb{N}_0^n \\ |\mathbf{d}|=3g-3+n+p+1}} \frac{\langle \tau_{d_1} \cdots \tau_{d_n} \tau_0^{p+1} \rangle}{2^{5g-6+2(n+p+1)} \mathbf{d}!} b_1^{2d_1} \cdots b_n^{2d_n} \quad \square \end{aligned}$$

*Proof of theorem.* We proceed by induction. The base case when  $p = 0$  corresponds to Theorem 4.4:

$$\mathcal{N}_{g,n,0} = \mathcal{N}_{g,n} = N_{g,n} + l.o.t$$

Assume the relation holds for some  $p$ . Combining the above two lemmas gives us

$$\begin{aligned}\mathcal{N}_{g,n,p+1}(b_1, \dots, b_n) &= \frac{1}{2} \mathcal{D}(\mathcal{N}_{g,n,p}(b_1, \dots, b_n)) + l.o.t \\ &= \frac{1}{2} \mathcal{D}(N_{g,n+p}(b_1, \dots, b_n, \underbrace{0, \dots, 0}_p)) + l.o.t \\ &= N_{g,n+p+1}(b_1, \dots, b_n, \underbrace{0, \dots, 0}_{p+1}) + l.o.t.\end{aligned}\quad \square$$

**Corollary 4.12.** *Let  $b_1, \dots, b_n$  be positive integers such that  $\sum_{i=1}^n b_i$  is even. Let  $p$  be a non-negative integer and let  $N = n + p - 3$ . Then*

$$\mathcal{N}_{0,n,p}(b_1, \dots, b_n) = \frac{1}{N! 2^{2N}} \sum_{\substack{\mathbf{d} \in \mathbb{N}_0^n \\ |\mathbf{d}|=N}} \binom{N}{d_1, \dots, d_n}^2 b_1^{2d_1} \cdots b_n^{2d_n} + l.o.t. \quad (4.9)$$

When  $n = 1$  with  $b$  even, we have the special case

$$\mathcal{N}_{0,1,p}(b) = \frac{b^{2(p-2)}}{(p-2)! 2^{2(p-2)}}. \quad (4.10)$$

**Remark 4.11.** Equation (4.9) mirrors [AEZ2, Theorem 1.1] which was obtained using combinatorial identities. There is a difference by a factor of a power of 2 since we are counting integer metrics on ribbon graphs, whereas the authors of [AEZ2] count half-integer metrics. In fact, we should be also be counting half-integer metric ribbon graphs, however, after rescaling our variables in Section 3.4, the factor of a power of 2 has been included as part of a prefactor in the volume formula.

We are now ready to recast the statement of Lemma 3.8 in terms of Kontsevich volume polynomials for principal strata. Note that working with undecorated stable graphs is sufficient since the number of simple zeros on each singular layer is completely determined.

**Theorem 4.13.** *The Masur-Veech volume of the principal stratum  $\mathcal{Q}(-1^n, 1^{4g-4+n})$  of genus  $g$  differentials with  $n$  simple poles is given by*

$$\text{Vol } \mathcal{Q}(-1^n, 1^{4g-4+n}) = \sum_{\Gamma \in \mathcal{G}_{g,n}} \text{Vol}(\Gamma) = C_{g,n} \sum_{\Gamma \in \mathcal{G}_{g,n}} \mathcal{Z}(P_\Gamma) = C_{g,n} \sum_{\Gamma \in \mathcal{G}_{g,n}/S_n} n_\Gamma \cdot \mathcal{Z}(P_\Gamma)$$

where

$$P_\Gamma = \frac{1}{2^{\#V(\Gamma)-1}} \cdot \frac{1}{|\text{Aut}(\Gamma)|} \cdot \prod_{e \in E(\Gamma)} b_e \cdot \prod_{v \in V(\Gamma)} N_{g_v, n_v + p_v}((b_e)_{e \in E_v(\Gamma)}, 0^{p_v})$$

and

$$C_{g,n} = \frac{2^{6g-5+2n} \cdot (4g-4+n)!}{(6g-7+2n)!}.$$

## 4.4 Examples of volume computations

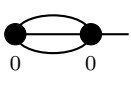
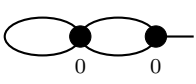
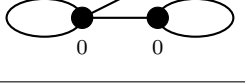
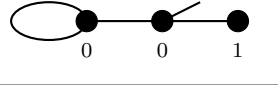
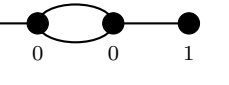
**Proposition 4.14.** *Using Theorem 3.12, we have the following formula for the volume of principal quadratic strata in genus 0:*

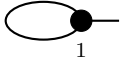
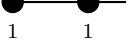
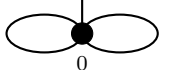
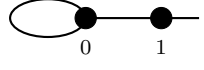
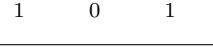
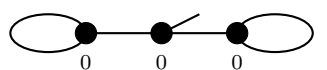
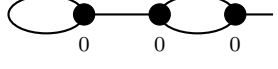
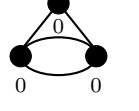
$$\text{Vol } \mathcal{Q}_{0,n} = \text{Vol } \mathcal{Q}(-1^n, 1^{n-4}) = 4 \left( \frac{\pi^2}{2} \right)^{n-3}.$$

Examples of small computations for  $\mathcal{Q}_{1,2}$  and  $\mathcal{Q}_{2,0}$  can be found in [DGZZ1]. We provide further computations for  $\mathcal{Q}_{2,1}$  and  $\mathcal{Q}_{1,3}$ . The Kontsevich volume polynomials for small  $g$  and  $n$  where  $2g + n - 2 > 0$  are given below.

$g$	$n$	$N_{g,n}(b_1, \dots, b_n)$
0	3	1
0	4	$\frac{1}{4}(b_1^2 + b_2^2 + b_3^2 + b_4^2)$
0	5	$\frac{1}{32} \sum_{i=1}^5 b_i^4 + \frac{1}{8} \sum_{1 \leq i < j \leq 5} b_i^2 b_j^2$
1	1	$\frac{1}{48} \cdot b_1^2$
1	2	$\frac{1}{348} (b_1^2 + b_2^2)^2$
1	3	$\frac{1}{4608} \sum_{i=1}^3 b_i^6 + \frac{1}{768} \sum_{i \neq j} b_i^4 b_j^2 + \frac{1}{384} \cdot b_1^2 b_2^2 b_3^2$

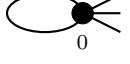
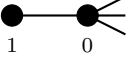
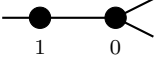
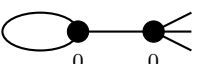
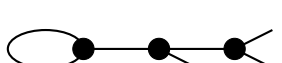
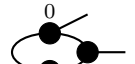
**Example 4.12.** Volume of  $\mathcal{Q}_{2,1}$ : The first two constants are  $\frac{1}{2\#V(\Gamma)}$  and  $\frac{1}{|\text{Aut}(\Gamma)|}$ .

$\Gamma \in \mathcal{G}_{2,1}$	$n_\Gamma \cdot P_\Gamma \xrightarrow{C_{2,1} \cdot \mathcal{Z}} \text{Vol}(\Gamma)$
	$\frac{1}{2} \cdot \frac{1}{6} \cdot b_1 b_2 b_3 \cdot N_{0,3}(b_1, b_2, b_3) N_{0,4}(b_1, b_2, b_3, 0)$ $= \frac{1}{48} \cdot b_1^3 b_2 b_3 + \frac{1}{48} \cdot b_1 b_2^3 b_3 + \frac{1}{48} \cdot b_1 b_2 b_3^3 \mapsto \frac{4}{2835} \cdot \pi^8$
	$\frac{1}{2} \cdot \frac{1}{4} \cdot b_1 b_2 b_3 \cdot N_{0,4}(b_1, b_1, b_2, b_3) N_{0,3}(b_2, b_3, 0)$ $= \frac{1}{16} \cdot b_1^3 b_2 b_3 + \frac{1}{32} \cdot b_1 b_2^3 b_3 + \frac{1}{32} \cdot b_1 b_2 b_3^3 \mapsto \frac{8}{2835} \cdot \pi^8$
	$\frac{1}{2} \cdot \frac{1}{4} \cdot b_1 b_2 b_3 \cdot N_{0,4}(b_1, b_1, b_2, 0) N_{0,3}(b_2, b_3, b_3)$ $= \frac{1}{16} \cdot b_1^3 b_2 b_3 + \frac{1}{32} \cdot b_1 b_2^3 b_3 \mapsto \frac{2}{945} \cdot \pi^8$
	$\frac{1}{4} \cdot \frac{1}{2} \cdot b_1 b_2 b_3 \cdot N_{0,3}(b_1, b_1, b_2) N_{0,3}(b_2, b_3, 0) N_{1,1}(b_3)$ $= \frac{1}{384} \cdot b_1 b_2 b_3^3 \mapsto \frac{1}{17010} \cdot \pi^8$
	$\frac{1}{4} \cdot \frac{1}{2} \cdot b_1 b_2 b_3 \cdot N_{0,3}(b_1, b_2, 0) N_{0,3}(b_1, b_2, b_3) N_{1,1}(b_3)$ $= \frac{1}{384} \cdot b_1 b_2 b_3^3 \mapsto \frac{1}{17010} \cdot \pi^8$
	$c_3(\mathcal{Q}_{2,1}) = \frac{11}{1701} \cdot \pi^8$

$\Gamma \in \mathcal{G}_{2,1}$	$P_\Gamma \xrightarrow{C_{2,1}, \mathcal{Z}} \text{Vol}(\Gamma)$
	$1 \cdot \frac{1}{2} \cdot b_1 \cdot N_{1,3}(b_1, b_1, 0)$ $= \frac{7}{4608} \cdot b_1^7 \mapsto \frac{4}{405} \cdot \pi^8$
	$\frac{1}{2} \cdot 1 \cdot b_1 \cdot N_{1,1}(b_1)N_{1,2}(b_1, 0)$ $= \frac{1}{36864} \cdot b_1^7 \mapsto \frac{1}{5670} \cdot \pi^8$
	$c_1(\mathcal{Q}_{2,1}) = \frac{19}{1890} \cdot \pi^8$
	$1 \cdot \frac{1}{8} \cdot b_1 b_2 \cdot N_{0,5}(b_1, b_1, b_2, b_2, 0)$ $= \frac{3 \cdot b_1^5 \cdot b_2}{128} + \frac{1}{16} \cdot b_1^3 b_2^3 + \frac{3}{128} \cdot b_1 b_2^5 \mapsto \frac{512}{33075} \cdot \pi^8$
	$\frac{1}{2} \cdot \frac{1}{2} \cdot b_1 b_2 \cdot N_{1,2}(b_1, b_2) \cdot N_{0,3}(b_1, b_2, 0)$ $= \frac{1}{1536} \cdot b_1^5 b_2 + \frac{1}{768} \cdot b_1^3 b_2^3 + \frac{1}{1536} \cdot b_1 b_2^5 \mapsto \frac{121}{297675} \cdot \pi^8$
	$\frac{1}{2} \cdot \frac{1}{2} \cdot b_1 b_2 \cdot N_{0,3}(b_1, b_1, b_2)N_{1,1}(b_2, 0)$ $= \frac{1}{1536} \cdot b_1 b_2^5 \mapsto \frac{2}{11907} \cdot \pi^8$
	$\frac{1}{2} \cdot \frac{1}{2} \cdot b_1 b_2 \cdot N_{0,4}(b_1, b_1, b_2, 0)N_{1,1}(b_2)$ $= \frac{1}{384} \cdot b_1^3 b_2^3 + \frac{1}{768} \cdot b_1 b_2^5 \mapsto \frac{142}{297675} \cdot \pi^8$
	$\frac{1}{4} \cdot \frac{1}{2} \cdot b_1 b_2 \cdot N_{1,1}(b_1)N_{0,3}(b_1, b_2)N_{1,1}(b_2)$ $= \frac{1}{18432} \cdot b_1^3 b_2^3 \mapsto \frac{1}{340200} \cdot \pi^8$
	$c_2(\mathcal{Q}_{2,1}) = \frac{25}{1512} \cdot \pi^8$
	$\frac{1}{4} \cdot \frac{1}{8} \cdot b_1 b_2 b_3 b_4 \cdot N_{0,3}(b_1, b_1, b_2)N_{0,3}(b_2, b_3, 0)N_{0,3}(b_3, b_4, b_4)$ $= \frac{1}{32} \cdot b_1 b_2 b_3 b_4 \mapsto \frac{1}{3402} \cdot \pi^8$
	$\frac{1}{4} \cdot \frac{1}{4} \cdot b_1 b_2 b_3 b_4 \cdot N_{0,3}(b_1, b_1, b_2)N_{0,3}(b_2, b_3, b_4)N_{0,3}(b_3, b_4, 0)$ $= \frac{1}{16} \cdot b_1 b_2 b_3 b_4 \mapsto \frac{1}{1701} \cdot \pi^8$
	$\frac{1}{4} \cdot \frac{1}{4} \cdot b_1 b_2 b_3 b_4 \cdot N_{0,3}(b_1, b_2, 0)N_{0,3}(b_1, b_3, b_4)N_{0,3}(b_2, b_3, b_4)$ $= \frac{1}{16} \cdot b_1 b_2 b_3 b_4 \mapsto \frac{1}{1701} \cdot \pi^8$
	$c_4(\mathcal{Q}_{2,1}) = \frac{5}{3402} \cdot \pi^8$

$$\text{Vol } \mathcal{Q}_{2,1} = c_1(\mathcal{Q}_{2,1}) + c_2(\mathcal{Q}_{2,1}) + c_3(\mathcal{Q}_{2,1}) + c_4(\mathcal{Q}_{2,1}) = \frac{29}{840} \cdot \pi^8.$$

**Example 4.13.** Volume of  $\mathcal{Q}_{1,3}$ . The first three constants are  $n_\Gamma$ ,  $\frac{1}{2\#V(\Gamma)-1}$  and  $\frac{1}{|\text{Aut}(\Gamma)|}$ .

$\Gamma \in \mathcal{G}_{1,3}/S_3$	$n_\Gamma \cdot P_\Gamma \xrightarrow{C_{1,3}, \mathcal{Z}} n_\Gamma \cdot \text{Vol}(\Gamma)$
	$1 \cdot 1 \cdot \frac{1}{2} \cdot b_1 \cdot N_{0,5}(b_1, b_1, 0, 0, 0) = \frac{3}{32} \cdot b_1^5 \mapsto \frac{8}{105} \cdot \pi^6$
	$1 \cdot \frac{1}{2} \cdot 1 \cdot b_1 \cdot N_{1,1}(b_1) \cdot N_{0,4}(b_1, 0, 0, 0) = \frac{1}{384} \cdot b_1^5 \mapsto \frac{2}{945} \cdot \pi^6$
	$3 \cdot \frac{1}{2} \cdot 1 \cdot b_1 \cdot N_{1,2}(b_1, 0) \cdot N_{0,3}(b_1, 0, 0) = \frac{1}{256} \cdot b_1^5 \mapsto \frac{1}{315} \cdot \pi^6$
	$c_1(\mathcal{Q}_{1,3}) = \frac{11}{135} \cdot \pi^6$
	$3 \cdot \frac{1}{2} \cdot \frac{1}{2} \cdot N_{0,3}(b_1, b_2) \cdot N_{0,4}(b_1, b_2, 0, 0) = \frac{3}{16} \cdot b_1^3 b_2 + \frac{3}{16} \cdot b_1 b_2^3 \mapsto \frac{2}{75} \cdot \pi^6$
	$1 \cdot \frac{1}{2} \cdot \frac{1}{2} \cdot b_1 b_2 \cdot N_{0,3}(b_1, b_1, b_2) \cdot N_{0,3}(b_2, 0, 0, 0) = \frac{1}{16} \cdot b_1 b_2^3 \mapsto \frac{1}{225} \cdot \pi^6$
	$3 \cdot \frac{1}{2} \cdot \frac{1}{2} \cdot b_1 b_2 \cdot N_{0,4}(b_1, b_1, b_2, 0) \cdot N_{0,3}(b_2, 0, 0, 0) = \frac{3}{8} \cdot b_1^3 b_2 + \frac{3}{16} \cdot b_1 b_2^3 \mapsto \frac{1}{25} \cdot \pi^6$
	$3 \cdot \frac{1}{4} \cdot 1 \cdot b_1 b_2 \cdot N_{1,1}(b_1) \cdot N_{0,3}(b_1, b_2, 0) \cdot N_{0,3}(b_2, 0, 0, 0) = \frac{1}{64} \cdot b_1^3 b_2 \mapsto \frac{1}{900} \cdot \pi^6$
	$c_2(\mathcal{Q}_{1,3}) = \frac{13}{180} \cdot \pi^6$
	$3 \cdot \frac{1}{4} \cdot \frac{1}{2} \cdot b_1 b_2 b_3 \cdot N_{0,3}(b_1, b_2, 0) \cdot N_{0,3}(b_1, b_2, b_3) \cdot N_{0,3}(b_3, 0, 0, 0) = \frac{3}{8} \cdot b_1 b_2 b_3 \mapsto \frac{1}{90} \cdot \pi^6$
	$3 \cdot \frac{1}{4} \cdot \frac{1}{2} \cdot b_1 b_2 b_3 \cdot N_{0,3}(b_1, b_1, b_2) \cdot N_{0,3}(b_2, b_3, 0) \cdot N_{0,3}(b_3, 0, 0, 0) = \frac{3}{8} \cdot b_1 b_2 b_3 \mapsto \frac{1}{90} \cdot \pi^6$
	$1 \cdot \frac{1}{4} \cdot \frac{1}{6} \cdot b_1 b_2 b_3 \cdot N_{0,3}(b_1, b_2, 0) N_{0,3}(b_2, b_3, 0) \cdot N_{0,3}(b_1, b_3, 0) = \frac{1}{4} \cdot b_1 b_2 b_3 \mapsto \frac{1}{135} \cdot \pi^6$
	$c_3(\mathcal{Q}_{1,3}) = \frac{4}{135} \cdot \pi^6$

$$\text{Vol } \mathcal{Q}_{1,3} = c_1(\mathcal{Q}_{1,3}) + c_2(\mathcal{Q}_{1,3}) + c_3(\mathcal{Q}_{1,3}) = \frac{11}{60} \cdot \pi^6.$$

**Example 4.14.** Let us consider one-cylinder volume contributions in  $\mathcal{Q}_{0,n}$ . The unlabeled stable graphs in  $\mathcal{G}_{0,n}(1)/S_n$  are of the form  $\Gamma_{n_1, n_2}$  where  $n = n_1 + n_2$ . The number of leg labelings is  $n_{\Gamma_{n_1, n_2}} = \binom{n}{n_1} = \binom{n}{n_2}$ . Note that  $\Gamma_{n_1, n_2} = \Gamma_{n_2, n_1}$  and

$$|\text{Aut}(\Gamma_{n_1, n_2})| = \begin{cases} 2, & n_1 = n_2 \\ 1, & n_1 \neq n_2 \end{cases}. \quad (4.11)$$



Using Corollary 4.12, the volume polynomial  $P_{\Gamma_{n_1, n_2}}$  is given by

$$\frac{1}{2} \cdot \frac{1}{|\text{Aut}(\Gamma_{n_1, n_2})|} \cdot b \cdot \mathcal{N}_{0,1,n_1}(b) \cdot \mathcal{N}_{0,1,n_2}(b) = \frac{1}{2} \cdot \frac{1}{|\text{Aut}(\Gamma_{n_1, n_2})|} \cdot \frac{b^{2n-7}}{(n_1-2)!(n_2-2)!2^{2(n-4)}}$$

The volume contribution is then

$$\begin{aligned} c_1(\mathcal{Q}_{0,n}) &= C_{0,n} \sum_{\Gamma_{n_1, n_2} \in \mathcal{G}_{0,n}(1)/S_n} n_{\Gamma_{n_1, n_2}} \cdot \mathcal{Z}(P_{\Gamma_{n_1, n_2}}) \\ &= \frac{2^{2n-5}(n-4)!}{(2n-7)!} \cdot \frac{(2n-7)! \cdot \zeta(2n-6)}{2^{2n-7}} \cdot \\ &\quad \sum_{\Gamma_{n_1, n_2} \in \mathcal{G}_{0,n}(1)/S_n} \frac{1}{|\text{Aut}(\Gamma_{n_1, n_2})|} \cdot \binom{n}{n_1} \cdot \frac{1}{(n_1-2)!(n-n_1-2)!} \\ &= 4 \cdot \zeta(2n-6) \cdot \frac{1}{2} \cdot \sum_{n_1=2}^{n-2} \binom{n}{n_1} \cdot \binom{n-4}{n_1-2} \\ &= 2 \cdot \zeta(2n-6) \cdot \binom{2n-4}{n-2} \end{aligned}$$

where in the final equality, we have used the identity  $\sum_{k=0}^n \binom{x}{k} \binom{y}{n-k} = \binom{x+y}{n}$ . Using Example 3.32, we also obtain the volume contribution in  $\mathcal{Q}_{0,n}$  coming from square-tiled surfaces constructed from a single band of squares:

$$\text{cyl}_1(\mathcal{Q}_{0,n}) = 2 \cdot \binom{2n-4}{n-2}.$$

# Chapter 5

## Application of Volumes

In this chapter, we briefly discuss some applications of Masur-Veech volumes.

### 5.1 Enumeration of meanders

This section will mostly follow results from [DGZZ2]. Meanders are combinatorial objects that arise in various fields of mathematics, physics, and biology (for example, polymer folding models). A *meander* is a simple closed curve in the plane transversely intersecting the horizontal axis, considered up to isotopy of the plane preserving this axis. The *order* of a meander is the integer  $N$  such that it intersects the horizontal axis  $2N$  times. There are many unsolved problems regarding meanders. For instance, let  $M(N)$  be the number of meanders of order  $N$ . An exact asymptotic count for  $M(N)$  is unknown, and the growth rate remains conjectural, although there are sharp theoretical bounds and approximations from computer simulations. If one however fixes some combinatorial data of the meanders, such a formula for the asymptotic count becomes possible.

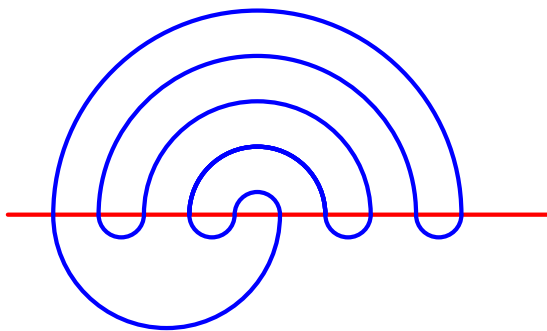


Figure 5.1: A meander with a maximal arc and five minimal arcs.

**Definition 5.1.** An *arc* of a meander is a connected portion of the curve lying completely above or below the horizontal axis. A *maximal arc* is an arc joining the leftmost and rightmost crossings. A *minimal arc* is an arc joining two adjacent crossings. Define  $M_p^+(N)$  to be the number of meanders with a maximal arc having at most  $2N$  crossings and exactly  $p$  minimal crossings.

**Theorem 5.1** ([DGZZ2, Theorem 1.1]). *For any fixed  $p$ , the number  $M_p^+(N)$  has the following asymptotics as  $N \rightarrow \infty$ :*

$$M_p^+(N) = 2(p+1) \cdot \frac{\text{cyl}_{1,1}(\mathcal{Q}(1^{p-3}, -1^{p+1}))}{(p+1)!(p-3)!} \cdot \frac{N^{2p-4}}{4p-8} + o(N^{2p-4}) \quad (5.1)$$

We require the following result regarding the equidistribution of certain subsets of square-tiled surfaces. The authors in [DGZZ2] prove more general results on arithmetic invariant suborbifolds, which are special subspaces of strata, however we will only be considering the special cases of these results to apply to meander enumeration. We first introduce some preliminary definitions.

**Definition 5.2.** Let  $\mathcal{L}$  be the lattice of square-tiled surfaces in a connected component  $\mathcal{C}$  of a stratum, and let  $\mathcal{D}$  be a subset of  $\mathcal{L}$ . We say  $\mathcal{D}$  has *uniform density* in  $\mathcal{C}$  if there exists a number  $\delta(\mathcal{D})$  such that for any subset  $U \subseteq \mathcal{C}$ , we have the asymptotic

$$\#(U \cap (\varepsilon\mathcal{D})) \sim \delta(\mathcal{D}) \frac{\nu(U)}{\varepsilon^{2d}}$$

where  $\nu$  is the Masur-Veech measure defined in Section 2.3 and  $d = \dim_{\mathbb{R}} \mathcal{C}$ .

**Example 5.3.** Let  $\mathcal{D} = \mathcal{L}$  be the full lattice of square-tiled surfaces in a stratum  $\mathcal{C}$ . By replacing  $\mathcal{H}_1(\mu)$  with any subset  $U$  in Equation (3.2), we obtain

$$\lim_{\varepsilon \rightarrow 0} \varepsilon^{2d} \cdot \#(U \cap (\varepsilon\mathcal{L})) = \nu(U)$$

where . In particular,  $\delta(\mathcal{L}) = 1$  so the full lattice has uniform density.

Let  $\mathcal{ST}_{\mathcal{D}}(\mathcal{C}, 2N)$  be the subset of square-tiled surfaces in  $\mathcal{D}$  tiled from at most  $2N$  squares. We will be interested in the cases when  $\mathcal{D}$  is the set of square-tiled surfaces in  $\mathcal{Q}(\mu)$  arranged into a single band of horizontal or vertical squares. Denote these subsets by  $\mathcal{D}_1^h$  and  $\mathcal{D}_1^v$  respectively. We also recall that

$$\#\mathcal{ST}(\mathcal{Q}(\mu), 2N) \sim \frac{1}{2d} \cdot \text{Vol } \mathcal{Q}(\mu) \cdot N^d$$

and we have a similar asymptotic for the 1-cylinder volume contributions:

$$\#\mathcal{ST}_{\mathcal{D}_1^h}(\mathcal{Q}(\mu), 2N) = \#\mathcal{ST}_{\mathcal{D}_1^v}(\mathcal{Q}(\mu), 2N) \sim \frac{1}{2d} \cdot \text{cyl}_1 \mathcal{Q}(\mu) \cdot N^d$$

$$\#\mathcal{ST}_{\mathcal{D}_1^h \cap \mathcal{D}_1^v}(\mathcal{Q}(\mu), 2N) \sim \frac{1}{2d} \cdot \text{cyl}_{1,1}(\mathcal{Q}(\mu)) \cdot N^d.$$

A subset  $\mathcal{D}$  of  $\mathcal{L}$  has a density  $\delta(\mathcal{D})$  if and only if

$$\#\mathcal{ST}_{\mathcal{D}}(\mathcal{C}, N) \sim \delta(\mathcal{D}) \cdot \frac{\text{Vol}(\mathcal{C})}{2d}$$

giving us

$$\text{cyl}_1(\mathcal{Q}(\mu)) = \delta(\mathcal{D}_1^h) \cdot \text{Vol } \mathcal{Q}(\mu) = \delta(\mathcal{D}_1^v) \cdot \text{Vol } \mathcal{Q}(\mu).$$

For two subsets  $\mathcal{D}$  and  $\mathcal{D}'$  of  $\mathcal{L}$  with uniform density, it is generally false that

$$\delta(\mathcal{D} \cap \mathcal{D}') = \delta(\mathcal{D}) \cdot \delta(\mathcal{D}').$$

We now set up the definitions necessary to describe special subsets that satisfy this equality. Using cohomological coordinates defined in Section 2.3, consider the chart map into the canonical decomposition

$$\Psi : \mathcal{Q}(\mu) \rightarrow H_-^1(\widehat{X}, \widehat{\Sigma}; \mathbb{C}) = H_-^1(\widehat{X}, \widehat{\Sigma}; \mathbb{R}) \oplus H_-^1(\widehat{X}, \widehat{\Sigma}; i\mathbb{R}).$$

Let  $\pi_{\text{Re}}$  and  $\pi_{\text{Im}}$  be the respective projection maps. The *Re-foliation* and *Im-foliation* are the level sets of  $\pi_{\text{Im}} \circ \Psi$  and  $\pi_{\text{Re}} \circ \Psi$  respectively. Geometrically, the complex numbers representing the edges of a polygon presentation of a surface lying in the Re-foliation (resp. Im-foliation) all have identical imaginary (resp. real) part.

**Definition 5.4.** Let  $X$  be a square-tiled in  $\mathcal{D}$  and let  $L_{\text{Re}}(X)$  resp.  $L_{\text{Im}}(X)$  be the leafs in the Re-foliation resp. Im-foliation passing through  $X$ . A subset  $\mathcal{D}$  of square-tiled surface is called *Re-invariant* resp. *Im-invariant* if  $L_{\text{Re}}(X) \subseteq \mathcal{D}$  and  $L_{\text{Im}}(X) \subseteq \mathcal{D}$  for all  $X \in \mathcal{D}$ .

**Theorem 5.2** ([DGZZ2, Theorem 4.16]). *Let  $\mathcal{D}^h$  and  $\mathcal{D}^v$  be subsets of  $\mathcal{L}$  that are respectively Re-invariant and Im-invariant. Then  $\mathcal{D}^h, \mathcal{D}^v$  and  $\mathcal{D}^h \cap \mathcal{D}^v$  admit uniform density and*

$$\delta(\mathcal{D}^h \cap \mathcal{D}^v) = \delta(\mathcal{D}^h) \cdot \delta(\mathcal{D}^v).$$

In particular, our subsets of interest  $\mathcal{D}_1^h$  and  $\mathcal{D}_1^v$  are Re-Invariant and Im-invariant respectively. By Theorem 5.2, we obtain

$$\text{cyl}_{1,1}(\mathcal{Q}(\mu)) = \delta(\mathcal{D}_1^h \cap \mathcal{D}_1^v) \text{Vol } \mathcal{Q}(\mu) = \delta(\mathcal{D}_1^h) \cdot \delta(\mathcal{D}_1^v) \cdot \text{Vol } \mathcal{Q}(\mu) = \frac{\text{cyl}_1(\mathcal{Q}(\mu))^2}{\text{Vol } \mathcal{Q}(\mu)}.$$

One can interpret this equality as the independence of the distribution of one horizontal and one vertical cylinder square-tiled surface. In particular, we have the ratio

$$\frac{\text{cyl}_{1,1}(\mathcal{Q}(\mu))}{\text{cyl}_1(\mathcal{Q}(\mu))} = \frac{\text{cyl}_1(\mathcal{Q}(\mu))}{\text{Vol } \mathcal{Q}(\mu)}.$$

In the principal stratum, combining the results from Example 4.14 and Proposition 4.14 gives us

$$\text{cyl}_{1,1}(\mathcal{Q}(-1^n, 1^{4g-4+n})) = \left(\frac{2}{\pi^2}\right)^{n-3} \binom{2n-4}{n-2}^2.$$

**Lemma 5.3** ([DGZZ2, Lemma 3.1]). *There is a natural bijection between meanders in the plane and square-tiled surfaces with a marked oriented vertical side of one of the squares that have a single horizontal and vertical band of squares.*

The  $p$  minimal arcs and the single maximal arc correspond to simple poles on the square-tiled surface. In particular, there are  $p + 1$  simple poles and  $p - 3$  simple zeros in the principal stratum.

In Equation (5.1), the value

$$\frac{\text{cyl}_{1,1}(\mathcal{Q}(1^{p-3}, -1^{p+1}))}{4p - 8} \cdot N^{4p-8}$$

counts the number of square-tiled surface with a single horizontal and a single vertical band of cylinders constructed from at most  $2N$  squares. This corresponds to meanders of order at most  $N$ . The factors  $(p + 1)!(p - 3)!$  convert the labelled counts into unlabelled counts. Finally, the factor  $2(p + 1)$  accounts for the number of markings for the maximal arc.

## 5.2 Siegel-Veech constants and Lyapunov exponents

In the study of flat surfaces, one may be interested in counting the number of closed geodesics of bounded length. We have seen in Section 2.1 that geodesics appear in families, each forming a cylinder embedded in the surface. Thus, we can consider counting the embeddings of cylinders of bounded circumference in a flat surface. For a cylinder  $\text{cyl}$ , denote by  $w(\text{cyl})$  its circumference. Let  $X$  be either a translation or half-translation surface. Let  $L > 0$ , and define the quantity

$$N_{\text{area}}(X, L) = \frac{1}{\text{Area}(X)} \sum_{\substack{\text{cyl} \subseteq X \\ w(\text{cyl}) \leq L}} \text{Area}(\text{cyl})$$

which is well-defined since the number of cylinders in  $X$  of bounded circumference is finite. This quantity represents the number of families of geodesics of length at most  $L$ , weighted by the area of the cylinder which they form. One can interpret this quantity as the density of geodesics of length at most  $L$  on the flat surface. Eskin and Masur proved the following result.

**Theorem 5.4.** *For non-negative integers  $g, n$  such that  $2g + n > 3$ , there exists a positive constant  $c_{\text{area}}(\mathcal{Q}_{g,n})$  such that*

$$\frac{1}{\pi L^2} \int_{\mathcal{Q}_{g,n}^{\text{Area}=1}} N_{\text{area}}(X, L) d\nu_1(X) = \text{Vol } \mathcal{Q}_{g,n} \cdot c_{\text{area}}(\mathcal{Q}_{g,n}).$$

The constant  $c_{\text{area}}(\mathcal{Q}_{g,n})$  is called the Siegel-Veech constant. In [DGZZ1], they showed that this constant satisfies the relation

$$\text{Vol } \mathcal{Q}_{g,n} \cdot c_{\text{area}}(\mathcal{Q}_{g,n}) = \frac{3}{\pi^2} \sum_{\Gamma \in \mathcal{G}_{g,n}} \mathcal{Z}(\partial_\Gamma P_\Gamma) \quad (5.2)$$

where  $\partial_\Gamma$  is a differential operator dependent on the structure of the stable graph  $\Gamma$ .

Many problems on a translation surface can be solved by studying its orbit under the  $\text{GL}_2(\mathbb{R})$  action, and the closure of this orbit. This construction has been extensively researched in recent years, with many breakthroughs linking dynamical problems to other areas of mathematics, such as algebraic geometry and number theory. The survey [Wr] provides an excellent introduction to these ideas.

Let  $g \in \text{GL}_2(\mathbb{R})$  and consider the vectors in  $\mathbb{R}^2$  that define the edges of a translation surface  $(X, \omega)$  in the polygon presentation. Then  $g \cdot (X, \omega)$  is defined to be the translation surface given by the collection of polygons obtained by acting on the vectors defining  $(X, \omega)$  by  $g$ . A special one-parameter family of deformations is generated by the diagonal subgroup

$$g_t = \begin{pmatrix} e^t & 0 \\ 0 & e^{-t} \end{pmatrix}$$

called the *Teichmuller geodesic flow*. The name comes from the fact that the projection of this flow onto Teichmuller space is a geodesic with respect to the Teichmuller metric.

We now give an informal description of Lyapunov exponents. These numbers show up in many dynamical problems, for example, diffusion rates in the wind-tree billiards [DHL], [DZ]. A proper treatment can be found in [Zo, Section 5.8]. Lyapunov exponents can be considered as certain abstract constants

$$\lambda_1 \geq \cdots \geq \lambda_{2g}$$

depending on the stratum of an Abelian or quadratic differentials. Roughly speaking, they are related to the logarithms of eigenvalues of the linear action on the fibres of the Hodge bundle, induced by applying the Teichmuller geodesic flow. The Kontsevich-Zorich (KZ) cocycle describes the evolution of fibres in the Hodge bundle under this flow, given by

$$A_t(X, \omega) : H^1(X, \mathbb{R}) \rightarrow H^1(g_t X; \mathbb{R}).$$

Recall that the fibres are  $2g$  real dimensional vector spaces, so there are  $2g$ -many real eigenvalues. The KZ cocycle preserves the symplectic intersection form on cohomology so the Lyapunov exponents are in fact symmetric. The full spectrum takes the form

$$\lambda_1 \geq \cdots \geq \lambda_g \geq 0 \geq -\lambda_g \geq \cdots \geq -\lambda_1,$$

in particular, we are only concerned about the first  $g$  exponents. Denote their sum by  $\Lambda$ . This quantity is a fundamental constant in the study of dynamical systems, and is closely related to the area Siegel-Veech constant.

**Theorem 5.5** ([EKZ, Theorem 1]). *The top  $g$  Lyapunov exponents of the Hodge bundle over the stratum  $\mathcal{H}(\mu)$  along Teichmuller geodesic flow satisfies*

$$\Lambda = \frac{1}{2} \sum_{i=1}^m \frac{\mu_i(\mu_i + 2)}{\mu_i + 1} + \frac{\pi^2}{3} \cdot c_{\text{area}}(\mathcal{H}(\mu)).$$

In the quadratic setting, the Hodge bundle on the double cover splits into two subbundles, corresponding to the invariant and anti-invariant subspaces with respect to the natural involution  $\tau$  as discussed in Section 2.3. See [EKZ, Page 12] for complete details. Let  $\Lambda^+$  and  $\Lambda^-$  denote the sum of positive Lyapunov exponents corresponding to these subbundles.

**Theorem 5.6** ([EKZ, Theorem 2]). *The Lyapunov exponents  $\lambda_1^+ \geq \dots \geq \lambda_g^+$  of the invariant subbundle  $H_+^1$  of the Hodge bundle over the stratum  $\mathcal{Q}(\mu)$  along Teichmuller geodesic flow satisfies*

$$\Lambda^+ = \frac{1}{24} \sum_{i=1}^m \frac{\mu_i(\mu_i + 4)}{\mu_i + 2} + \frac{\pi^2}{3} \cdot c_{\text{area}}(\mathcal{Q}(\mu)).$$

Furthermore,  $\Lambda^+ = 0$  for  $g = 0$ . The Lyapunov exponents  $\lambda_1^- \geq \dots \geq \lambda_{g_{\text{eff}}}^-$  of the anti-invariant subbundle  $H_-^1$  of the Hodge bundle over the stratum  $\mathcal{Q}(\mu)$  along Teichmuller geodesic flow satisfies

$$\Lambda^- - \Lambda^+ = \frac{1}{4} \sum_{\mu_i \text{ odd}} \frac{1}{\mu_i + 2}.$$

Applying this theorem to the principal strata  $\mathcal{Q}(-1^n, 1^{4g-4+n})$  of quadratic differentials, we obtain

$$\begin{aligned} \Lambda^+ &= \frac{5g - n - 5}{18} + \frac{\pi^2}{3} \cdot c_{\text{area}}(\mathcal{Q}_{g,n}) \\ \Lambda^- &= \Lambda^+ + \frac{g + n - 1}{3}. \end{aligned}$$

Using Equation (5.2), the authors in [DGZZ1] were also able to obtain values for sums of Lyapunov exponents after computing volumes of the associated principal strata. Theorem 5.6 allows us to obtain a closed formula for the Siegel-Veech constant for all genus 0 quadratic strata. By expressing Siegel-Veech constants in terms of ratios of volumes of “boundary strata”, Athreya, Eskin, and Zorich [AEZ1] were able to obtain identities on the volumes of genus 0 quadratic strata which were used to recursively compute the volumes of all genus 0 quadratic strata, giving us Theorem 3.12.

# Chapter 6

## Conclusion

In this thesis, we began by introducing the theory of flat surfaces and their moduli spaces. We discussed their stratification and constructed local coordinates on strata, from which the Masur-Veech measure was constructed.

In Chapter 3, we defined the Masur-Veech volume and showed it can be computed by counting square-tiled surfaces. Some combinatorial tools were required to execute these counts, which included stable graphs and ribbon graphs. We then proved a geometric and combinatorial formula for the evaluation of these volumes which followed the techniques from [DGZZ1] for principal strata. In sufficiently nice cases, this framework can be extended to non-principal strata. We also discussed possible extensions to handle cases when the count functions are certain piecewise polynomials. This chapter concluded with some examples using our extended approach.

In Chapter 4, we derived an intersection theory approach to evaluating volumes in principal strata of quadratic differentials introduced in [DGZZ1]. We first provided an exposition of Kontsevich's proof of Witten's conjecture, which related the counts of ribbon graphs to intersection numbers. This allowed us to express volumes in principal strata in terms of Kontsevich volume polynomials. We then presented some further hand computations, extending the smaller examples provided in [DGZZ1].

In Chapter 5, we discussed some applications of Masur-Veech volumes. We began by introducing the problem of meander enumeration, and showed that after fixing some combinatorial features, the asymptotics can be expressed in terms of certain 1-cylinder volume contributions in genus 0. We also briefly discussed Siegel-Veech constants and Lyapunov exponents, which are closely related to volumes and are important numbers showing up in certain counting and dynamical problems.

# Appendix A

## Riemann surfaces and differentials

**Definition A.1.** A *Riemann surface* is a pair  $(X, \mathcal{A})$  where  $X$  is a two real-dimensional manifold and  $\mathcal{A}$  is a complex atlas of charts  $(U_i, \varphi_i)$  where the sets  $U_i$  cover  $X$  and  $\varphi_i : U_i \rightarrow V_i \subseteq \mathbb{C}$  is a homeomorphism onto an open subset. Moreover, all charts are holomorphically compatible, that is, the transition maps  $\varphi_i \circ \varphi_j^{-1}$  are biholomorphic.

**Remark A.2.** Two complex atlases are equivalent if their union is also a complex atlas. This defines an equivalence relation on the set of complex atlases which we refer to as a complex structure. Every complex structure contains a unique maximal atlas which contains all holomorphically compatible charts.

For a detailed treatment of sheaves and differential forms on Riemann surfaces, see [Fo, Sections 6 and 9]. The *canonical line bundle* is the holomorphic cotangent bundle. Sections of this bundle can locally be written as  $f(z)dz$  where  $f$  is a holomorphic function. The *canonical sheaf* is the sheaf of holomorphic sections denoted by  $K_X$  defined by  $K_X(U) = \Gamma(T^{*(1,0)}U)$ , where  $T^{*(1,0)}U$  is the holomorphic cotangent bundle on  $U$ .

**Definition A.3.** The space of *holomorphic one-forms* or *Abelian differentials* on  $X$  is the set of global sections  $H^0(X, K_X)$  of the sheaf  $K_X$ .

**Definition A.4.** The space of holomorphic *quadratic differentials* is the set of global sections  $H^0(X, K_X^{\otimes 2})$  where  $K_X^{\otimes 2}$  is the symmetric square of  $K_X$ .

**Remark A.5.** Locally, a holomorphic one-form can be expressed as  $\omega = f(z)dz$  for some holomorphic function  $f$ . Let  $w = w(z)$  be another coordinate. By the chain rule, we have  $\omega = f(z(w))z'(w)dw$ . Therefore, a holomorphic one-form can be considered as a collection of functions  $f_i$  for each chart  $U_i$  where on overlaps, we have  $f_j(z_j) = f(z_i(z_j))z'_i(z_j)$ . An identical observation follows for a quadratic differential locally expressed as  $q = f(z)dz^2$ , where on overlaps we have  $f_j(z_j) = f(z_i(z_j))z'_i(z_j)^2$ . Moreover, every quadratic differential  $q$  induces a metric  $|q|$  since it locally transforms identically to a metric.

**Proposition A.1.** *Let  $X$  be a Riemann surface equipped with a quadratic differential  $q$  that is not the square of an Abelian differential. Let  $\Sigma$  be the set of singularities (both zeros and poles) of  $q$ . There exists a canonical ramified double cover  $\pi : \widehat{X} \rightarrow X$  such that  $\pi^*q = \widehat{\omega}^2$  for some Abelian differential  $\widehat{\omega}$  on  $\widehat{X}$ .*

*Proof.* Consider the punctured surface  $X' = X \setminus \Sigma$  and let  $\mathcal{A} = \{(U_i, z_i)\}_{i \in I}$  be an atlas on  $X'$ . Assume all charts of  $\mathcal{A}$  are connected and simply-connected so the square root of  $q$  exists on each chart. We can express  $q$  locally on each  $U_i$  as  $f_i(z_i)dz_i^2$  with the collection of functions  $f_i$  satisfying the relations

$$f_i(z_i(z_j))dz_i^2 = f_j(z_j)dz_j^2$$

on  $U_i \cap U_j \neq \emptyset$ . Note that  $f_i$  is a non-zero function on  $U_i$  since we have punctured all zeros. Consider two copies  $(U_i^+, \zeta_i^+)$  and  $(U_i^-, \zeta_i^-)$  of each chart  $(U_i, z_i) \in \mathcal{A}$ , one for each branch of  $g_i^\pm(z_i) = \sqrt{f_i(z_i)}$ . Choose the sign on each chart such that the subsets of  $U_i^\pm$  and  $U_j^\pm$  corresponding to  $U_i \cap U_j$  are identified so

$$g_i^\pm(\zeta_i^\pm(\zeta_j^\pm)) = g_j^\pm(\zeta_j^\pm)$$

on  $U_i^\pm \cap U_j^\pm \neq \emptyset$ . Now define the Abelian differential  $\widehat{\omega}$  by

$$\widehat{\omega}|_{U_i^\pm} = g_i^\pm(\zeta_i^\pm)d\zeta_i^\pm.$$

Let  $U_p \subseteq C$  be an open neighbourhood containing a singularity  $p$  of order  $m$  and no other singularities. There is a chart  $z$  such that  $z(p) = 0$  so that locally we have  $q|_{U_p} = z^m dz^2$ . Pulling back  $q$  via  $\zeta^2 = z$ , we obtain

$$\pi^*q|_{U_p^\pm} = (\zeta^m)^2(d(\zeta^2))^2 = \zeta^{2m}(2\zeta d\zeta)^2 = (2\zeta^{m+1}d\zeta)^2$$

which is the square of an Abelian differential. This produces a punctured Riemann surface equipped with a holomorphic 1-form  $\widehat{\omega}$ .  $\square$

**Remark A.6.** Let  $g$  denote the genus of  $X$  and  $\widehat{g}$  denote the genus of the double cover  $\widehat{X}$ . Some authors refer to the difference  $g_{\text{eff}} = \widehat{g} - g$  as the *effective genus*. This can be computed using the Riemann-Hurwitz formula, in particular,  $\widehat{g} = 2g - 1 + \frac{b}{2}$  where  $b$  is the number of distinct odd singularities corresponding to the branch points.

**Proposition A.2.** *The natural involution  $\tau : \widehat{X} \rightarrow \widehat{X}$  that interchanges the two sheets satisfies  $\tau^*\widehat{\omega} = -\widehat{\omega}$ .*

*Proof.* Using the property  $\pi \circ \tau = \pi$ , one obtains by pulling back  $q$  the relation  $\widehat{\omega}^2 = (\tau^*\widehat{\omega})^2$  so  $\tau^*\widehat{\omega} = \pm\widehat{\omega}$ . If  $\tau^*\widehat{\omega} = \widehat{\omega}$  then  $\widehat{\omega}$  descends to a well-defined form  $\omega$  on  $X$  so

$$\pi^*q = \widehat{\omega}^2 = (\pi^*\omega)^2 = \pi^*(\omega^2).$$

Since  $\pi$  is surjective,  $\pi^*$  is injective and thus  $q = \omega^2$  which is a contradiction.  $\square$

# Appendix B

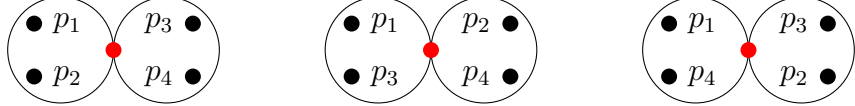
## Moduli space examples

**Example B.1.** Let  $g = 0$  and  $n = 3$ . There exists a unique Möbius transformation mapping any genus 0 Riemann surface with three marked points  $(X, p_1, p_2, p_3)$  to  $(\mathbb{CP}^1, 0, 1, \infty)$  so  $\mathcal{M}_{0,3}$  is a singleton.

**Example B.2.** Let  $g = 0$  and  $n = 4$ . There exists a unique Möbius transformation mapping any genus 0 Riemann surface with four marked points  $(X, p_1, p_2, p_3, p_4)$  to  $(\mathbb{CP}^1, 0, 1, \infty, t)$  where  $t \neq 0, 1, \infty$ . Since  $t$  is free to vary,  $\mathcal{M}_{0,4} \cong \mathbb{CP}^1 \setminus \{0, 1, \infty\}$ .

**Example B.3.** Let  $g = 1$  and  $n = 1$ . Every complex torus, also called an elliptic curve, arises as a quotient  $\mathbb{C}/\Lambda$  where  $\Lambda$  is a lattice spanned by linearly independent complex numbers  $z_1, z_2 \in \mathbb{C}$ . The image of  $\Lambda$  gives the single marked point. Two tori  $\mathbb{C}/\Lambda$  and  $\mathbb{C}/\Lambda'$  are isomorphic if  $\Lambda = \alpha\Lambda'$  for some  $\alpha \in \mathbb{C}^*$ . Normalising so that  $z_1 = 1$  and  $z_2 = \tau$  for some  $\tau \in \mathbb{H}$ , we observe that any  $\text{SL}(2, \mathbb{Z})$  action on  $\tau$  gives another number that generates the same lattice. Therefore,  $\mathcal{M}_{1,1} \cong \mathbb{H}/\text{SL}(2, \mathbb{Z})$ .

**Example B.4.** The space  $\overline{\mathcal{M}}_{0,3}$  is a singleton. Since  $\mathcal{M}_{0,4} \cong \mathbb{CP}^1 \setminus \{0, 1, \infty\}$ , we have for the compactification  $\overline{\mathcal{M}}_{0,4} \cong \mathbb{CP}^1$ . The points  $0, 1, \infty$  correspond to the stable curves shown below.



**Example B.5.** The compactification of  $\mathcal{M}_{1,1} \cong \mathbb{H}/\text{SL}(2, \mathbb{Z})$  is obtained by adding the point at infinity, corresponding to a degenerated torus with one nodal point. That is,  $\overline{\mathcal{M}}_{1,1} \cong (\mathbb{H} \cup \{\infty\})/\text{SL}(2, \mathbb{Z})$ .

# Appendix C

## Additional proofs

**Lemma C.1** (Proof of Equation (4.4)). *Let  $G \in \mathcal{R}_{g,n}$  be a ribbon graph and let  $\lambda_i$  be the variable associated with the  $i$ -th boundary component with length  $b_i$ . Then*

$$\sum_{i=1}^n b_i \lambda_i = \sum_{f \in F(G)} \ell(f) \lambda(f) = \sum_{e \in E(G)} \ell(e) \tilde{\lambda}(e). \quad (\text{C.1})$$

*Proof.* First expand the left hand side using half-edge representatives for each boundary component and substitute the definition of the length function on boundaries. We will also denote by  $\lambda$  the function on  $F(G)$  which returns the corresponding variable  $\lambda_i$ .

$$\sum_{i=1}^n b_i \lambda_i = \sum_{[x]_2 \in F(G)} \ell([x]_2) \lambda([x]_2) = \sum_{[x]_2 \in F(G)} \sum_{i=1}^{\#[x]_2} \ell([\tau_2^i x]_1) \lambda([x]_2) = \sum_{x \in X} \ell([x]_1) \lambda([x]_2)$$

The final equality follows by observing that  $[x]_2 = [\tau_2^i x]_2$  and that the set  $X$  is equal to the disjoint union of orbit sets of representatives of boundaries. Invoking a similar argument for representatives of edges in reverse, we obtain the right hand side of the Lemma.

$$= \sum_{[x]_1 \in E(G)} \ell([x]_1) \lambda([x]_2) + \underbrace{\ell([\tau_1 x]_1)}_{=\ell([x]_1)} \lambda([\tau_1 x]_2) = \sum_{[x]_1 \in E(G)} \ell([x]_1) \tilde{\lambda}([x]_1) = \sum_{e \in E(G)} \ell(e) \tilde{\lambda}(e).$$

□

# Bibliography

- [KaZe] A. B. Katok and A. N. Zemlyakov. “Topological transitivity of billiards in polygons”. In: *Mathematical Notes of the Academy of Sciences of the USSR* 18 (1975), pp. 760–764. DOI: [10.1007/BF01818045](https://doi.org/10.1007/BF01818045).
- [Fo] O. Forster. *Lectures on Riemann Surfaces*. Vol. 81. Graduate Texts in Mathematics. New York: Springer New York, NY, 1981. DOI: [10.1007/978-1-4612-5961-9](https://doi.org/10.1007/978-1-4612-5961-9).
- [Ma] H. Masur. “Interval exchange transformations and measured foliations”. In: *Annals of Mathematics* 115 (1982), pp. 169–200. DOI: [10.2307/1971341](https://doi.org/10.2307/1971341).
- [Ve] W. Veech. “Gauss measures for transformations on the space of interval exchange maps”. In: *Annals of Mathematics* 115 (1982), pp. 201–242. DOI: [10.2307/1971391](https://doi.org/10.2307/1971391).
- [Ha] J. L. Harer. “The virtual cohomological dimension of the mapping class group of an orientable surface”. In: *Inventiones Mathematicae* 84 (Feb. 1986), pp. 157–176. DOI: [10.1007/BF01388737](https://doi.org/10.1007/BF01388737).
- [Pe] R. C. Penner. “The Decorated Teichmüller Space of Punctured Surfaces”. In: *Communications in Mathematical Physics* 113 (1987), pp. 299–339. DOI: [10.1007/BF01223515](https://doi.org/10.1007/BF01223515).
- [BoEp] B.H. Bowditch and D.B.A. Epstein. “Natural triangulations associated to a surface”. In: *Topology* 27.1 (1988), pp. 91–117. DOI: [10.1016/0040-9383\(88\)90008-0](https://doi.org/10.1016/0040-9383(88)90008-0).
- [W91] E. Witten. “Two-dimensional gravity and intersection theory on moduli space”. In: *Surveys in Differential Geometry* 1 (1991), pp. 243–310. DOI: [10.4310/SDG.1990.v1.n1.a5](https://doi.org/10.4310/SDG.1990.v1.n1.a5).
- [K92] M. Kontsevich. “Intersection theory on the moduli space of curves and the matrix Airy function”. In: *Comm. Math. Phys.* 147 (1992), pp. 1–23. DOI: [10.1007/BF02099526](https://doi.org/10.1007/BF02099526).
- [Mi95] R. Miranda. *Algebraic Curves and Riemann Surfaces*. Vol. 5. Graduate Studies in Mathematics. American Mathematical Society, 1995.
- [HM98] J. Harris and I. Morrison. *Moduli of Curves*. Vol. 187. Graduate Texts in Mathematics. Springer-Verlag, 1998.
- [MuPe] M. Mulase and M. Penkava. “Ribbon Graphs, Quadratic Differentials on Riemann Surfaces, and Algebraic Curves Defined over  $\overline{\mathbb{Q}}$ ”. In: *arXiv: Mathematics*

- ical Physics* (1998). URL: <https://api.semanticscholar.org/CorpusID:2075745>.
- [EO] A. Eskin and A. Okounkov. “Asymptotics of numbers of branched coverings of a torus and volumes of moduli spaces of holomorphic differentials”. In: *Inventiones mathematicae* 145 (2001), pp. 59–103. DOI: [10.1007/s002220100142](https://doi.org/10.1007/s002220100142).
- [Zo2] A. Zorich. “Square Tiled Surfaces and Teichmüller Volumes of the Moduli Spaces of Abelian Differentials”. In: *Rigidity in Dynamics and Geometry*, 459-471 (2002) (Jan. 2002). DOI: [10.1007/978-3-662-04743-9\\_25](https://doi.org/10.1007/978-3-662-04743-9_25).
- [Zvo2] D. Zvonkine. “Strebel differentials on stable curves and Kontsevich’s proof of Witten’s conjecture”. In: *arXiv: Algebraic Geometry* (2002). URL: <https://api.semanticscholar.org/CorpusID:13634236>.
- [KoZo] M. Kontsevich and A. Zorich. “Connected components of the moduli spaces of Abelian differentials with prescribed singularities”. In: *Inventiones Mathematicae* 153.3 (2003), pp. 631–678. DOI: [10.1007/s00222-003-0303-x](https://doi.org/10.1007/s00222-003-0303-x).
- [EO2] A. Eskin and O. Okounkov. “Pillowcases and quasimodular forms”. In: ed. by Victor Ginzburg. Boston, MA: Birkhäuser Boston, 2006, pp. 1–25. DOI: [10.1007/978-0-8176-4532-8\\_1](https://doi.org/10.1007/978-0-8176-4532-8_1).
- [Jo] J. Jost. *Compact Riemann Surfaces: An Introduction to Contemporary Mathematics*. 3rd. Universitext. Berlin: Springer-Verlag, 2006. DOI: [10.1007/978-3-540-33067-7](https://doi.org/10.1007/978-3-540-33067-7).
- [Zo] A. Zorich. “Flat surfaces”. In: (2006). Ed. by Pierre Cartier, Bernard Julia, Pierre Moussa, and Philippe Vanhove, pp. 439–585. DOI: [10.1007/978-3-540-31347-2\\_17](https://doi.org/10.1007/978-3-540-31347-2_17).
- [Mirz] M. Mirzakhani. “Weil–Petersson Volumes and Intersection Theory on the Moduli Space of Curves”. In: *Journal of the American Mathematical Society* 20.1 (2007), pp. 1–23. DOI: [10.1090/S0894-0347-06-00526-1](https://doi.org/10.1090/S0894-0347-06-00526-1).
- [Do] N. Do. “Intersection theory on moduli spaces of curves via hyperbolic geometry”. PhD thesis. The University of Melbourne, 2008.
- [La] E. Lanneau. “Connected components of the strata of the moduli spaces of quadratic differentials”. In: *Annales Scientifiques de l’École Normale Supérieure* (4) 41.1 (2008), pp. 1–56.
- [Si09] J.H. Silverman. *The Arithmetic of Elliptic Curves*. 2nd. Vol. 106. Graduate Texts in Mathematics. Springer, 2009.
- [Nor] Paul Norbury. “Counting lattice points in the moduli space of curves”. In: *Mathematical Research Letters* 17 (2010), pp. 467–481. DOI: [10.4310/MRL.2010.v17.n3.a7](https://doi.org/10.4310/MRL.2010.v17.n3.a7).
- [CMS] K.M. Chapman, M. Mulase, and B. Safnuk. “The Kontsevich constants for the volume of the moduli of curves and topological recursion”. In: *Communications in Number Theory and Physics* 5.4 (2011), pp. 643–698. DOI: [10.48550/arXiv.1009.2055](https://doi.org/10.48550/arXiv.1009.2055).

- [Zvo] D. Zvonkine. “An Introduction to Moduli Spaces of Curves and Their Intersection Theory”. In: *Handbook of Teichmüller Theory 3* (2012), pp. 667–716. DOI: [10.4171/103-1/12](https://doi.org/10.4171/103-1/12).
- [AEZ2] J.S. Athreya, A. Eskin, and A. Zorich. “Counting generalized Jenkins–Strebel differentials”. In: *Geometriae Dedicata* 170.1 (2014), pp. 195–217. DOI: [10.1007/s10711-013-9877-7](https://doi.org/10.1007/s10711-013-9877-7).
- [DHL] Vincent Delecroix, Pascal Hubert, and Samuel Lelièvre. “Diffusion for the periodic wind-tree model”. In: *Annales scientifiques de l’École Normale Supérieure* Ser. 4, 47.6 (2014), pp. 1085–1110. DOI: [10.24033/asens.2234](https://doi.org/10.24033/asens.2234).
- [EKZ] A. Eskin, M. Kontsevich, and A. Zorich. “Sum of Lyapunov exponents of the Hodge bundle with respect to the Teichmüller geodesic flow”. In: *Publications Mathématiques de l’Institut des Hautes Études Scientifiques* 120 (2014), pp. 207–333. DOI: [10.1007/s10240-013-0060-3](https://doi.org/10.1007/s10240-013-0060-3).
- [FoMa] C. Matheus G. Forni. “Introduction to Teichmuller theory and its applications to dynamics of interval exchange transformations, flows on surfaces and billiards”. In: *J. Mod. Dyn.* 8 (2014), no. 3–4, 271–436.
- [DZ] V. Delecroix and A. Zorich. “Cries and whispers in wind-tree forests”. In: *arXiv preprint arXiv:1502.06405* (2015).
- [Wr] A. Wright. “Translation surfaces and their orbit closures: An introduction for a broad audience”. In: *EMS Surveys in Mathematical Sciences* 2.1 (2015), pp. 63–108. DOI: [10.4171/EMSS/9](https://doi.org/10.4171/EMSS/9).
- [AEZ1] J.S. Athreya, A. Eskin, and A. Zorich. “Right-angled billiards and volumes of moduli spaces of quadratic differentials on  $\mathbb{CP}^1$ ”. In: *Annales scientifiques de l’École Normale Supérieure, Série 4* 49.6 (2016), pp. 1311–1386. DOI: [10.24033/asens.2310](https://doi.org/10.24033/asens.2310).
- [Go] Elise Goujard. “Volumes of strata of moduli spaces of quadratic differentials: getting explicit values”. In: *Annales de l’Institut Fourier* 66.6 (2016), pp. 2203–2251. DOI: [10.5802/aif.3062](https://doi.org/10.5802/aif.3062).
- [Ch] Y. Chou. *Kontsevich’s Proof of Witten Conjecture*. Lecture notes, National Taiwan University. 2019.
- [DGZZ2] V. Delecroix, E. Goujard, P. Zograf, and A. Zorich. “Enumeration of Meanders and Masur–Veech Volumes”. In: *Forum of Mathematics, Pi* 8.e2 (2020). Published online; arXiv preprint version 2017 available at arXiv:1705.05190, pp. 1–71. DOI: [10.1017/fmp.2020.2](https://doi.org/10.1017/fmp.2020.2).
- [AtMa] J.S. Athreya and H. Masur. *Translation Surfaces*. Vol. 78. Student Mathematical Library. American Mathematical Society, 2021. ISBN: 978-1-4704-6486-9. DOI: [10.1090/stml/078](https://doi.org/10.1090/stml/078).
- [DGZZ1] V. Delecroix, É. Goujard, P. Zograf, and A. Zorich. “Masur–Veech volumes, frequencies of simple closed geodesics, and intersection numbers of moduli spaces of curves”. In: *Duke Mathematical Journal* 170.12 (2021), pp. 2633–2718. DOI: [10.1215/00127094-2021-0054](https://doi.org/10.1215/00127094-2021-0054).
- [MPS] S. Molcho, R. Pandharipande, and J. Schmitt. “The Hodge bundle, the universal 0-section, and the log Chow ring of the moduli space of curves”. In:

- arXiv preprint arXiv:2101.08824* (2021). MPIM-Bonn-2021, revised 2022. DOI: [10.48550/arXiv.2101.08824](https://doi.org/10.48550/arXiv.2101.08824).
- [CMS2] D. Chen, M. Möller, and A. Sauvaget. “Masur-Veech volumes and intersection theory: the principal strata of quadratic differentials”. In: *Duke Mathematical Journal* 172.9 (2023), pp. 1735–1779. DOI: [10.1215/00127094-2022-0063](https://doi.org/10.1215/00127094-2022-0063).
- [KaZu] R.M. Kaufmann and J. Zúñiga. “A combinatorial model for the moduli of bordered Riemann surfaces and a compactification”. In: *Contemporary Mathematics* 802 (2024), pp. 117–137. DOI: [10.1090/conm/802/01706](https://doi.org/10.1090/conm/802/01706).
- [BC] D. Chen A. Bud. *Moduli of Differentials and Teichmüller Dynamics*. Available online at <https://arxiv.org/abs/2004.05762>.
- [Al] J. Alper. “Stacks and Moduli”. URL: <https://sites.math.washington.edu/~jarod/moduli.pdf>.